CHARACTERIZATION OF THE PHOSPHODIESTERASE SUBTYPES THAT REGULATE MOUSE ATRIAL MYOCYTE ELECTROPHYSIOLOGY

by

Andrew P. Adamczyk

Submitted in partial fulfilment of the requirements
for the degree of Master of Science

at

Dalhousie University
Halifax, Nova Scotia
July of 2011

DALHOUSIE UNIVERSITY

DEPARTMENT OF PHYSIOLOGY AND BIOPHYSICS

The undersigned hereby certify that they have read and recommend to the Faculty of Graduate Studies for acceptance a thesis entitled "CHARACTERIZATION OF THE PHOSPHODIESTERASE SUBTYPES THAT REGULATE MOUSE ATRIAL MYOCYTE ELECTROPHYSIOLOGY" by Andrew P. Adamczyk in partial fulfilment of the requirements for the degree of Master of Science.

Dated: July 26th, 2011

Supervisor: _____

Readers: _____

_____

_____

Departmental Representative: _____

DALHOUSIE UNIVERSITY

DATE: July 26th , 2011

AUTHOR: Andrew P. Adamczyk

TITLE: CHARACTERIZATION OF THE PHOSPHODIESTERASE SUBTYPES THAT REGULATE MOUSE ATRIAL MYOCYTE ELECTROPHYSIOLOGY

DEPARTMENT OR SCHOOL: Department of Physiology and Biophysics

DEGREE: MSc CONVOCATION: October YEAR: 2011

_____

Signature of Author

TABLE OF CONTENTS

LIST OF TABLES

LIST OF FIGURES

ABSTRACT

Phosphodiesterases (PDEs) are the enzymes responsible for the hydrolysis of cyclic nucleotides including cAMP and cGMP. We recently discovered that natriuretic peptides elicit effects in the atrial myocardium via a PDE dependant pathway; however, the role(s) of specific PDE subtypes in atrial myocytes are not clear. Thus, I studied the effects of PDE selective blockers on mouse atrial action potentials (APs) and L-type Ca^{2+} currents ($I_{Ca,L}$). AP duration (APD) was significantly increased in the presence of IBMX (inhibits all PDEs) as well as EHNA (PDE2 inhibitor) and rolipram (PDE4 inhibitor). The PDE 3 inhibitor milrinone had no effect on APD. Applying milrinone and rolipram (PDE3/PDE4 inhibition) or EHNA, milrinone, and rolipram (PDE2/ PDE3/PDE4 inhibition) in combination prolonged APD as effectively as IBMX. A similar pattern of results was obtained for atrial $I_{Ca,L}$. These data provide novel insight into the unique effects of PDE inhibitors in atrial myocytes.

LIST OF ABBREVIATIONS USED

AC	Adenelyl cyclase
Ach	Acetylcholine
Ang II	Angiotensin II
ANP	Atrial natriuretic peptide
AP	Action potential
APD50	Action potential duration at 50% repolarization time
APD70	Action potential duration at 70% repolarization time
APD90	Action potential duration at 90% repolarization time
AVN	Atrioventricular node
β-AR	β-adrenergic receptor
BNP	Brain type natriuretic peptide
CICR	Calcium induced calcium release
CN	Cyclic nucleotide
CNG	Cyclic nucleotide gated
CNP	C-type natriuretic peptide
CREB	cAMP response element binding protein
cAMP	Cyclic 3', 5' adenosine monophosphate
cGMP	Cyclic 3', 5' guanosine monophosphate
E-C	Excitation-contraction
ED	Erectile disfunction

EHNA	Erythro-9-(2-hydroxy-3-nonyl) adenine
Epac	Exchange protein activated by cAMP
ERK	Extracellular signal regulated kinases
ERP	Effective refractory period
GAF	cGMP, adenylyl cyclase, Fh1A
GC	Guanylyl cyclase
G_i	Inhibitory G protein
GPCR	G-protein coupled receptor
G_s	Stimulatory G protein
$I_{Ca,L}$	L-type Ca^{2+} current
ICER	Inducible cyclic AMP early repressor
I_{CNG}	cGMP gated current
I_{Na}	Fast, inward Na^+ current
I_{K1}	Inwardly rectifying K^+ current
$I_{K,s}$	Rapidly activating, slow inactivating outward K^+ current
I_{Kur}	Rapidly activating outward K^+ current
I_{ss}	Non inactivating steady state current
$I_{to,f}$	Fast, transient outward K^+ current
LTCC	L-type Ca^{2+} channel
M_2	Muscarinic receptor
mAKAP	Muscle A-kinase anchoring protein
MIMX	8-methoxy-1-methyl-3-isobutylxanthine
NCX	Sodium-calcium exchanger
NHR	NH_2 terminal hydrophobic region
NO	Nitric oxide

NOS	Nitric oxide synthase
NP	Natriuretic peptide
pGC	Particulate guanylyl cyclase
PAS	Per-ARNT-Sim
Po	Open probability
PDE	Phosphodiesterase
PKA	Protein kinase A
PKG	Protein kinase G
RMP	Resting membrane potential
RYR	Ryanodine receptor
sGC	Soluble guanylyl cyclase
SAN	Sinoatrial node
SCD	Sudden cardiac death
SR	Sarcoplasmic reticulum
SERCA	Sarcoendoplasmic reticulum Ca^{2+} ATPase
TnC	Troponin C
TnI	Troponin I
UCR	Upstream conserved regulatory region
V_{max}	Rate of depolarization
$V_{1/2}$	Membrane potential at which 50% of channels are activated

ACKNOWLEGMENTS

I would like to dedicate my MSc thesis to my mom and dad, who have supported and motivated me along this journey, and who have always been there in both the good times and the bad. Without you both, I would not be where I am today. I cannot thank you enough and I hope to have made you both proud.

I would also like to give a special thanks to my supervisor Dr. Robert Rose for first and foremost giving me the opportunity to conduct research in such a high quality lab. His passion for cardiovascular research and desire to produce only the best work have been ingrained in me and have not only made me a better researcher but student as well. Your guidance, supervision and knowledge of cardiac electrophysiology have been much appreciated

In addition to my supervisor, I would also like to thank the members of my supervisory committee Dr. Susan Howlett and Dr. Paul Linsdell. Without their help and direction the completion of this thesis would not have been possible.

To the other members of Dr. Rose's lab, your friendship, encouragement, and help have made my experience here at Dalhousie one to remember. Having the ability to work with you all on a day to day basis has been a privilege and I would like to wish you all the best in your future endeavours.

Lastly, I would like to thank the funding agencies who without their support this work would not be possible. These include the Canadian Institute of Health Research, the Heart and Stroke Foundation of Nova Scotia, and the Dalhousie Medical Research Foundation.

CHAPTER 1: INTRODUCTION

1.1 Cyclic Nucleotides

The cyclic nucleotides (CNs) cyclic adenosine 3', 5' –monophosphate (cAMP) and cyclic guanosine 3', 5' –monophophate (cGMP) are two second messengers that are crucial in the modulation of many physiological processes in many organs including the heart (Fischmeister *et al.*, 2006). Sutherland and colleagues, who were the first to discover cAMP over 50 years ago, were also the first to coin the term "second messenger" when describing cAMP (Suthurland & Rall, 1958). Soon after, this same term was applied to cGMP after its discovery (Ashman *et al.*, 1963). Since then, many efforts have been put forth in order to understand these two second messengers. How are they synthesized and degraded? What controls their levels within the cell? How do they target their effectors, whether it be by phosphorylation or direct binding to proteins, as well as numerous other cellular functions (Fimia & Sassone-Corsi, 2001;Beavo & Brunton, 2002;Pawson & Scott, 2005;Hofmann, 2005). Although these questions have been extensively looked at, many questions still remain unanswered. This is the case for the heart, where cAMP and cGMP are important regulators of cardiac function. Precise regulation of CN levels within cardiomyocytes is crucial for normal physiological function; therefore, understanding their roles and regulation in the myocardium is of paramount importance.

cAMP which is synthesized by adenylyl cyclase (AC) upon G-protein coupled receptor (GPCR) stimulation by catecholamines, activates the cAMP dependant protein kinase A (PKA) pathway. PKA can modulate cardiac rhythm (chronotropy) as well as contractile force (inotropy) and relaxation (lusitropy) of the heart (Bers, 2002). cGMP,

which is synthesized by guanylyl cyclase (GC) in response to nitric oxide (NO) and natriuretic peptides (NPs), is able to modulate inotropy and metabolic responses via the activation of its downstream effectors including, protein kinase G (PKG), cyclic nucleotide gated channels, and phosphodiesterases (PDEs) (Shah & MacCarthy, 2000;Vandecasteele *et al.*, 2001). The cAMP and cGMP pathways have often been associated with opposing influences on cardiac function, largely due to the opposing effects of PKA and PKG on target proteins; however, this theory is likely overly simplistic due to the interactions of cAMP/cGMP with a large number of downstream targets, including PDEs, which can elicit a range of effects in the myocardium (Lohmann *et al.*, 1991;Vandecasteele *et al.*, 2001;Fischmeister *et al.*, 2005). These issues will be discussed in more detail below.

In addition to the factors regulating their synthesis, intracellular concentrations of cAMP and cGMP are critically regulated by their degradation by PDEs (Conti & Beavo, 2007;Francis *et al.*, 2001). PDEs represent the only CN degrading enzymes; therefore, they are critical in controlling the levels of cAMP and cGMP within cells. PDEs are encoded by 21 different genes which are grouped based on sequence similarity, regulatory properties, and substrate specificity, into 11 families (PDEs 1-11) (Bender & Beavo, 2006;Beavo, 1995;Conti & Beavo, 2007;Francis *et al.*, 2001;Francis *et al.*, 2011;Maurice *et al.*, 2003). In the heart, 7 PDE families have been described: PDE1, PDE2, PDE3, PDE4, PDE5, PDE8 and PDE9 (Loughney *et al.*, 1996;Meacci *et al.*, 1992;Kostic *et al.*, 1997a;Senzaki *et al.*, 2001;Soderling & Beavo, 2000;Soderling *et al.*, 1998;Onody *et al.*, 2003), where most attention has been given to PDE1-5, but important roles for additional subtypes are being identified (Maurice *et al.*, 2003;Takimoto *et al.*,

2005b). PDE1, PDE2 and PDE3 are capable of hydrolysing both cAMP and cGMP, making them dual specific enzymes; PDE4 and PDE8 hydrolyse only cAMP; and PDE5 and PDE9 hydrolyse only cGMP (Lugnier, 2006).

Our lab, which is currently investigating the electrophysiological effects of NPs, has recently shown that these peptides are able to modulate L-type Ca^{2+} currents ($I_{Ca,L}$) in mouse atrial myocytes via a PDE dependant pathway that modulates intracellular cAMP. We believe that this could be associated to the fact that NPs, when bound to their GC linked receptors, are able to increase intracellular levels of cGMP resulting in the modulation of PDE activity. In particular PDE2, PDE3, and PDE4 because PDE2 and PDE3 are directly regulated by cGMP and all three subtypes tightly regulate cAMP in cardiomyocytes (Fischmeister *et al.*, 2006). By investigating the role(s) that these specific PDE subtypes have in regulating atrial electrophysiology, we aim to further understand the mechanism(s) responsible for the effects of NPs in the atrial myocardium in normal physiological conditions as well in the context of protecting against atrial arrhythmias. Indeed mutations in NP genes have been associated with atrial fibrillation (Hodgson-Zingman *et al.*, 2008;Tsang *et al.*, 2005;Stambler & Guo, 2005), which is a very common atrial arrhythmia resulting in the loss of coordinated atrial electrical activation and contraction. This loss results in reduced ventricular filling and blood stasis in the atria, which predisposes individuals to heart failure and thromboembolic stroke (Wang *et al.*, 2003;Wolf *et al.*, 1991).

This study will also help further understand possible regional differences in the regulation of CNs by PDEs in the heart. In particular, which PDE subtypes are responsible for maintaining basal cAMP and cGMP levels in the atrial myocardium of the

heart verses the ventricles or the sinoatrial node (SAN)? Although many studies have examined the roles of specific PDEs in the myocardium, the majority of studies have focused on ventricular myocytes.

In order to gain a better understanding of the topics discussed above, as well as the approaches that were taken to characterize the atrial region of the heart, the contribution made by selective PDEs and their ability to modulate its electrophysiology. A more in depth analysis of CNs and their ability to regulate cardiac function and CN phosphodiesterases will be done in the sections to follow.

1.2 Regulation of Cardiac Function by Cyclic Nucleotides

1.2.1 Cardiac Excitation-Contraction Coupling

Cardiac excitation-contraction (E-C) coupling is the process that converts electrical signals (action potentials (APs)) into contractile responses enabling cardiomyocytes to contract and pump blood to the organs and tissues in our bodies. When the AP occurs the sarcolemmal membrane is depolarized causing the opening of L-type Ca^{2+} channels (LTCCs) and allowing Ca^{2+} ions to enter the cell generating an inward current, called the L-type Ca^{2+} current ($I_{Ca,L}$). This $I_{Ca,L}$ results in the release of Ca^{2+} stores from the sarcoplasmic reticulum (SR) via the ryanodine receptors (RyR), a mechanism known as calcium induced calcium release (CICR) (Fabiato & Fabiato, 1978). Ca^{2+} ions bind to contractile proteins, such as troponin C (TnC), resulting in the cross bridging of actin and myosin filaments; hence, a muscle contraction (Bers, 2002). During relaxation, most of the cytosolic Ca^{2+} is taken back up into the SR through the ATP dependant Ca^{2+} pump (sarcoendoplasmic reticulum Ca^{2+} -ATPase, SERCA). This pump is regulated by phospholamban (PLB). Some of the cytosolic Ca^{2+} is also is

pumped out of the cell via the sodium-calcium exchanger (NCX) and sarcolemmal Ca^{2+}ATPase, thereby lowering the intracellular Ca^{2+} concentration and removing calcium from the contractile proteins (Bers, 2002;Bers, 2008). This phenomenon occurs in all working myocardium including that of the atria and ventricles

1.2.2 Pathways Regulating cAMP in the Heart

The autonomic nervous system plays a major role in controlling intracellular cAMP due to the opposing actions of the sympathetic and parasympathetic branches of the nervous system on AC activity (Bers, 2002).

Activation of the sympathetic system occurs when catecholamines (epinephrine and norepinephrine), which are produced in the adrenal glands, are released from sympathetic nerve terminal into the synaptic cleft where they bind to β-adrenergic receptors (β-ARs). In the heart, two types of β-AR (β_1-AR and β_2-AR) participate in the sympathetic stimulation of cardiac function. A third (β_3-AR) which is also found in the heart, is coupled to NO stimulation (Xiao *et al.*, 2004). β_1-AR and β_2-AR are coupled to stimulatory G proteins (Gs), which activate ACs that catalyze conversion of ATP to cAMP. In the heart , AC5 and AC6 represent the dominant isoforms (Defer *et al.*, 2000) which seem to be preferentially localized in T-tubules (Gao *et al.*, 1997;Laflamme & Becker, 1999). A rise in intracellular cAMP levels results in the activation of cAMP-dependant PKA, which can phosphorylate downstream targets, including the LTCC and the RyR (Keef *et al.*, 2001;Takasago *et al.*, 1989). This has been shown to increase the mean open probability (Po) of both LTCCs and RYRs, leading to a higher cytosolic Ca^{2+} concentration and increased contractility and chronotropy (Brette *et al.*, 2006;Bers, 2002). Additional PKA targets include PLB, which results in the stimulation of SERCA

activity increasing its ability to sequester Ca^{2+} into the SR (MacLennan & Kranias, 2003), as well as Troponin I (TnI) which decreases its sensitivity to Ca^{2+} (Layland *et al.*, 2005) . Both the increase in SERCA activity and the decrease in Ca^{2+} sensitivity of TnI contribute to the enhanced lusitropic effects mediated by β-adrenergic stimulation. PKA also has the ability to alter gene expression in cardiac myocytes via cAMP response element binding protein (CREB) (Muller *et al.*, 2001).

cAMP also elicits effects in a number of ways independently of PKA. These include the direct activation of Epac (Morel *et al.*, 2005) , a guanine nucleotide exchange factor for the small GTPase Rap1 (Bos, 2003), and cyclic nucleotide gated channels (HCN) (Baruscotti *et al.*, 2005). To summarize, the result of increased levels of intracellular cAMP is in most cases an increase in inotropy, lusitropy or chronotropy, and at times a combination of the three.

The production of cAMP is inhibited or reduced by the parasympathetic nervous system. This occurs when the parasympathetic neurotransmitter acetylcholine (ACh) is released into the synaptic cleft and binds muscarinic (M_2) receptors. M_2 receptors are coupled to inhibitory G proteins ($G_{i/o}$), which reduce AC activity and the production of cAMP leading to a decrease in PKA activity (Brodde & Michel, 1999)

1.2.2.1 Degradation of Intracellular cAMP

The intracellular levels of cAMP are not only regulated by their synthesis but also via their hydrolysis by PDEs. PDEs are found not only in the cytosol, but in a variety of membranes, including nuclear and cytoskeletal locations (Lugnier, 2006). Although several PDE subtypes are expressed in the heart (see above) the present study focuses on three subtypes: PDE2, which is stimulated by cGMP and hydrolyses both cAMP and

cGMP; PDE3, which is inhibited by cGMP and preferentially hydrolysis cAMP but has the ability to hydrolyse both; and finally PDE4 which hydrolysis cAMP only (Maurice *et al.*, 2003). PDE3 and PDE4 have both proven to be very important in preventing cAMP diffusion within cardiomyocytes. In rat ventricular myocytes, PDE3 and PDE4 have both shown to potentiate β_1-AR cAMP signals. PDE3 and PDE4 were also able to control β_1 and β_2-AR regulation of $I_{Ca,L}$ in these preparations (Rochais *et al.*, 2006;Nikolaev *et al.*, 2006). PDE2 has also demonstrated the ability to control cAMP signaling, as a prominent role in selectively shaping the cAMP response to catecholamines was demonstrated via a pathway involving β_3-adrenergic receptors, NO generation and cGMP production in primary cultured ventricular myocytes (Mongillo *et al.*, 2006). Therefore, PDE2, PDE3 and PDE4, all play a significant role in regulating intracellular cAMP gradients, and by doing so controlling cAMPs ability to stimulate its downstream targets.

1.2.3 Pathways Regulating cGMP in the Heart

In the heart cGMP is produced by two different forms of guanylyl cyclase. The first being the soluble form (sGC), which is activated by NO (Padayatti *et al.*, 2004;Pyriochou & Papapetropoulos, 2005) and the second being the particulate form (pGC) which is activated by NPs (ANP, BNP and CNP) (D'Souza *et al.*, 2004;Kuhn, 2003;Padayatti *et al.*, 2004).

1.2.3.1 Nitric Oxide Signaling in the Heart

There are three isoforms of nitric oxide synthase (NOS) found to be expressed in cardiomyocytes and other cell types of the heart. These include the neuronal (nNOS or NOS1), the inducible (iNOS or NOS2) and the endothelial (eNOS or NOS3) isoforms (Moncada *et al.*, 2000;Massion & Balligand, 2003). eNOS and nNOS are found to be

constitutively expressed in cardiomyocytes. eNOS localizes to caveolae (Feron *et al.*, 1998;Garcia-Cardena *et al.*, 1997), where they have been found to be compartmentalized with β-AR and LTCC (Schwencke *et al.*, 1999) allowing NO to inhibit β-AR induced inotropy (Hare *et al.*, 1998). nNOS, on the other hand, has been shown to be located on SR membrane vesicles (Xu *et al.*, 1999). Contrary to eNOS, nNOS stimulates Ca^{2+} influx through LTCC (Sears *et al.*, 2003), and has also been linked to stimulation of SR Ca^{2+} release via the RyR *in vitro* (Xu *et al.*, 1998;Eu *et al.*, 2000).

1.2.3.2 Natriuretic Peptide Signaling in the Heart

NPs (ANP, BNP and CNP) are a family of related hormones which bind two classes of receptors: the GC- linked natriuretic peptide A and B receptors (NPR-A and NPR-B), and the natriuretic peptide C receptor (NPR-C) which does not contain a transmembrane GC but has been linked to G_i (Rose & Giles, 2008;Rose *et al.*, 2003). The fact that both NPR-A and NPR-B contain a cytosolic GC makes them able to catalyze the synthesis of cGMP from GTP (Wedel & Garbers, 1998). NPR-C lacks direct GC stimulatory activity, but is functionally linked to the activation of G_i proteins (Murthy & Makhlouf, 2000). ANP and BNP are primarily synthesized in the atria in normal (non-diseased) conditions, whereas, CNP is predominantly found in the central nervous system, pituitary, kidney, and vascular endothelial cells (Fowkes & McArdle, 2000). In the context of the GC-linked NPRs, NPR-A binds ANP and BNP, whereas NPR-B preferentially binds CNP (Potter *et al.*, 2006).

1.2.3.3 cGMP Signaling

cGMP has the ability to act on three main enzymes found in cardiomyocytes: PDE2, PDE3, and cGMP dependant PKG (Fischmeister *et al.*, 2005;Lohmann *et al.*,

1991), each of which can contribute to the regulation of cardiac function. It has been shown that the activation of PKG by cGMP results in a decrease in cardiac contractility due to the decrease in LTCC activity and reduction of myofilament Ca^{2+} sensitivity of these cells (Fischmeister *et al.*, 2005;Mery *et al.*, 1991;Schroder *et al.*, 2003;Layland *et al.*, 2002). Low submicromolar concentrations of cGMP increase contractility and heart rate by inhibition of PDE3 and increased cAMP levels (Mohan *et al.*, 1996;Preckel *et al.*, 1997;Vila-Petroff *et al.*, 1999); however, at higher concentrations of cGMP (5μM), the opposite occurs via the stimulation of PDE2 and a resultant decrease in cAMP (Lohmann *et al.*, 1991;Vandecasteele *et al.*, 2001). These findings demonstrate that the effects of cGMP are concentration dependant and also dependant on the level of expression, localization, and activity of PKG, PDE2, and PDE3, which may vary considerably depending on the animal model, region of the heart, and the levels of cAMP and cGMP production (basal versus stimulated).

1.3 Cyclic Nucleotide Phosphodiesterases

Cyclic nucleotide phosphodiesterases function by selectively catalyzing the hydrolysis of the 3' cyclic phosphate bond of both cAMP and cGMP to generate 5'AMP and 5'GMP, which are inactive in their respective CN signaling pathways (Beavo, 1995;Francis *et al.*, 2011). PDEs were first discovered in 1962 by Butcher and Sutherland, not long after Sutherland and colleagues had made the novel discovery of cAMP (Butcher & Sutherland, 1962). The discovery of an enzyme that could catalyze the degradation of cAMP and cGMP played an enormous role in validating the physiological importance of these second messengers. As time went on and technologies developed, it

became clear that there were multiple forms of PDEs with different kinetic and regulatory properties (Thompson *et al.*, 1979;Beavo *et al.*, 1982).

To date, 11 distinct PDE families (PDEs 1-11), which are derived from 21 genes, have been identified and classified based on their amino acid sequences, regulatory properties, and catalytic characteristics (Table 1.1) (Bender & Beavo, 2006;Beavo, 1995;Conti & Beavo, 2007;Francis *et al.*, 2001;Francis *et al.*, 2011;Maurice *et al.*, 2003). Some of these genes contain multiple promoters resulting in a myriad of splice variants (> 100 mRNA products), further contributing to their molecular diversity (Bender & Beavo, 2006;Conti & Beavo, 2007). Certain PDEs are highly specific for cAMP (PDEs 4, 7 and 8) or cGMP (PDEs 5, 6 and 9), and others hydrolyze both CNs (PDEs 1,2,3,10, and 11); isoforms within the dual specificity families can differ significantly in preference for cAMP or cGMP as occurs among PDE1 isoforms (Bender & Beavo, 2006). The diversity among their catalytic activities provides PDEs the ability to breakdown CNs over a wide range of concentrations in all cells. PDEs in a given cell type frequently vary across species, which further complicates the understanding of their function (bi-Gerges *et al.*, 2009;Dodge *et al.*, 2001). The fact that PDEs are also differentially regulated enables them to integrate and cross-talk with a myriad of signaling pathways which will be discussed in more detail in the following section. In recent years, it has been well established that PDEs are able to be targeted to discrete compartments inside the cell, where they are responsible for controlling CN levels and shaping microenvironments for a variety of CN effectors: CN dependant protein kinases (PKA and PKG), Epacs (exchange protein activated by cAMP), phosphoprotein phosphatases, and/or CN gated cation channels (Baillie, 2009;Bender & Beavo,

2006;Castro *et al.*, 2006;Conti & Beavo, 2007;Fischmeister *et al.*, 2006;Houslay, 2010;Houslay *et al.*, 2007;Jarnaess & Tasken, 2007;Leroy *et al.*, 2008;Richter *et al.*, 2008;Vandecasteele *et al.*, 2006;Zaccolo, 2009;Zaccolo & Movsesian, 2007).

Despite the fact that PDEs and their functional characteristics have been investigated for over 50 years there is still much to be learned due to the complexity of this superfamily of enzymes which continues to grow as more advanced technologies are developed. The spatial distribution and specificity of action of these PDEs in different cell types, the various levels of expression and activity, as well as knowledge of their structure and function are only some of the areas being heavily investigated. Although this study primarily focuses on understanding roles of cardiac PDEs, it still remains important to first and foremost understand these enzymes as a whole.

Table 1.1 PDE enzyme kinetic properties for PDE 1-5

Isoform	Substrate	K_m		V_{max} (purified)	
		cGMP	cAMP	cGMP	cAMP
		μM		μmol/min/mg	
PDE1A	cAMP<cGMP	2.6-3.5	72.7-124	50-300	70-450
PDE1B	cAMP<cGMP	1.2-5.9	10-24	30	10
PDE1C	cAMP=cGMP	0.6-2.2	0.3-1.1	-	-
PDE2A	cAMP=cGMP	10	30	123	120
PDE3A	cAMP>cGMP	0.02-0.15	0.18	0.34	3.0-6
PDE3B	cAMP>cGMP	0.28	0.38	2.0	8.5
PDE4A	cAMP>cGMP	-	2.9-10	-	0.58
PDE4B	cAMP>cGMP	-	1.5-4.7	-	0.13
PDE4C	cAMP>cGMP	-	1.7	-	0.31
PDE4D	cAMP>cGMP	-	1.2-5.9	-	0.03-1.56
PDE5A	cGMP>cAMP	2.9-6.2	290	1.3	1.0

Substrate specificities, which outline weather the PDE isoform preferentially hydrolyses cAMP or cGMP; K_m values, the concentration of substrate which leads to half-maximal hydrolyzing rates and V_{max}, the limiting hydrolyzing rate at higher concentrations of substrate have been outlined in the above table for PDEs 1-5. (Modified from Bender & Beavo, 2006)

1.3.1 General PDE Structure

Typically, PDEs have an NH_2-terminal regulatory domain (R domain) and a COOH-terminal catalytic domain (C domain) of ≈ 270 amino acids; however, some also contain regulatory features in the C domain such is the case for PDE4 (Bender & Beavo, 2006;Conti & Beavo, 2007;Houslay & Baillie, 2003;Omori & Kotera, 2007).

1.3.1.1 Regulatory Domain

The regulatory domain is situated between the amino terminus and the catalytic domain. This is where calmodulin binding sites for PDE1, allosteric cGMP binding sites called GAF (cGMP, adenylyl cyclase, Fh1A) domains for PDE1,PDE2, PDE5, PDE6, PDE10 and PDE11, phosphorylation sites and phosphatidic binding sites for PDE4, PAS (Per-ARNT-Sim) domain for PDE8, upstream conserved regulatory (UCR) domain for PDE4 and autoinhibitory sequences for PDE1 and PDE4 are found (Francis *et al.*, 2001;Lugnier, 2006). GAF and UCR domains are two of the major regulatory subdomains. The UCR domains directly regulate PDE4 function (Houslay & Adams, 2003;Houslay *et al.*, 2007;Richter & Conti, 2002), and interact with heterologous proteins allowing PDE4 to form protein complexes (Bjorgo *et al.*, 2010;Houslay, 2010;McCahill *et al.*, 2008). The GAF domain has also shown to serve many different functions. Similar to the UCR domain, GAF also participates in heterologous protein-proteins interactions. It also permits protein-protein interactions within PDEs causing dimerization and CN binding, allowing cGMP to bind and activate these particular PDE subtypes (Martinez *et al.*, 2002;Zoraghi *et al.*, 2004). There are other PDEs which contain other characteristic regions, enabling them to insert into the membrane. PDE3 is well known to contain two regions enabling them to accomplish this task: NHR1 and NHR2

(NH2-terminal hydrophobic regions 1 and 2). PDE3A, which lacks NHR domains is mostly cytosolic; therefore, demonstrating the importance of this regions for membrane insertion (Kenan *et al.*, 2000;Shakur *et al.*, 2000).

1.3.1.2 The Catalytic Domain

The catalytic domain is found in all PDEs and is essential for their ability to catalyze the hydrolysis of CN. There seems to be much similarity between the overall folds and functional structural elements between the PDE families (Lugnier, 2006). The similarities they demonstrate in amino acid sequence have been shown to range from 25-50% (Bender & Beavo, 2006;Omori & Kotera, 2007); however, high sequence identity does not necessarily translate into functional similarities. For example, PDE 5, 6 and 11 are among the most similar in sequence identity, but their substrate preferences, catalytic rates, and substrate affinities vary markedly (Bender & Beavo, 2006;Conti & Beavo, 2007;Omori & Kotera, 2007). Substrate preference is not always associated to similarities in crystal structure either. This has been demonstrated by the similarities between the x – ray crystallographic structures of PDE9 and PDE4, of which PDE9 is specific for cGMP and PDE4 is specific for cAMP; although they are similar structurally, their substrate specificity oppose each other (Huai *et al.*, 2004).

Other important lessons have been learned from crystal structures of the catalytic domain as well. One thing that is consistent among PDE families is that all catalytic domains contain three subdomains composed largely of 16 helices. The active site seems to be formed at the junction of theses helices by residues that are highly conserved among all of the PDEs (Bender & Beavo, 2006). Situated at the bottom of this substrate binding pocket are two divalent metal binding sites for Zn^{2+} and Mg^{2+} (Wang *et al.*, 2005;Xu *et*

al., 2000). The zinc metal binding site has two histidines and two aspartic acid residues which are conserved among all PDEs and which also form part of the CN recognition site. These residues form part of the signature recognition sequence for CN PDEs, which is itself only a piece of a larger HD (histidine/ aspartate) domain with a known phosphohydrolase activity. Therefore, these highly conserved residues are absolutely necessary for the activity of phosphodiesterases.

1.3.1.3 Cyclic Nucleotide Recognition

Now that the structure and location of the binding pocket for CNs has been established, how does this pocket recognize cAMP or cGMP and in some cases both? The proposed mechanism is that an invariant glutamine stabilizes the binding of the purine ring in the binding pocket via hydrogen bonds that form with either cAMP or cGMP, depending on the orientation of the glutamine (Zhang *et al.*, 2004). This is also known as the "glutamine switch". For this pocket to be able to bind both CNs, the glutamine must be able to rotate freely. For the PDEs, which are highly selective for a particular CN, the glutamine is held in place by neighbouring residues, not allowing it to change its position, whereas the dual specific PDEs are not restricted and can go into the proper orientation for both cAMP and cGMP.

This binding pocket is not only where CNs bind to get degraded, but it is also where selective PDE inhibitors act to block PDE activity. PDE inhibitors that are presently being used clinically are PDE5 inhibitors for the treatment of erectile dysfunction (ED) and pulmonary hypertention (Barnett & Machado, 2006;Coward & Carson, 2008;Dorsey *et al.*, 2010;Galie *et al.*, 2009), PDE3 inhibitors for the treatment of intermittent claudication and acute heart failure (Kambayashi *et al.*, 2003;Mebazaa *et al.*,

2010;Movsesian, 2000), a PDE4 inhibitor for the treatment of chronic obstructive pulmonary disease (COPD) (Hatzelmann *et al.*, 2010), as well as other non selective PDE inhibitors for the treatment of asthma and blood clotting following stroke or heart valve replacement (Burke *et al.*, 2010;Dengler *et al.*, 2010).

1.3.2 Pharmacology

As outlined in the previous section, PDE inhibitors are now being used clinically in order to improve the therapeutic treatment of various diseases and ailments. However, when using PDE inhibitors several facets of selectivity should be considered. First of all, the word specific or selective is often misused when talking about PDE inhibitors. All PDE inhibitors have some level of cross-reactivity with the other families. In order for a PDE inhibitor to be "selective" it must have at least a 30-fold and preferably greater than a 100-fold selectivity over all other PDEs to be truly called selective in an *in vitro* experiment. This means that, the IC_{50} (the concentration at which 50% inhibition occurs) if determined at a low substrate concentration, for the PDE in question should be 100 times lower than all other PDEs. If these guidelines are followed, the blocker should achieve 90% inhibition of the PDE in question and 10% or less inhibition of the other PDEs (Beavo *et al.*, 2006). There are now many widely used PDE "selective" inhibitors in experimental and in some cases clinical settings, some of these as well as their IC_{50} values are outlined in the following review (Bender & Beavo, 2006).

1.3.3 Role of PDEs in Cardiomyocyte Physiology

As described in the sections above, cAMP and cGMP influence many facets of cardiomyocyte physiology. Accordingly, changes in the activity, expression, or subcellular localization of PDEs in cardiomyocytes play a crucial role in regulating the

ability of cAMP and cGMP to modulate cardiac function. PDE1, PDE2, PDE3, PDE4 and PDE5 have been well characterized in the heart (Maurice *et al.*, 2003;Verde *et al.*, 1999;Zaccolo & Movsesian, 2007;Takimoto *et al.*, 2005b) . Each of their respective roles in CN compartmentation, as well as their ability to modulate cardiac physiology in different regions of the myocardium will be addressed in the following sections.

1.3.3.1 Phosphodiesterase 1

PDE1 is known as the $Ca^{2+/}$calmodulin PDE due to its regulatory domain, and its activation properties which are dependent on Ca^{2+}/calmodulin binding (Kakkar *et al.*, 1999;Lugnier, 2006). To date, three PDE1 genes (PDE1A, PDE1B and PDE1C) have been characterized each encoding for multiple variants with distinct hydrolyzing kinetics and Ca^{2+}/calmodulin sensitivities. PDE1A and PDE1B selectively hydrolyse cGMP with much higher affinity then cAMP, whereas PDE1C is able to hydrolyse both with equal affinities (Kakkar *et al.*, 1999).

Of these, PDE1A and PDE1C are found to be expressed in cardiac tissue isolated from several species (Kakkar *et al.*, 1999;Rybalkin *et al.*, 1997;Osadchii, 2007). PDE1A expression has been described in cardiac tissues from human (Loughney *et al.*, 1996), cow (Sonnenburg *et al.*, 1993), dog (Clapham & Wilderspin, 2001), rat (Yanaka *et al.*, 2003) and mouse (Miller *et al.*, 2009). PDE1A has been shown to regulate cardiac hypertrophy, as it was found to be upregulated in hearts and cardiomyocytes from various pathological hypertrophy models and in isolated neonatal and adult rat ventricular myocytes which were treated with angiotensin II (Ang II) (Miller *et al.*, 2009). PDE1C, on the other hand, has been found to be expressed in human cardiomyocyte localizing itself along the Z-lines and M-lines of the myofilaments (Vandeput *et al.*, 2007). PDE1C

expression was also found in mouse hearts and/or cardiomyocytes (Miller *et al.*, 2009;Lukowski *et al.*, 2010). However, contrary to PDE1A, there was no significant change in expression of PDE1C protein levels observed in a pressure overload mouse model of cardiac remodelling (Lukowski *et al.*, 2010). When PDE1 was investigated in terms of its role in modulating cardiac electrophysiology in rat ventricular myocytes by measuring $I_{Ca,L}$ following the application of the selective PDE1 blocker 8-methoxy-1-methyl-3-isobutylxanthine (MIMX) in basal conditions, no significant difference was observed in peak $I_{Ca,L}$. However, following β-adrenergic stimulation with isoproterenol a small, but significant increase was observed (Verde *et al.*, 1999).

Although the cardiac gene products of PDE1, which are found to be expressed in the heart, have been predominantly found in non myocyte fractions, such as vascular smooth muscle cells (Bode *et al.*, 1991;Rybalkin *et al.*, 1997;Rybalkin *et al.*, 2002), it is clear based on the studies mentioned above that PDE1 plays a role in cardiac myocyte physiology as well. Even though some electrophysiological effects have been observed, under pre stimulated conditions, the role of PDE1 in the heart seems to be predominantly in regulating cardiac myocyte hypertrophy and myocardial remodelling.

1.3.3.2 Phosphodiesterase 2

PDE2, identified as the cyclic GMP-stimulated PDE, was discovered in 1971 by Beavo and colleagues (Beavo *et al.*, 1971). Its family contains only a single gene (PDE2A), which codes for three different splice variants: PDE2A1(Sonnenburg *et al.*, 1991), PDE2A2 (Yang *et al.*, 1994), and PDE2A3 (Rosman *et al.*, 1997). PDE2 hydrolyses both cAMP and cGMP and is allosterically regulated by both with positive and cooperative kinetics; however, favours cGMP as a substrate and effecter (Erneux *et*

al., 1981). This is demonstrated by the change in the rate of cAMP hydrolysis observed in the presence of low concentrations of cGMP, which was shown to be increased by 2-6-fold (Martins *et al.*, 1982;Muller *et al.*, 1992).

Two GAF (GAF-A and GAF-B) domains are present on the N-terminal regions of PDE2, and each is believed to play different roles in dimerization and in cGMP binding of this enzyme (Martinez *et al.*, 2002). GAF-B is thought to be responsible for the binding of cGMP and activating the catalytic properties of the enzyme (Wu *et al.*, 2004); therefore, this becomes of great interests for CN signaling in tissues expressing PDE2 and in which rapid changes in CN levels have been observed, such as the heart.

One PDE2 variant, PDE2A2, has been found in both atrial and ventricular myocytes in various species from frog to human (Osadchii, 2007). PDE2 is the most abundant PDE subtype expressed in frog myocardium, whereas in the rat it only accounts for 3% of the total cAMP-hyrolyzing activity, demonstrating the potential for species variability (Lugnier *et al.*, 1992;Mongillo *et al.*, 2006). In terms of its localization within the cell, it is found in both the cytosol and associated with membrane structures such as the plasma membrane, sarcoplasmic reticulum, golgi apparatus and nuclear envelope (Lugnier, 2006). Although in most species, PDE2 activity is relatively small compared to other cardiac PDEs such as PDE3 and PDE4, its presence in the plasma membrane enables it to contribute to the modulation of LTCCs when cGMP is present (Fischmeister *et al.*, 2005). The first studies to demonstrate this were done by Fischmeister and Harztell in the late 1980s whereby using frog ventricular myocytes they were able to show that PDE2 is able to hydrolize cAMP and reduce $I_{Ca,L}$ upon application of cGMP, even though the cell was being dialysed with >5μmol/L cAMP via the patch pipette (Hartzell &

Fischmeister, 1986;Fischmeister & Hartzell, 1987). The information involving PDE2 and its ability to contribute to the regulation of cardiac function was facilitated by the discovery that erythro-9-(2-hyroxy-3-nonyl) adenine (EHNA) behaved as a selective PDE2 inhibitor (Mery *et al.*, 1995;Podzuweit *et al.*, 1995). This helped further understand the physiological implications of the cross-talk between the cAMP and cGMP signaling pathways being mediated through PDE2.

It was shown in experiments using frog ventricular and human atrial myocytes, that application of high concentrations of cGMP or NO donors result in a significant decrease in $I_{Ca,L}$; however, when the PDE2 blocker EHNA was subsequently applied this effect was rescued. These experiments clearly demonstrate that these effects were being mediated by PDE2 and its ability to hydrolyse cAMP (Mery *et al.*, 1995;Kirstein *et al.*, 1995;Vandecasteele *et al.*, 2001). Furthermore, EHNA was also able to result in a significant increase in $I_{Ca,L}$ in human atrial myocytes under basal conditions, which may suggest a higher constitutively active guanylyl cyclase in these cells (Rivet-Bastide *et al.*, 1997). This effect was attributed to a cGMP dependant inhibition of PDE3, which will be discussed in the following section. In rabbit sinoatrial node (SAN) myocytes, it was shown that heart rate was negatively affected by the application of NO, partially due to inhibition of $I_{Ca,L}$ via a signaling pathway involving cGMP and its association with PDE2 (Han *et al.*, 1998).

PDE2 has also been shown to make a significant contribution to the compartmentation and regulation of β-adrenergic signaling. Experiments conducted by Mongillo and colleagues (Mongillo *et al.*, 2006) have found that this control is mediated partially via the stimulation of β_3-ARs, which in turn activate eNOS. This activation

results in NO stimulation of sGC and increased cGMP levels, which activate PDE2 and its ability to increase cAMP hydrolyzing activity (Mongillo *et al.*, 2006). It is also important to remember; however, that PDE2 also hydrolyses cGMP as well, and in fact contributes to its compartmentation. Recent studies have shown that PDE2 is in fact exclusively responsible for regulating the particulate pool of cGMP. These experiments were performed in rat ventricular myocytes using the cyclic nucleotide gated channel (CNG) technique, whereby rat olfactory CNG channel α-subunits are expressed in the sarcolemmal membrane and changes in subsarcolemmal concentrations of cGMP are monitored by changes in associated cGMP gated current (I_{CNG}). This study compared the effects of activators of pGC (ANP and BNP) and sGC (NO donors) on subsarcolemmal concentrations of cGMP (Castro *et al.*, 2006). By doing so, they were able to determine that the particulate cGMP pool is readily accessible at the plasma membrane, whereas the soluble pool is not. Using PDE selective blockers they were also able to show that PDE5 controls the soluble but not the particulate pool of cGMP, whereas the particulate pool is under the exclusive control of PDE2; therefore, it is clear that different spatiotemporal distributions of cGMP may contribute to the specific effects of natriuretic peptides and NO donors on cardiac function.

Thus, PDE2 is not only a key player in controlling intracellular levels of CN and their compartmentation within the cells, but they are also able to modulate myocardial electrophysiology by specifically localizing themselves in particular regions involved in these processes. Therefore, PDE2 and its ability to affect atrial electrophysiology in the murine model need to be further investigated.

1.3.3.3 Phosphodiesterase 3

PDE3 has probably been the most characterized out of the cardiac PDEs when it comes to the human heart, as pharmacological agents which specifically inhibit this family have been used for treatment of heart failure for over two decades (Zaccolo & Movsesian, 2007).

The PDE3 family consists of 2 genes (PDE3A and B), each containing multiple splice variants. PDE3, similar to PDE2, is able to hydrolyse both cAMP and cGMP with K_m values in submicromolar ranges (K_m cGMP ~ 0.2μM; K_m cAMP ~ 0.1μM); however, PDE3 hydrolyses cAMP at a 10-fold higher rate than cGMP (Lugnier, 2006). Therefore, PDE3 is often called the cGMP inhibited cAMP hydrolyzing PDE (Beavo, 1995). PDE3 contains two regions in the regulatory domain which help with the localization of this enzyme within the cell, called NHR1 and NHR2. These two regions differ in the fact that NHR1 consists of hydrophobic loops that insert into intracellular membranes and NHR2 appears to localize the enzyme through protein-protein interactions (Kenan *et al.*, 2000;Shakur *et al.*, 2000). PDE3 is also regulated by PKB and PKA mediated phosphorylation, increasing its activity (Han *et al.*, 2006).

Both PDE3A and PDE3B have been found to be expressed in the heart. In the human heart, 3 isoforms which are generated by the PDE3A gene have been identified. These differ in the length of their N-terminal sequence; therefore, making their localization within the cell different from each other. The PDE3A1 isoform is located exclusively in the microsomal fraction of human myocardium, because it contains both NHR1 and 2 in the N-terminal domain (Kenan *et al.*, 2000;Shakur *et al.*, 2000). The PDE3A2 isoform is found in both in microsomal and cytosolic fraction, because it is

without the NHR1 domain. It is also thought to lack the PKB binding; however, maintains the PKA sites. The last isoform, PDE3A3, lacks both NHR1 and 2 domains resulting in a primarily cytosolic distribution, and is also missing all phosphorylation sites (Hambleton *et al.*, 2005). In the mouse, both PDE3A and PDE3B have been found to be expressed in equal amounts when analyzing whole heart preparations (Patrucco *et al.*, 2004); however, PDE3A is the most abundant form found in cardiomyocytes, whereas PDE3B is almost exclusively found in vascular smooth muscle of the heart (Movsesian, 2002;Maurice *et al.*, 2003).

Pharmacological inhibition of PDE3 activity has been associated with increases in $I_{Ca,L}$ in various species, an effect contributing to the positive inotropic effects of these inhibitors. In human atrial myocytes application of milrinone, a PDE3 selective blocker, significantly increased $I_{Ca,L}$ under basal conditions similar to that seen under the presence of isoproterenol (ISO) a β-adrenergic agonist (Kirstein *et al.*, 1995). Significant increases in $I_{Ca,L}$ have been observed in human ventricular myocytes as well (Li *et al.*, 1994). In rat ventricular myocytes; however, PDE3 inhibition under basal condition was unable to increase $I_{Ca,L}$, but was able to do so in cells pre stimulated with ISO or when inhibited in conjunction with PDE4 (Verde *et al.*, 1999). The inability of PDE3 specific block to elicit changes in $I_{Ca,L}$ in basal conditions was also observed in mouse ventricular myocytes (Kerfant *et al.*, 2007).These differences suggest species and regional difference in the role of PDE3 as a regulator of CNs and ion channel function.

As mentioned above, PDE3 is also called the cGMP inhibited PDE due to its higher affinity but lower hydrolyzing rate for cGMP. This gives PDE3 the ability to participate in both the cAMP and cGMP dependant pathways, resulting in much cross-

talk between PDE3 and PDE2. This property of PDE3 accounts for the stimulatory effects of low concentrations of cGMP on $I_{Ca,L}$ in human atrial myocytes (Kirstein *et al.*, 1995;Vandecasteele *et al.*, 2001),whereas at higher concentrations, PDE2 activity dominates resulting in the hydrolysis of cAMP rather than its increase. Therefore two different effects can be seen in the same pathway depending on the concentration of cGMP.

Although pharmacological inhibition of PDE3 showed beneficial hemodynamic and contractile effects in individuals with heart failure in the early phases of trials, further analysis of these patients showed that these beneficial effects were often short lived. Increased mortality associated with arrhythmias and sudden cardiac death (SCD) was observed in many clinical trials (Movsesian & Alharethi, 2002;DiBianco *et al.*, 1989). The further deterioration and worsening of heart failure conditions after chronic inhibition of PDE3 is thought be mediated by PDE3s association to the proapoptotic transcriptional repressor ICER (Inducible Cyclic AMP Early Repressor). Studies done using isolated cardiomyocytes have shown that chronic inhibition of PDE3 results in a significant increase in cardiac apoptosis similar to that observed after chronic β-AR or angiotensin II stimulation (Ding *et al.*, 2005a;Ding *et al.*, 2005b). When ICER levels become elevated, it represses antiapoptotic proteins such as Bcl-2 and the PDE3A gene itself, thus creating a positive feedback loop further decreasing PDE3 levels and increasing ICER levels (Yan *et al.*, 2007).

In summary, PDE3 plays a major role in the heart, especially in humans, as it is able to not only regulate second messengers and their ability to modulate cardiac ion channel activity but control the development and progression of heart failure at the level

of transcription. However, there seems to be some degree of variability in terms of its contribution to regulation of $I_{Ca,L}$ .This difference seems to be both species and region dependant and warrants further investigation.

1.3.3.4 Phosphodiesterase 4

The PDE4 family, formerly known as the cAMP-PDE for its high affinity for cAMP and insensitivity for cGMP, is the largest of the 11 families of PDEs. It consists of 4 genes (PDE4A, PDE4B, PDE4C, and PDE4D), each with multiple mRNA products encoding both long and short forms of PDE4, which form a group of at least 35 isoforms (Lugnier, 2006).

As its former name states, PDE4 is a cAMP specific PDE (Km ~ 2-4μM), which similarly to the other families contains a unique signature region in its amino acid sequence. Contrary to having a Ca^{2+}/calmodulin, GAF or NHR1/2 domains, PDE4 contains a region called upstream conserved regulatory (UCR1 and UCR2) domain (Bolger *et al.*, 1993), which are located between the end of the N-terminal tail and the beginning of the catalytic domain. The long form of the PDE4 protein contains both conserved regions, whereas the short version only contains the UCR2 domain (Houslay *et al.*, 1998).

In terms of its regulation, PDE4 activity is increased upon phosphorylation. This is due to the fact that PDE4 contains an acceptor site in the UCR1 domain for PKA-mediated phosphorylation. This was demonstrated when PDE4 activity rose after cAMP levels increased subsequent to the application of forskolin, an AC activator (MacKenzie *et al.*, 2002). Located on the C-terminal side of the catalytic region, is another phosphorylation site sensitive to extracellular signal-regulated kinase (ERK).

Phosphorylation of PDE4 by ERK has been associated with the activation of PDE4D short form, but inhibition of the long forms (MacKenzie *et al.*, 2000).

In the heart, PDE4A, PDE4B and PDE4D have been found to be expressed in human, mouse and rat (Richter *et al.*, 2010). These genes and their respective protein products seem to be localized to defined compartments of the cell, regulating particular sets of intracellular signaling processes associated to increases in cAMP (Houslay & Adams, 2003). This specificity is highly associated to the uniqueness of each of their N-terminal domains, which target these isoforms to their specific subcellular locations (Baillie & Houslay, 2005). PDE4A, for example, can be targeted to specific cellular membranes because it contains a specific lipid binding domain called TAPAS (Baillie *et al.*, 2002). PDE4D, on the other hand, is targeted to sarcomeric regions, through its ability to bind to an anchor protein called myomegalin, as well as to the perinuclear region via its association to muscle A-kinase anchoring protein (mAKAP) (Verde *et al.*, 2001;Dodge *et al.*, 2001).What is interesting about mAKAP is that it is able to bind a plethora of proteins enabling certain PDE4 isoforms to form macromolecular complexes serving multiple functions in the same distinct compartment.

This is the case for PDE4D and its association with the RYR/Ca^{2+} release channel complex situated at the SR membrane (Lehnart *et al.*, 2005). This complex also contains PKA, FKBP12.6 (calstabin 2, a negative modulator of the RyR), and the protein phosphotases PP1 and PP2A (Marx *et al.*, 2000;Wehrens *et al.*, 2005). This particular complex has been associated to arrhythmias observed in heart failure patients, which is usually associated to the hyperphosphorylation of the RyR, making these channels "leaky" (Wehrens *et al.*, 2005). This is thought to be due to decreased PDE4D activity

which is observed in human failing hearts and has been tested using the genetic inactivation of this protein in mice (Lehnart *et al.*, 2005). Other protein complexes that PDE4 has been associated with are β-arrestins, a scaffolding protein that initiates the internalization of β_2-AR at the sarcolemmal membrane; and PI3Kγ, which localizes PDE4 near phospholamban regulating its phosphorylation. Hence, changes in SR Ca^{2+} ATPase activity resulting in changes in both Ca^{2+} transients and SR Ca^{2+} content (Perry *et al.*, 2002;Bolger *et al.*, 2003;Kerfant *et al.*, 2007).

Selective block of PDE4 in mouse and rat ventricular myocytes resulted in no significant increase in $I_{Ca,L}$ under basal conditions (Verde *et al.*, 1999;Kerfant *et al.*, 2007). However, in cells pre-stimulated with a submaximal concentration of ISO, PDE4 inhibition did result in a significant increase, suggesting that the lack of effect in basal conditions is related to cAMP threshold (Verde *et al.*, 1999). PDE4 inhibition only seems to increase $I_{Ca,L}$ in ventricular myocytes under basal conditions when blocked in combination with PDE3 (Verde *et al.*, 1999), which seems to be consistent with kinetic properties of PDE3 and PDE4 isoforms by which PDE3 K_m values for cAMP are 10 fold lower (Osadchii, 2007).

The information discussed above illustrates that PDE4 plays a major role in regulating the function and activity of multiple proteins found within isolated cardiomyocytes, by regulating the levels of cAMP and PKA phosphorylation in these distinct compartments of the cell. However, PDE4 does not regulate $I_{Ca,L}$ under basal conditions in ventricular myocytes. Investigating the electrophysiological role of PDE4 in the atrial myocardium will hopefully help us understand the different effects observed in ventricular myocytes: ISO pre-stimulated conditions verses basal, as well those in which

PDE4 was blocked in combination with PDE3.These differences are potentially associated to species variability, PDE4 protein expression levels or simply due to differences in cAMP threshold.

1.3.3.5 Phosphodiesterase 5

PDE5, which was previously named the cGMP-PDE, due to its selectivity for cGMP is encoded by a single gene (PDE5A) which has three protein products (PDE5A1-3) (Omori & Kotera, 2007). Similarly to PDE2, PDE5 contains two GAF domains (GAF A and GAF B) in its regulatory domain, in which GAF A has been associated to the allosteric binding of cGMP (Liu *et al.*, 2002). There are also two phosphorylation sites in the N-terminal region, one for PKA and the other for PKG, which are related to activation of the PDE5A enzyme (Corbin *et al.*, 2000). The binding of cGMP to the GAF A domain promotes this phosphorylation, which not only increases catalytic function but the binding affinity of cGMP as well (Zoraghi *et al.*, 2005;Francis *et al.*, 2002).

PDE5 has mostly been found to be expressed in vascular smooth muscle, and although its contribution to cardiac function had been debated (Maurice *et al.*, 2003;Semigran, 2005;Takimoto *et al.*, 2005b), there is still evidence demonstrating its presence in cardiac myocytes at both the mRNA (Kotera *et al.*, 1998) and protein levels (Senzaki *et al.*, 2001;Takimoto *et al.*, 2005a). Recently, it was shown that PDE5 inhibition is able to decrease the β-adrenergic stimulation of cardiac systolic and diastolic function in dog (Senzaki *et al.*, 2001), mouse (Takimoto *et al.*, 2005a), and human (Borlaug *et al.*, 2005), as well as the β-AR stimulated $I_{Ca,L}$ in guinea pig ventricular myocytes (Ziolo *et al.*, 2003) and mouse ventricular myocytes via a NOS3 dependant pathway (Wang *et al.*, 2009) . These studies demonstrate that PDE5 is not only expressed

in the heart but is functional as well. PDE5 inhibition has also been associated to the block of the apoptotic pathways in mouse ventricular myocytes (Das *et al.*, 2005), and the reversal of cardiac hypertrophy in mouse heart exposed to sustained pressure overload (Takimoto *et al.*, 2005b).

PDE5, similarly to other PDEs, is found to regulate CN compartmentation in cardiac myocytes (Castro *et al.*, 2006;Castro *et al.*, 2010). Using the I_{CNG} channel approach in rat ventricular myocytes, Castro and colleagues were able to demonstrate that PDE5 regulates intracellular cGMP synthesized by NO donors; however, it had no control over the current generated upon application of ANP. This suggest that PDE5 is able to controls pools of cGMP generated by sGC but not those generated by pGC, which as mentioned earlier are under the exclusive control of PDE2 (Castro *et al.*, 2006). Based on the studies outlined above, it is clear that although initially PDE5 was thought to only be expressed in vascular smooth muscle, it still plays a role in cardiac myocytes as a mediator of NO effects.

1.4 The Cardiac Action Potential

As can be deduced from the above sections, PDEs are not only able to ensure regulation and compartmentation of CNs in specific microdomains within the cell, but the inhibition of these PDEs has been associated with changes in cardiac ion channel activity also. For this particular study, investigating the ion channels involved in atrial electrophysiology are of interest since the role of PDE specific subtypes in modulating this regions electrophysiology is in question. The mouse atrial AP is generated by multiple ion channels (Figure 1.1). Phase 0 of the atrial AP, is the fast depolarization phase. This phase is due to the activation of the fast inward Na^+ current (I_{Na}), which

results in membrane potential depolarization from resting which is usually situated between -70mV and -80mV. The process by which atrial cells return from their depolarized state to the resting state is known as repolarization, and depends on a series of time-dependent outward K^+ currents (Nattel, 2003). This repolarization begins with phase 1 which is the result of the activation of fast, transient outward K^+ currents ($I_{to,\,f}$). In the atrial action potential phase 2 and 3, which form the bulk of membrane repolarization, are combined. There is no distinct plateau phase (phase 2), as is observed in ventricular APs. Currents involved in phase 2 and 3 are the inward L-type Ca^{2+} current ($I_{Ca,L}$), the rapidly activating slowly inactivating outward K^+ current ($I_{K,Slow}$), the rapidly activating outward K^+ current (I_{Kur}), and the non inactivating steady state current (I_{ss}) (Nerbonne & Kass, 2005;Bou-Abboud *et al.*, 2000). Following these two phases, resting membrane potential has usually been reached, which is phase 4 of the action potential and is maintained by the inwardly rectifying K^+ current (I_{K1}) (Nerbonne & Kass, 2005).

Therefore, examining APs can help isolate what cardiac channels may be regulated by changes in CN levels. This can be done by analysing different parameters of the AP, such as peak AP amplitude, resting membrane potential (RMP), rate of depolarization (V_{max}) and different phases of AP repolarization: AP duration at 50%, 70% and 90% repolarization times (APD50, APD70 and APD90).

1.5 L-Type Calcium Channels

Based on the fact that subtype specific PDE inhibition has already been shown to modulate $I_{Ca,L}$ in isolated cardiac myocytes, a more detailed review on these particular channels is warranted. Not only is L-type Ca^{2+} current involved in the generation of the APs but it is crucial in the phenomenon known as E-C coupling which is induced by

CICR (Bers, 2002). L-type Ca^{2+} channels, which are members of the voltage gated ion channel family are heteromultimeric complexes consisting of multiple subunits: α1-subunit, a disulfide-linked complex of α2- and δ -subunits, and an intracellular β- and γ-subunit, in which the α1-subunit is responsible for forming the channel pore, the voltage sensor, gating apparatus, and contain the known sites of channel regulation by second messengers, drugs, and toxins (Catterall, 1995; Walker & Waard, 1998).

Two isoforms of the L-type Ca^{2+} channel are expressed in the heart, the Ca_v 1.2 (α_{1C}) and the Ca_v 1.3 (α_{1D}) forms. The Ca_v 1.2 α subunit is the predominant molecular determinant of the $I_{Ca,L}$ in ventricular myocytes. This subunit is also expressed in the purkinje fibers, the atria, the atrioventricualr node (AVN) and the SAN regions of the heart (Mangoni & Nargeot, 2008). The Ca_v 1.3 α subunit, on the other hand, is only expressed in the supraventricular region, contributing to the L-type Ca^{2+} currents generated in isolated atrial, AVN and SAN myocytes (Zhang *et al.*, 2002; Zhang *et al*., 2005). This results in the activation of these channels at more negative potentials in comparison to the kinetics observed in ventricular myocytes. This was demonstrated in experiments conducted in both isolated atrial and SAN myocytes, where it was shown that by knocking out the Cav 1.3 gene, membrane potentials at which half the channels were activated ($V_{1/2}$) were significantly shifted in the positive direction (Zhang *et al.*, 2002; Zhang *et al*., 2005).

As mentioned above, these channels can be modulated by secondary messengers. To be more specific, their open probabilities are increased by cAMP- dependant PKA phosphorylation (Bers, 2002). Since PDEs are critical regulators of intracellular cAMP, the L-type Ca^{2+}current serves as a valuable functional parameter for measuring the

potential electrophysiological effects of subtype specific PDE inhibitors in mouse right atrial myocytes.

1.6 Study Motivation

As mentioned in the introduction, our lab is studying the electrophysiological effects of natriuretic peptides in the heart, and we have recently discovered that natriuretic peptides are able to modulate $I_{Ca,L}$ in the atrial region of the myocardium by modulating cGMP-dependant PDEs leading to a change in intracellular cAMP (unpublished data). Although cardiac PDEs and their respective roles in modulating cardiac electrophysiology in the ventricular region of the myocardium have been extensively studied, very little has been done to characterize their roles in the atrial myocardium in mice. Due to the fact that NPs are able to modulate intracellular cGMP levels within the cell, it was important to investigate the role of the specific PDE subtypes that are regulated by this CN, PDE2 and PDE3 in particular. PDE5, also regulated by and able to hydrolyse cGMP, was not investigated because this particular PDE is primarily responsible for the regulation of cGMP generated by NO downstream of sGC, not pGC as is the case for NPs. Even though PDE4 has no association to cGMP, it was important to investigate the role of this PDE as well and its ability to modulate atrial electrophysiology because of the enormous role it has in regulating intracellular cAMP and its downstream effectors, which are also highly involved in modulating cardiac electrical activity (Nikolaev *et al.*, 2006). Finally, PDE1, which is also highly expressed in the heart, seems to play more of a prominent role in regulating cardiac myocyte hypertrophy and myocardial remodelling in comparison to electrical activity and was not investigated. Therefore, the purpose of this study was to characterize the respective roles

of PDE2, PDE3 and PDE4 and their ability to modulate atrial electrophysiology by using PDE subtype selective blockers on mouse right atrial myocytes.

1) First, the effects of isoproterenol (ISO), a β-adrenergic agonist, IBMX (a broad spectrum PDE inhibitor) and PDE selective blockers for PDE2 (EHNA), PDE3 (milrinone) and PDE4 (rolipram) as well as a combinations of PDE blocker (milrinone+rolipram and EHNA+milrinone+rolipram) were tested on atrial APs. AP peak amplitude, maximum rate of depolarization (V_{max}), resting membrane potential (RMP), as well as AP duration at 50%, 70% and 90% repolarization times (APD50, APD70 and APD90) were analyzed.

2) Second, based on previous publications demonstrating the ability of PDEs to modulate $I_{Ca,L}$ in isolated cardiac myocytes, as well as the known sensitivity of this critical current to cAMP/PKA levels, $I_{Ca,L}$ was recorded under the same pharmacological conditions as used for AP measurements. These experiments provide novel insight into the contributions of specific PDEs to the regulation of atrial myocyte electrophysiology.

Figure 1.1. A schematic representation of the mouse atrial action potential and the membrane currents that generate it. A: Resting (4), upstroke (0), early repolarization/indistinguishable plateau (1&2) and late repolarization (3) are the five phases of the mouse atrial action potential. Phase 2, is much more distinct in the ventricular myocardium as mentioned in section 1.4. The inward currents, I_{Na} and $I_{Ca,L,}$ and outward currents, I_{K1}, $I_{to,f}$, I_{Kur}, $I_{K,Slow}$ and I_{ss}, are labelled with downward and upwards arrows respectively.

A

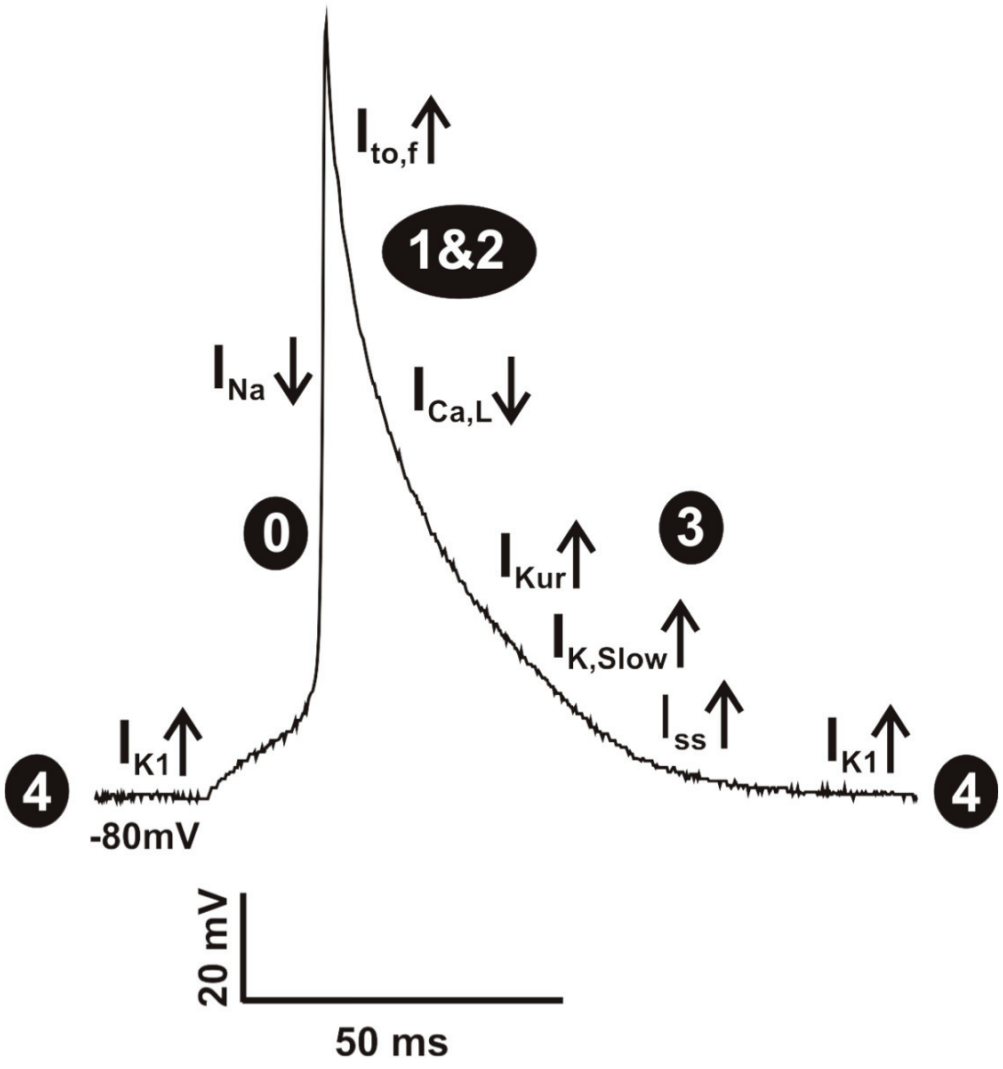

CHAPTER 2: MATERIALS AND METHODS

2.1 Animals

In the present study only male wildtype C57BL6 mice between the ages of 9-12 weeks were used. All experimental procedures were in accordance with the regulations of The Canadian Council on Animal Care and Dalhousie Animal Care Committee.

2.2 Isolation of Mouse Right Atrial Myocytes

The procedures for isolating working right atrial myocytes from the mouse have been described previously (Lomax *et al.*, 2003) and were as follows. Mice were administered a 0.2 ml intraperitoneal injection of heparin (1000IU/ml) to prevent blood clotting and given 5 min for it to be absorbed. Following this, mice were anaesthetized with isoflurane and killed by cervical dislocation. The heart was then excised and transferred to a dissecting dish where the right atrial appendage was isolated from the remaining supraventricular structures. This was done in Tyrode's solution consisting of (in mmol/L): 140 NaCl, 5.4 KCl, 1.0 $MgCl_2$, 1.8 $CaCl_2$, 5 HEPES, 1.2 KH_2PO_4 and 5.5 D-glucose, warmed to 35°C; pH was adjusted to 7.4 by the addition of NaOH. The right atrial appendage was then transferred to a second dissecting dish, containing the same Tyrode's solution, where it was pinned open and cut into 8-10 strips. The strips were then transferred via a modified pasteur pipette to a 5ml tube containing 2.5ml of a low Ca^{2+} - Mg^{2+} free solution consisting of (in mmol/L): 140 NaCl, 5.4 KCl, 0.07 $CaCl_2$, 1.2 KH_2PO_4, 50 taurine, 18.5 D-glucose, 5 HEPES and 1 mg/ml bovine serum albumin (BSA); pH was adjusted to 6.9 by the addition of NaOH. After three washes in this 'low Ca^{2+}, Mg^{2+} free' solution, the tissue was transferred to a 10ml tube containing 5 ml of the same solution to undergo enzymatic digestion by the addition of 3.8 mg of collagenase

(type II,Worthington; 280 U/mg), 75 µl of elastase (Worthington; 4.5 U/mgP), and 65.2 µl of 1mg/100 µl protease solution (type XIV, Sigma; 4.3 U/mg). Enzymatic digestion took place for 30 min at 35°C, with manual agitation of the tube every 5 min. Tissue strips were then washed three times in a modified Kraftbrühe solution consisting of (in mmol/L): 100 K^+ glutamate, 10 K^+ aspartate, 25 KCl, 10 KH_2PO_4, 2 $MgSO_4$, 20 taurine, 5 creatine base, 0.5 EGTA, 5 HEPES, 20 D-glucose, and 1 mg/ml BSA (pH adjusted to 7.2 with KOH). After this washing procedure, the tissue was mechanically agitated (triturated) using a wide-bore pipette in order to isolate working right atrial myocytes. Aliquots of this cell suspension were monitored by using a phase-contrast microscope (Nikon ECLIPSE TE300) as trituration progressed. Trituration was continued until an acceptable yield (~100-200) of single right atrial myocytes was achieved, usually within 10 min. The myocytes were then left to sit for one hour at room temperature after the addition of an extra 3.5ml of Kraftbrühe solution and then used in electrophysiology experiments.

2.3 Drugs

Isoproterenol (Iso; 1µM) was used as a β-adrenergic receptor agonist in order to stimulate adenelyl cyclase activity and increase intracellular cAMP levels (Verde *et al.*, 1999). *Erythro*-9-[2-hydroxy-3-nonly]adenine (EHNA; 10µM) was used to selectively inhibit PDE2 (Castro *et al.*, 2006), milrinone (MIL; 10µM) was used to selectively inhibit PDE3 (Maurice *et al.*, 2003), and rolipram (ROL; 10µM) was used to selectively inhibit PDE4 (Maurice *et al.*, 2003) in these experiments. The concentrations for half maximal inhibition (IC_{50}) of PDE2, PDE3 and PDE4 by each of these selective inhibitors are 1µmol/L for EHNA, 0.15µmol/L for MIL, and 1µmol/L for ROL, and each compound

has no effects on other PDE subtypes at the concentrations of 10μmol/L used in these experiments (Beavo, 1995;Lugnier, 2006;Fischmeister & Hartzell, 1991). IsoButyl-Methyl-Xanthine (IBMX; 100μM), which is a broad spectrum PDE inhibitor (IC_{50} 2-50μM) was also used in some experiments in order to inhibit all PDE activity (Verde *et al.*, 1999). IBMX, EHNA, milrinone and rolipram were all prepared as stock solutions in dimethyl sulfoxide (DMSO) in which the final concentration was 0.01%. Each compound was then aliquoted into 25μL tubes and stored at -80°C for future use. Drugs were dissolved in Tyrode's solution during experiments to attain required concentration. All pharmacological compounds were obtained from Sigma Chemical Company.

2.4 Electrophysiology

Micropipettes used for recording APs and $I_{Ca,L}$ were pulled from borosilicate glass (with filament, 1.5 mm OD, 0.75 mm ID, Sutter Instrument Company) using a Flaming/Brown pipette puller (model P-97, Sutter Instrument Company). The resistance of these pipettes was between 5-8MΩ when filled with recording solution. Micropipettes were positioned with a micromanipulator (Burleigh PCS-5000 system) mounted on the stage of an inverted microscope (Nikon ECLIPSE TE300). Seal resistance was between 2-10GΩ.

2.4.1 Action Potential Recordings

APs were recorded using the perforated patch-clamp technique as previously described (Rae *et al.*, 1991). An aliquot of cell suspension from the right atrium was first allowed to settle for 15 min in a 35-mm petri dish that was mounted on the stage of the Nikon ECLIPSE TE300 inverted microscope. After settling, the recording chamber was superfused at a flow rate of 2.0 ml/min with normal Tyrode's solution (22-23°C)

containing (in mmol/L): 140 NaCl, 5.4 KCl, 1 $CaCl_2$, 1 $MgCl_2$, 10 HEPES, and 5.5 D-glucose (pH adjusted to7.4 with NaOH). The pipette filling solution contained (in mmol/L): 140 KCl, 5 NaCl, 0.2 $CaCl_2$, 5 EGTA, 4 Mg-ATP, 1 $MgCl_2$, 10 HEPES, 6.6 Na-phosphocreatine, and 0.3 Na-GTP. pH was adjusted to 7.2 by the addition of KOH. Amphotericin B (200μg/ml) was added to this pipette solution to record APs with the perforated patch clamp technique.

To record APs using the perforated patch-clamp technique gigaseals were achieved and access resistance (Ra) was monitored for the development of capacitative transients. Typically, access resistance became less than 40 MΩ within 10 min of sealing onto the cell, which is sufficient for recoding APs in current clamp mode (Rose *et al.*, 2007).

APs were recorded in response to 0.04-0.08 nA depolarization pulses lasting 20 ms every 5 seconds using the Axopatch 200B amplifier (Molecular Devices) in current clamp mode. Action potentials were recorded under control conditions for 1-2 min. After stable control action potentials had been acquired, cells were superfused with Tyrode's solution containing drugs at the concentrations listed in section 2.3. The drug containing solution was superfused into the recording chamber for 5 minutes or until the effect had reached a plateau. This was then followed by a washout phase usually in the range of 10-20 min depending on the drug(s). Several AP parameters were analyzed. These included the AP duration at 50%, 70% and 90% repolarization times (APD50, APD70 and APD 90 respectively), AP peak amplitude, the maximum rate of depolarization (V_{max}) and the resting membrane potential (RMP).

2.4.2 Calcium Current Recordings

$I_{Ca,L}$ was measured by voltage clamping single right atrial myocytes using the patch-clamp technique in the whole cell configuration (Hamill *et al.*, 1981). Cell suspensions for $I_{Ca,L}$, were superfused with a sodium free Tyrode's solution (22-23°C, 2.0 ml/min) containing the following (in mmol/L): 140 CsCl, 5.4 TEA-Cl, 3 $CaCl_2$, 1 $MgCl_2$, 10 HEPES, and 5.5 D-glucose (pH adjusted to7.4 with CsOH). The pipette solution for $I_{Ca,L}$ contained in (mmol/L): 135 CsCl, 5 NaCl, 0.2 $CaCl_2$, 5 EGTA, 4 Mg-ATP, 1 $MgCl_2$, 10 HEPES, 6.6 Na-phosphocreatine, 0.3 Na-GTP (pH adjusted to 7.2 with CsOH). Inclusion of 5 mmol/L EGTA in the pipette solution is able to reduce the $[Ca^{2+}]_i$ to subnanomolar levels (Kerfant *et al.*, 2007). This allows us to record $I_{Ca,L}$ without having to worry about Ca^{2+} transients, which can strongly affect $I_{Ca,L}$ amplitudes and decay rates.

$I_{Ca,L}$ was recorded in the whole cell configuration. Rupturing the sarcolemma in the patch for voltage clamp experiments resulted in access resistances of 5-20 MΩ. After gaining access to the cell and allowing it to stabilize, access resistance, capacitance (Cm) and seal were recorded before beginning experiments to ensure that any changes in the current amplitude were due to the drug and not due to the condition of the cell over the course of the recording. Subsequently, series resistance was electronically compensated by 80-85% using the Axopatch 200B amplifier (Molecular Devices).

After gaining access to the cell and compensating for series resistance, $I_{Ca,L}$ was recorded by continuously stimulating myocytes every 5 seconds with a 250-ms voltage step to 0 mV after applying a 200-ms prepulse step to -60 mV from a holding potential of -80 mV. The myocytes were continuously superfused with external bath solution during this time. This latter protocol was used for all time course experiments. $I_{Ca,L}$ current-

voltage (I-V) relationships were measured by recording $I_{Ca,L}$ in response to 250-ms depolarizing steps ranging between voltage steps to -60 and +60 mV after a 200-ms prepulse step to -60 mV from a holding potential of -80 mV. Both time course and I-V relation voltage clamp protocols were used to measure drug effects on $I_{Ca,L}$. Drugs were applied for 5 min or until the drug effect had reached a plateau. Once the recordings were complete the compensation was turned off and the values for the Ra and seal where recorded for any changes. If the seal had been lost or the Ra had changed by >20% over the course of the experiment, the cell was discarded.

$I_{Ca,L}$ (I-V) relationships were determined by plotting the peak of the $I_{Ca,L}$ as a function of the step depolarization (i.e. peak $I_{Ca,L}$-V). $I_{Ca,L}$ activation kinetics were determined by calculating cord conductance (G) with the equation G=peak $I_{Ca,L}/(V_m-E_{rev})$ where V_m represents the depolarizing voltages and E_{rev} is the apparent reversal potential estimated from the I-V relationship. The maximal conductance (G_{max}), the voltage at which 50% activation occurs ($V_{1/2}$) and the slope factor (k) were obtained by fitting conductance to the Boltzman function: $A_1 = G$, $A_2 = Gmax$, $x = V_m$, $x_0 = V_{1/2}$ and dx = slope (k).

$$y = \frac{A_1 - A_2}{1 + e^{(x - x_0 / dx)}} + A_2$$

All electrophysiological recordings were performed using an Axopatch 200 B patch clamp amplifier which was linked to a Digidata 1440A data-acquisition system that was driven by Clampex version 10.2 software (all from Molecular Devices). All data

acquired over the course of this study was saved to the computer hard drive and filed for post experiment analysis. This analysis was done using pCLAMP software (Molecular Devices) and Origin 6.0 (Microcal Software).

2.5 Statistical Analysis

The data are presented as means ± SEM. The data were analyzed using an ANOVA with Dunn's multiple comparison procedure or paired Student's *t*-tests, as appropriate, to identify the significant differences. In all instances, $P<0.05$ was considered statistically significant.

CHAPTER 3: RESULTS

3.1 Effects of ISO and PDE Inhibitors on Action Potentials

In the first set of experiments, APs were measured in right atrial myocytes in control conditions and after the application of ISO, subtype specific PDE inhibitors or combined PDE inhibition. This was done by analyzing different parameters of the action potential, including different phases of repolarization.

Figure 3.1A shows representative effects of the β-AR agonist ISO (1 μM) on action potentials from single mouse right atrial myocytes. ISO increased (P<0.05) AP duration (APD) at 50%, 70% and 90% repolarization times (APD50, APD70 and APD90); however, it did not cause any significant change in RMP (P=0.18), peak AP amplitude (P=0.27) or V_{max} (P=0.15). Summary data for APD50, APD70 and APD90 is presented in Figure 3.1B. ISO increased APD50, APD70 and APD90 by 96.3 ± 7.9%, 94.2 ± 16.3% and 32.1 ± 9.2% respectively (P<0.05; n=10 myocytes).

Next, the effects of the broad spectrum PDE inhibitor IBMX (100μM) on right atrial APs were measured. Figure 3.2A shows representative AP recordings in control conditions and after the application of IBMX. These effects were similar to those seen with ISO. APD50, APD70 and APD90 values were increased (P<0.05; n=13 myocytes) by 105.9 ± 15.4, 90.5 ± 12.6% and 25.5 ± 3.5 % respectively as demonstrated in Figure 3.2B. RMP (P=0.21), peak AP amplitude (P=0.79) and V_{max} (P=0.38) were unchanged by IBMX.

After using both a β-adrenergic agonist and a broad spectrum PDE inhibitor, it was important to examine which PDE subtypes were involved in modulating AP

duration. This was accomplished using subtype specific PDE inhibitors as well as combinations of selective inhibitors.

The first selective inhibitor tested was EHNA (10μM), which selectively blocks PDE2 at this concentration (Podzuweit *et al.*, 1995). Figure 3.3A shows representative effects of EHNA on action potentials. Although the effects were not as robust as ISO or IBMX, EHNA still resulted in an increase ($P<0.05$) in APD at 50%, 70% and 90% repolarization times (see Figures 3.8-3.10 and Table 3.1 for a comparison of each drug treatment group on APD). Summary data for these parameters is shown in Figure 3.3B and is based on the analysis of 13 cells. EHNA caused an average increase of 21.7 ± 9.5% for APD50, 24.9 ± 8.8% for APD70 and 11.9 ± 5.7% for APD90. There was no difference found between control and EHNA for RMP ($P=0.09$), peak AP amplitude ($P=0.77$) and V_{max} ($P=0.24$).

The next compound tested was milrinone (10μM), which is a selective blocker of PDE3 at this concentration (Kirstein *et al.*, 1995;Verde *et al.*, 1999;Shakur *et al.*, 2002;Verde *et al.*, 1999). As shown in Figure 3.4A (representative AP recordings) and 3.4B (summary data; $n=9$ myocytes), milrinone had no effect on any of the AP parameters measured.

Rolipram (10μM), a PDE4 selective blocker (Kerfant *et al.*, 2007;Maurice *et al.*, 2003), increased ($P<0.05$) atrial myocyte APD as shown in the representative action potential recording in Figure 3.5A. This effect, again, was not as robust as ISO or IBMX (Figures 3.8-3.10 and Table 3.1). The application of rolipram resulted in an average increase of 31.7 ± 5.6% for APD50, 31.2 ± 5.2% for APD70 and 12.8 ± 2.9% increase for

APD90 (Figure 5B, n=7 cells). RMP (P=0.4), peak AP amplitude (P=0.71) and V_{max} (P=0.32) showed no significant difference.

Next, the effects of combinations of subtype specific PDE inhibitors on atrial APs were studied. Specifically, a combination of milrinone + rolipram (both at 10μM) and EHNA + milrinone + rolipram (all at 10μM) were investigated. Although milrinone at this concentration had no effect on APD by itself (Figure 3.4B), milrinone in combination with rolipram (i.e combined PDE3 and PDE4 inhibition) elicited robust effects that were similar to IBMX as illustrated in the representative AP recordings in Figure 3.6A, as well as Table 2.1. Summary data demonstrate that milrinone + rolipram increased APD50, APD70 and APD90 by an average of 110.6 ± 18.8%, 90.8 ± 15.9% and 29.9 ± 8.1% respectively (P<0.05; n=10).

Adding a PDE2 inhibitor to the combination of PDE3 and PDE4 inhibitors (i.e. EHNA + milrinone + rolipram; all at 10 μM) also elicited robust effects on atrial APs as illustrated in Figure 3.7A. Summary data demonstrated that the combination of EHNA + milrinone + rolipram increased APD50, APD70 and APD90 by an average of 108 ± 15.4%, 95.2 ± 12.8% and 20.4 ± 5.3% (P<0.05, n=9 cells, Figure 3.7B). These effects were very similar to those observed with milrinone + rolipram (Figures 3.8-3.10 and Table 3.1)

Figure 3.1. Effects of isoproterenol on action potential duration in adult mouse right atrial myocytes. A: representative action potential recordings in control conditions and after the application of ISO (1μM). B: Average effects of ISO (red bars) on 50%, 70% and 90 % repolarization time (APD50, APD70 and APD90) in comparison to control (black bars). Data are means ±SEM, n=10 myocytes, *P<0.05 vs. control for each parameter. Values in ISO were significantly greater than control (Table 3.1).

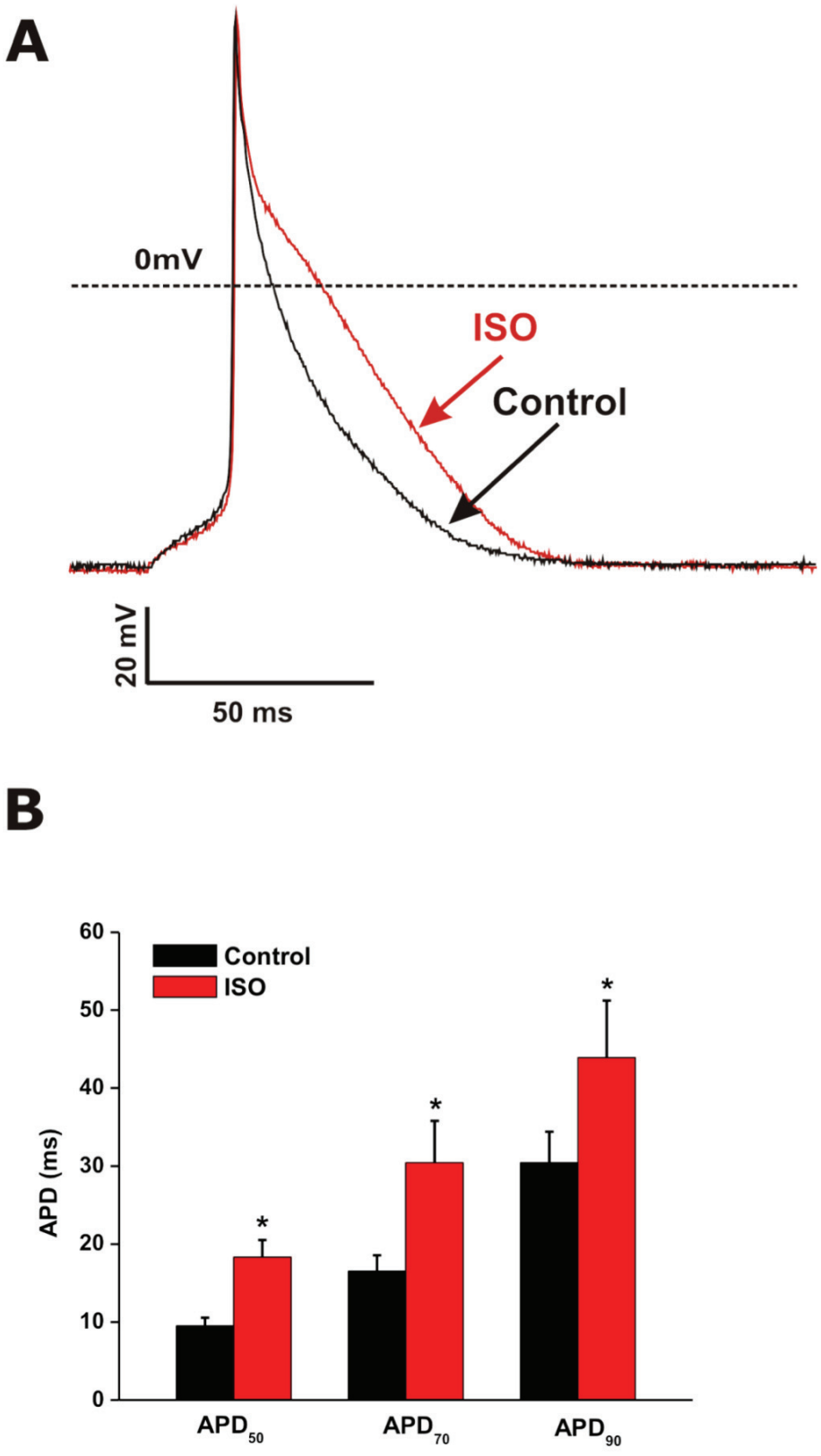
A
0mV
ISO
Control
20 mV
50 ms
B
Control
ISO
APD (ms)
60
50
40
30
20
10
0
*
*
*
APD50
APD70
APD90

Figure 3.1.

Figure 3.2. Effects of IBMX on action potential duration in adult mouse right atrial myocytes. A: representative action potential recordings in control conditions and after the application of IBMX (100μM). B: Average effects of IBMX (red bars) on 50%, 70% and 90 % repolarization time (APD50, APD70 and APD90) in comparison to control (black bars). Data are means ±SEM, n=13 myocytes, *P<0.05 vs. control for each parameter. Values for IBMX were significantly greater than control (Table 3.1).

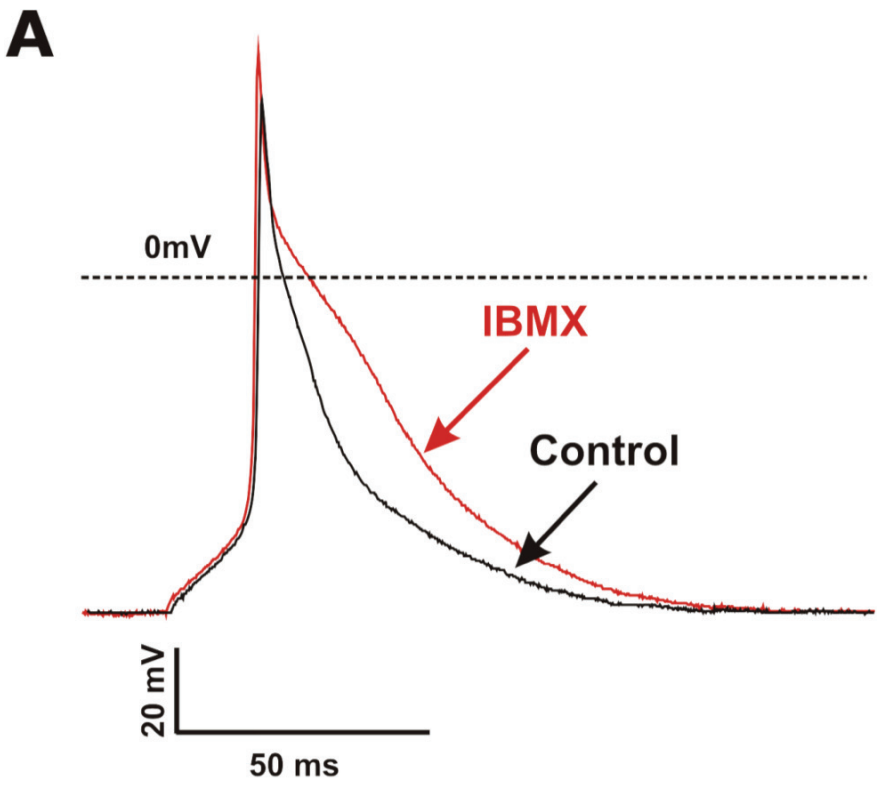
A
0mV
IBMX
Control
20 mV
50 ms

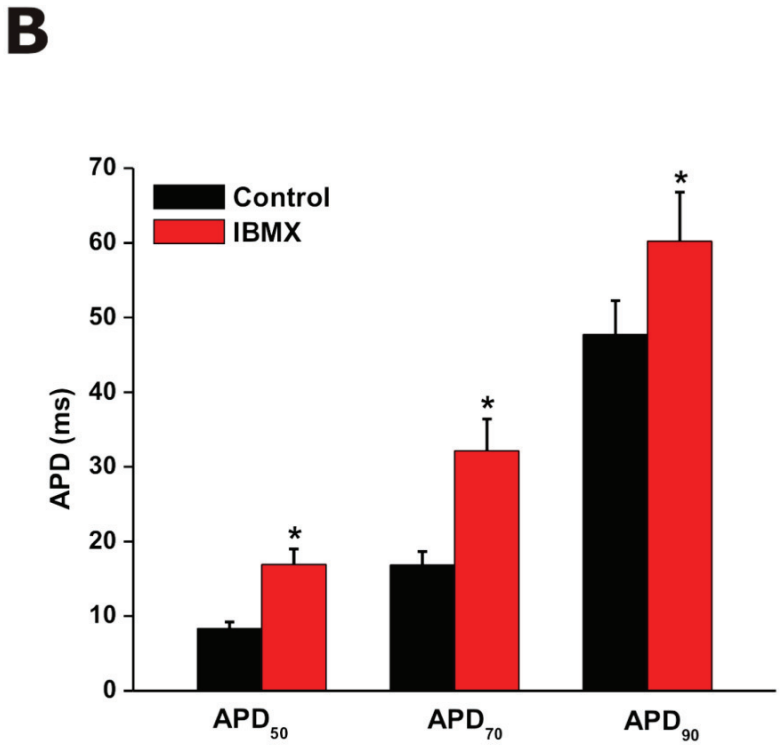
B
Control
IBMX
APD (ms)
70
60
50
40
30
20
10
0
*
*
*
APD50
APD70
APD90

Figure 3.2.

Figure 3.3. Effects of EHNA on action potential duration in adult mouse right atrial myocytes. A: representative action potential recordings in control conditions and after the application of EHNA (10μM). B: Average effects of EHNA (red bars) on 50%, 70% and 90 % repolarization time (APD50, APD70 and APD90) in comparison to control (black bars). Data are means ±SEM, n=13 myocytes, *P<0.05 vs. control for each parameter. Values in EHNA were significantly greater than control (Table 3.1).

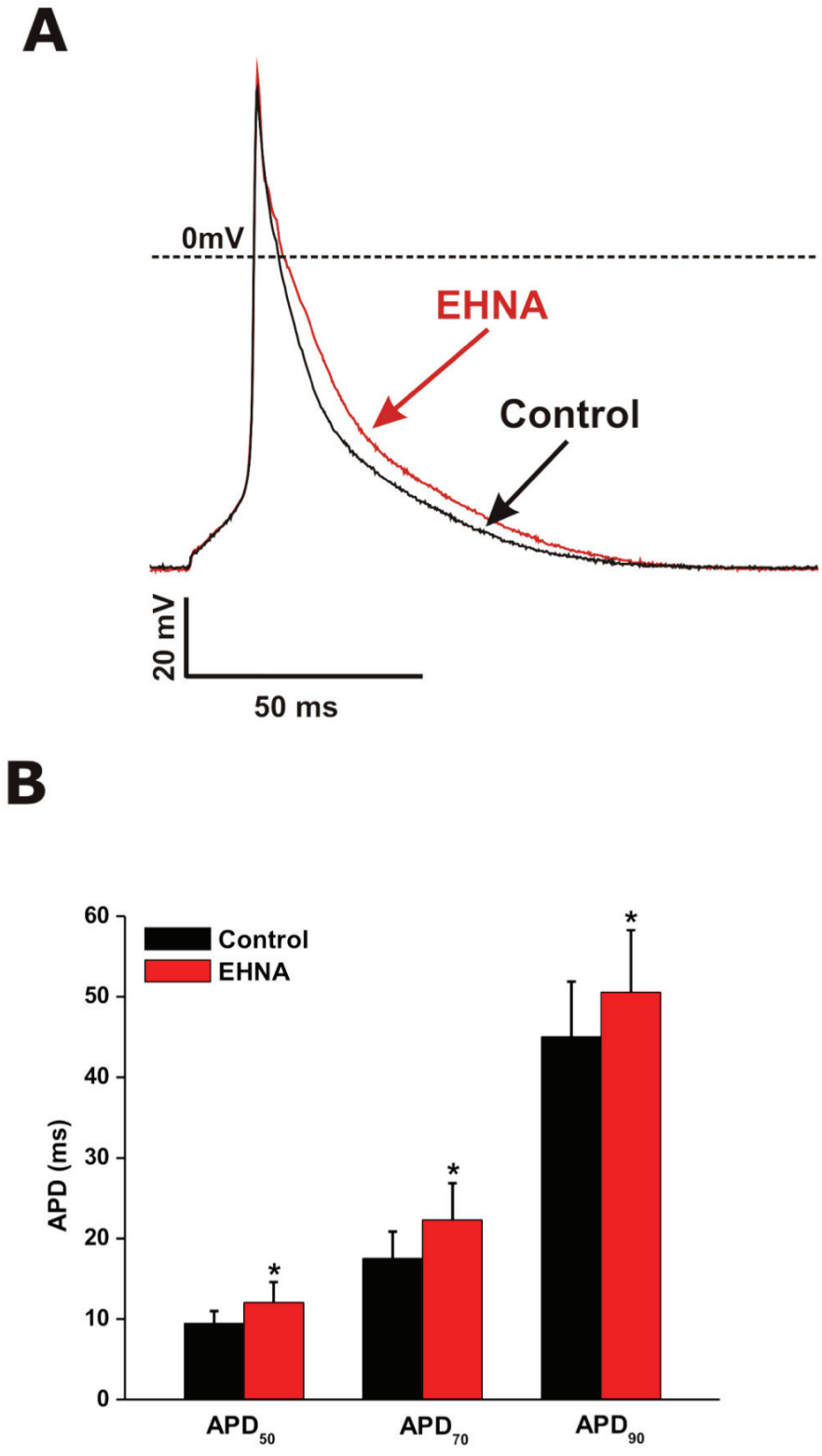
A
0mV
EHNA
Control
20 mV
50 ms
B
Control
EHNA
APD (ms)
60
50
40
30
20
10
0
*
*
*
APD50
APD70
APD90

Figure 3.3.

Figure 3.4. Effects of milrinone on action potential duration in adult mouse right atrial myocytes. A: representative action potential recordings in control conditions and after the application of milrinone (10μM). B: Average effects of milrinone (red bars) on 50%, 70% and 90 % repolarization time (APD50, APD70 and APD90) in comparison to control (black bars). Data are means ±SEM, *n*=9 myocytes, *P<0.05 vs. control for each parameter. Milrinone did not yield any significance difference in APD in comparison to control, P>0.05 (Table 3.1).

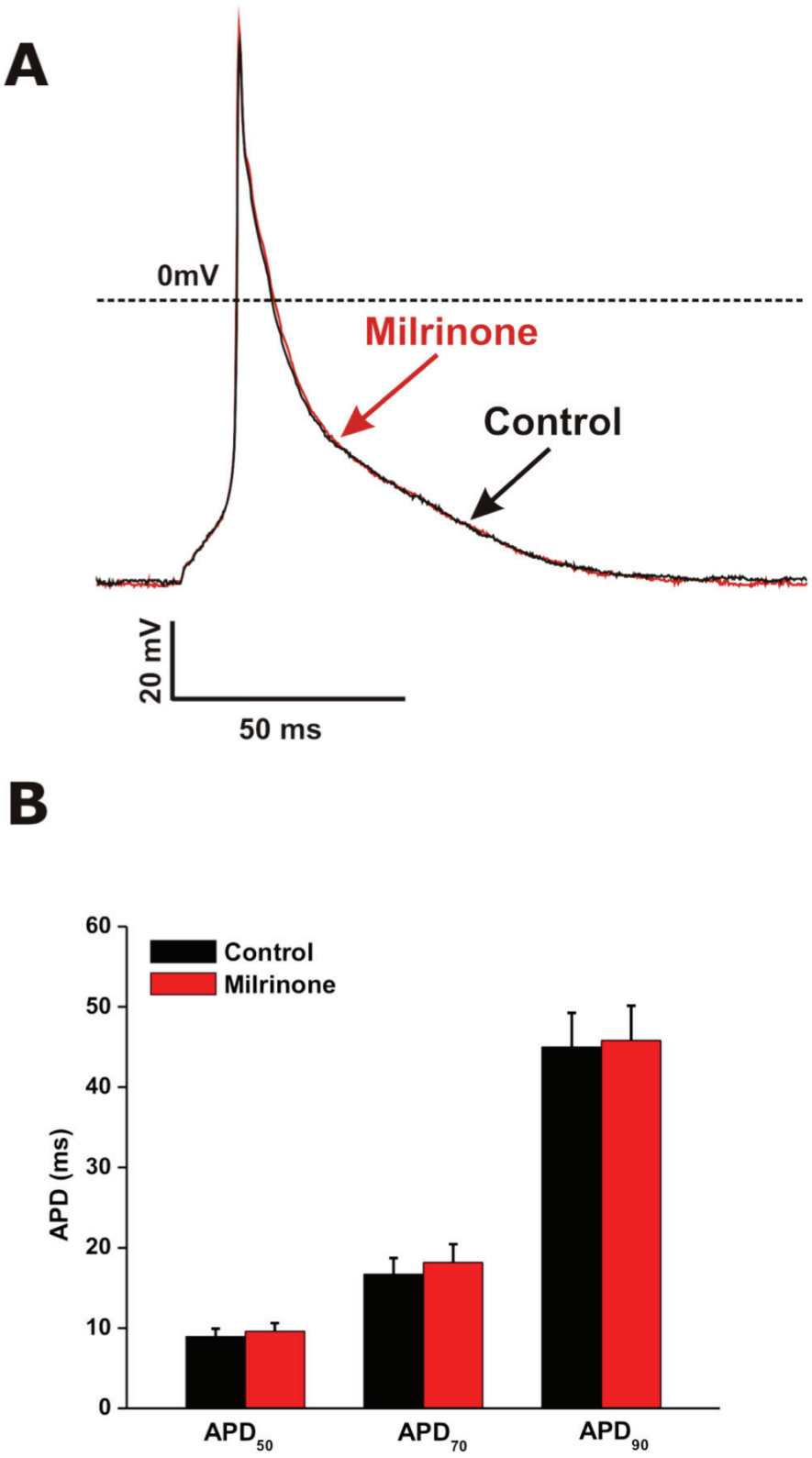
A
0mV
Milrinone
Control
20 mV
50 ms
B
Control
Milrinone
APD (ms)
60
50
40
30
20
10
0
APD50
APD70
APD90

Figure 3.4.

Figure 3.5. Effects of rolipram on action potential duration in adult mouse right atrial myocytes. A: representative action potential recordings in control conditions and after the application of rolipram (10μM). B: Average effects of rolipram (red bars) on 50%, 70% and 90 % repolarization time (APD50, APD70 and APD90) in comparison to control (black bars). Data are means ±SEM, n=7 myocytes, *P<0.05 vs. control for each parameter. Values in rolipram were significantly greater than control (Table 3.1).

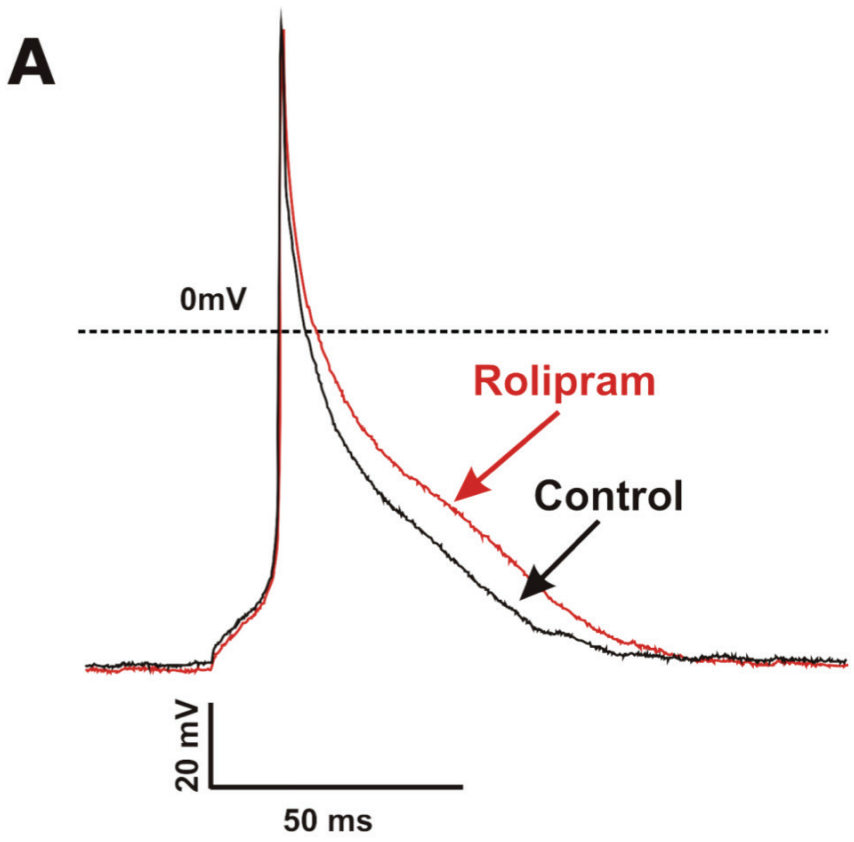
A
0mV
Rolipram
Control
20 mV
50 ms

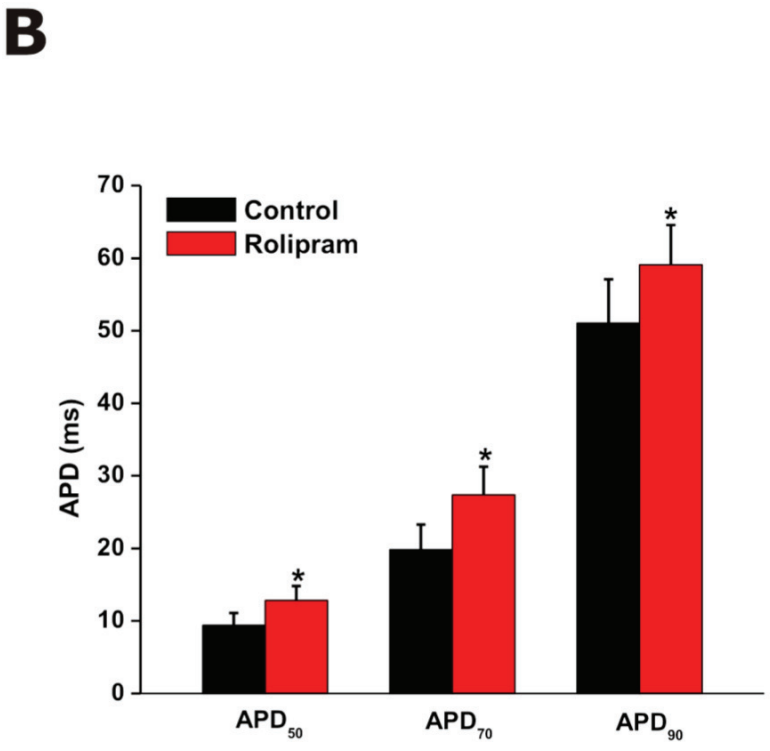
B
Control
Rolipram
APD (ms)
0
10
20
30
40
50
60
70
*
*
*
APD50
APD70
APD90

Figure 3.5.

Figure 3.6. Effects of milrinone and rolipram combined on action potential duration in adult mouse right atrial myocytes. A: representative action potential recordings in control conditions and after the application both MIL+ROL (10μM). B: Average effects of MIL+ROL (red bars) on 50%, 70% and 90 % repolarization time (APD50, APD70 and APD90) in comparison to control (black bars). Data are means ±SEM, n=10 myocytes, *P<0.05 vs. control for each parameter. Values in MIL+ROL were significantly greater than control (Table 3.1).

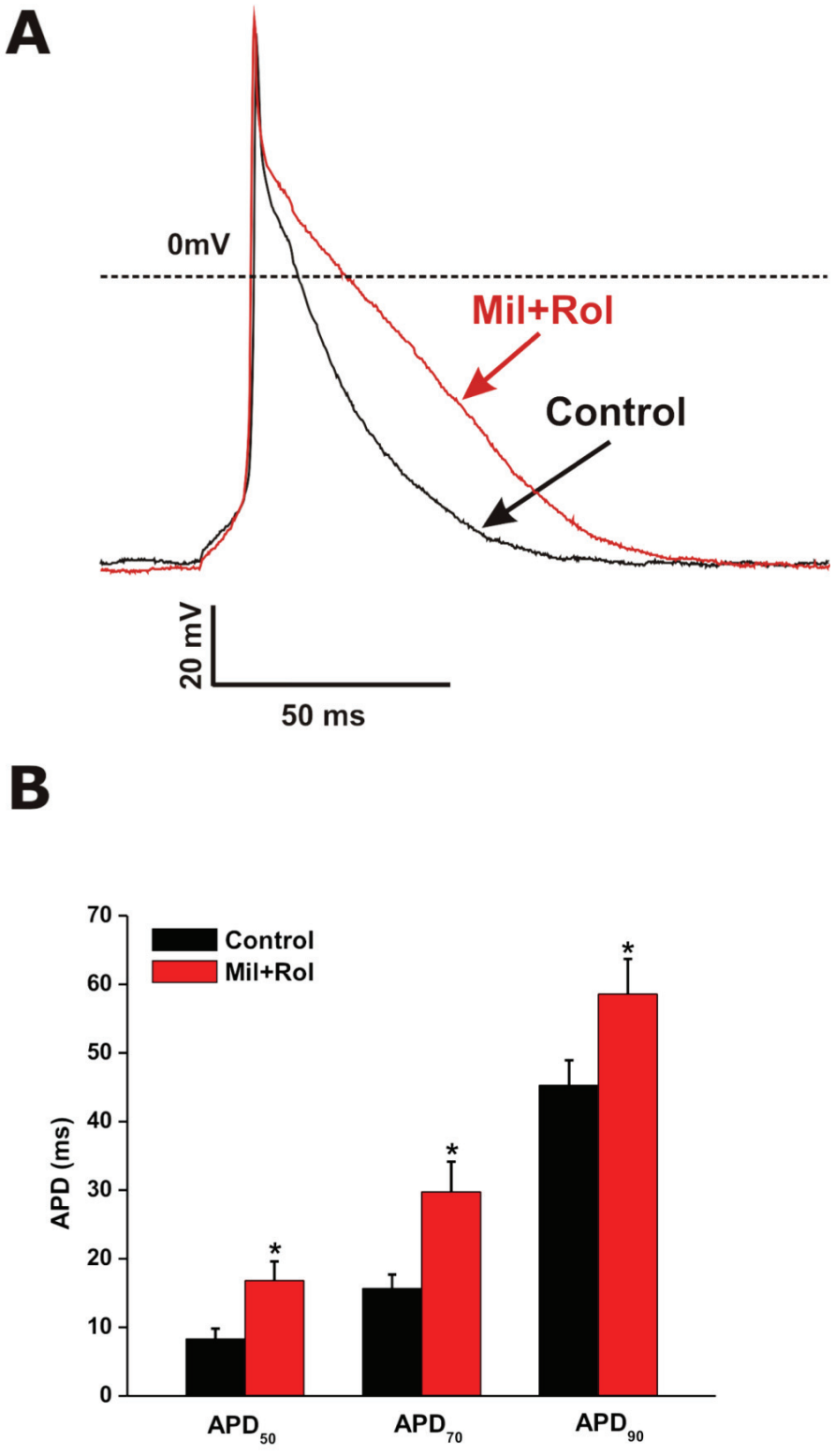
A
0mV
Mil+Rol
Control
20 mV
50 ms
B
Control
Mil+Rol
APD (ms)
0
10
20
30
40
50
60
70
*
*
*
APD50
APD70
APD90

Figure 3.6.

Figure 3.7. Effects of EHNA, milrinone and rolipram combined on action potential duration in adult mouse right atrial myocytes . A: representative action potential recordings in control conditions and after the application of EHNA+MIL+ROL (10μM). B: Average effects of EHNA+MIL+ROL (red bars) on 50%, 70% and 90% repolarization time (APD50, APD70 and APD90) in comparison to control (black bars). Data are means ±SEM, n=9 myocytes, *P<0.05 vs. control for each parameter. Values in EHNA+MIL+ROL were significantly greater than control (Table 3.1).

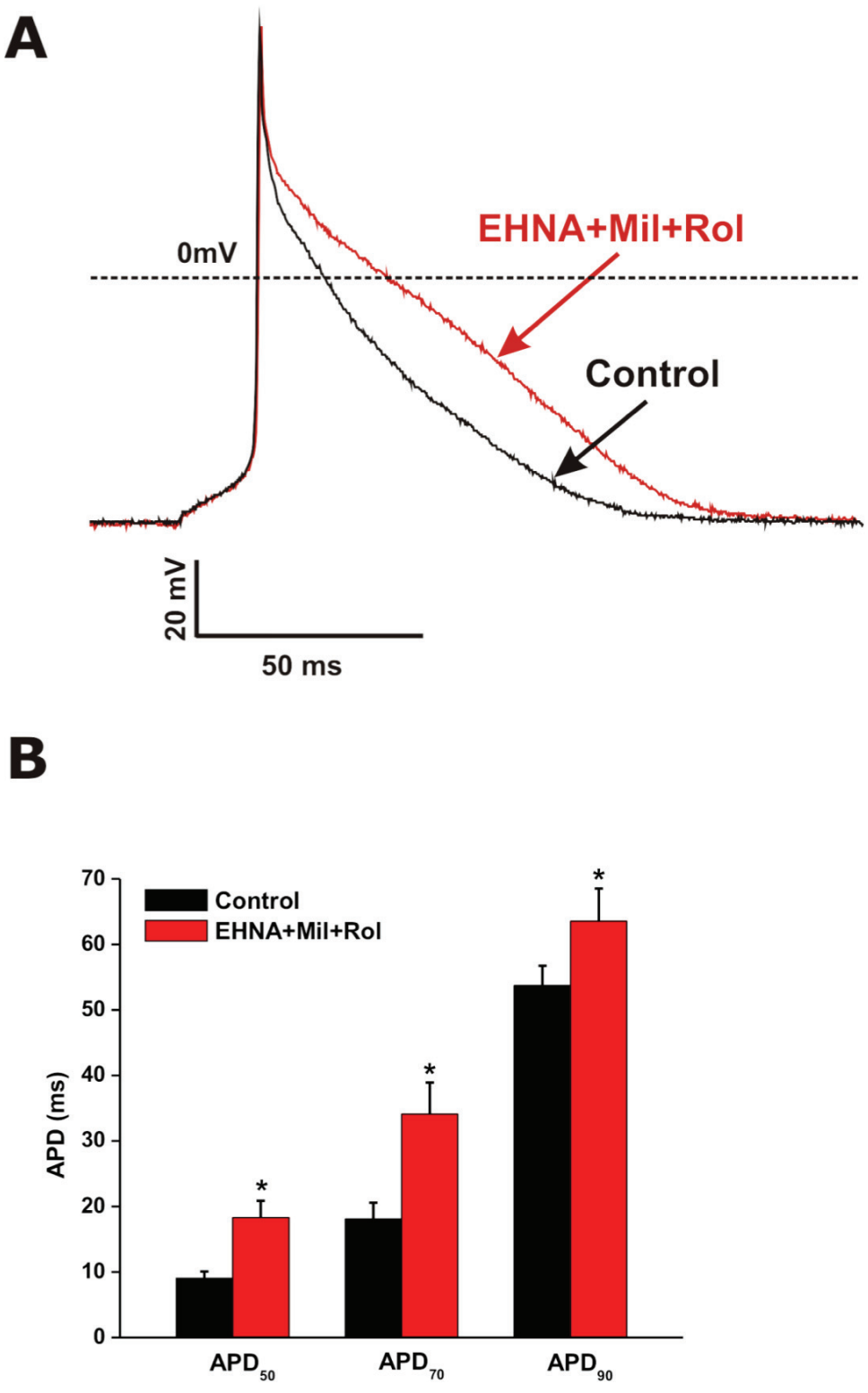
A
0mV
EHNA+Mil+Rol
Control
20 mV
50 ms
B
Control
EHNA+Mil+Rol
APD (ms)
0
10
20
30
40
50
60
70
*
*
*
APD50
APD70
APD90

Figure 3.7.

Figure 3.8. Summary data comparing the effects of isoproterenol, subtype specific and combined PDE inhibition on APD50 in adult mouse right atrial myocytes. A: Summary bar graph illustrating the effects of ISO (1 μM; gray bar), IBMX (100 μM; red bar), EHNA (10 μM; blue bar), milrinone (MIL 10 μM; green bar), rolipram (ROL 10 μM; orange bar) MIL+ROL (10 μM; white bar) and EHNA+MIL+ROL (10 μM; yellow bar) on 50% repolarization time (APD50) in comparison to control (black bars). Data are means ±SEM, with *n* values in parentheses,**P*<0.05 verses control.

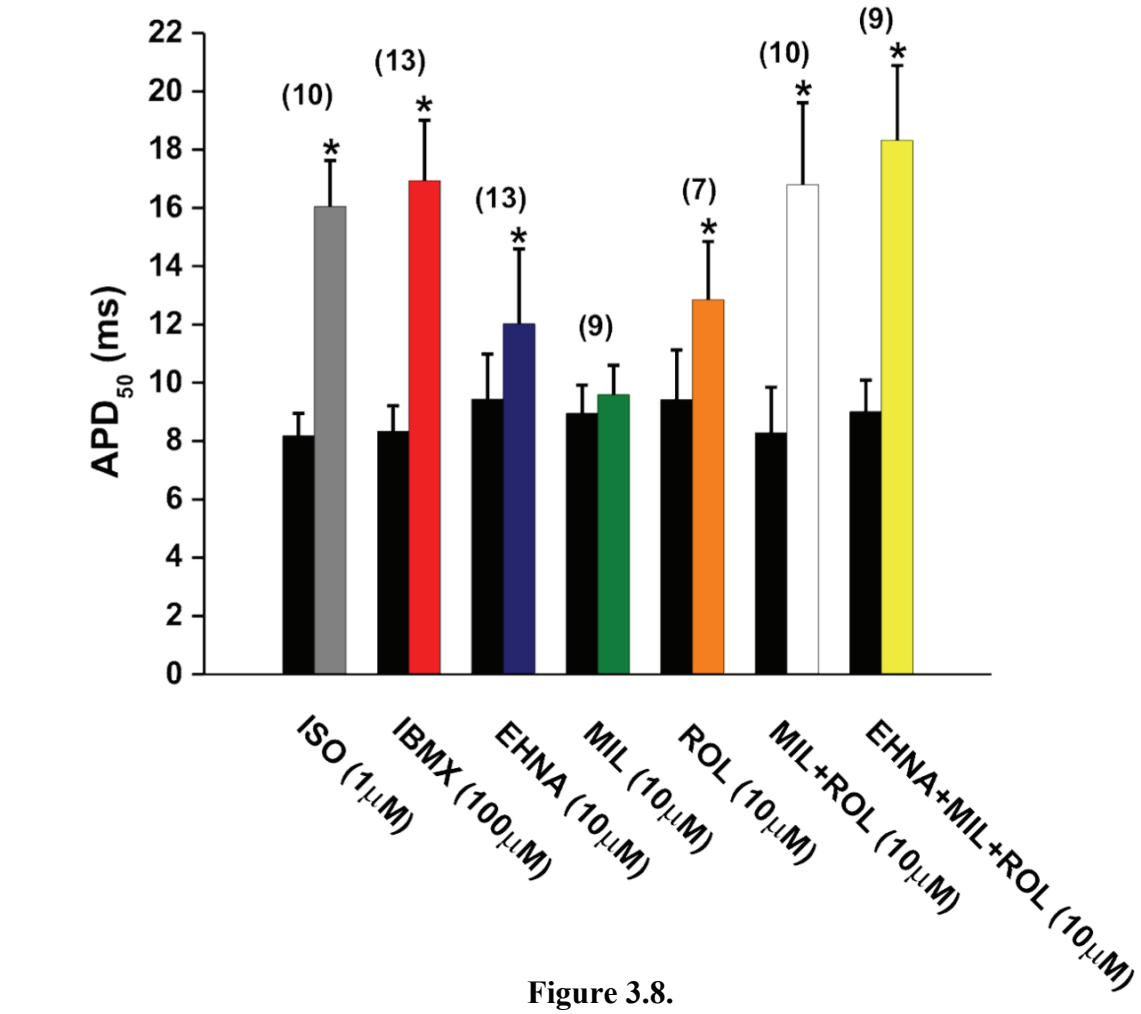
A
APD50 (ms)
0
2
4
6
8
10
12
14
16
18
20
22
(10)
(13)
(13)
(9)
(7)
(10)
(9)
*
ISO (1μM)
IBMX (100μM)
EHNA (10μM)
MIL (10μM)
ROL (10μM)
MIL+ROL (10μM)
EHNA+MIL+ROL (10μM)

Figure 3.8.

Figure 3.9. Summary data comparing the effects of isoproterenol, subtype specific and combined PDE inhibition on APD70 in adult mouse right atrial myocytes. A: Summary bar graph illustrating the effects of ISO (1 μM; gray bar), IBMX (100 μM; red bar), EHNA (10 μM; blue bar), milrinone (MIL 10 μM; green bar), rolipram (ROL 10 μM; orange bar) MIL+ROL (10 μM; white bar) and EHNA+MIL+ROL (10 μM; yellow bar) on 70% repolarization time (APD70) in comparison to control (black bars). Data are means ±SEM, with *n* values in parentheses, **P*<0.05 versus control.

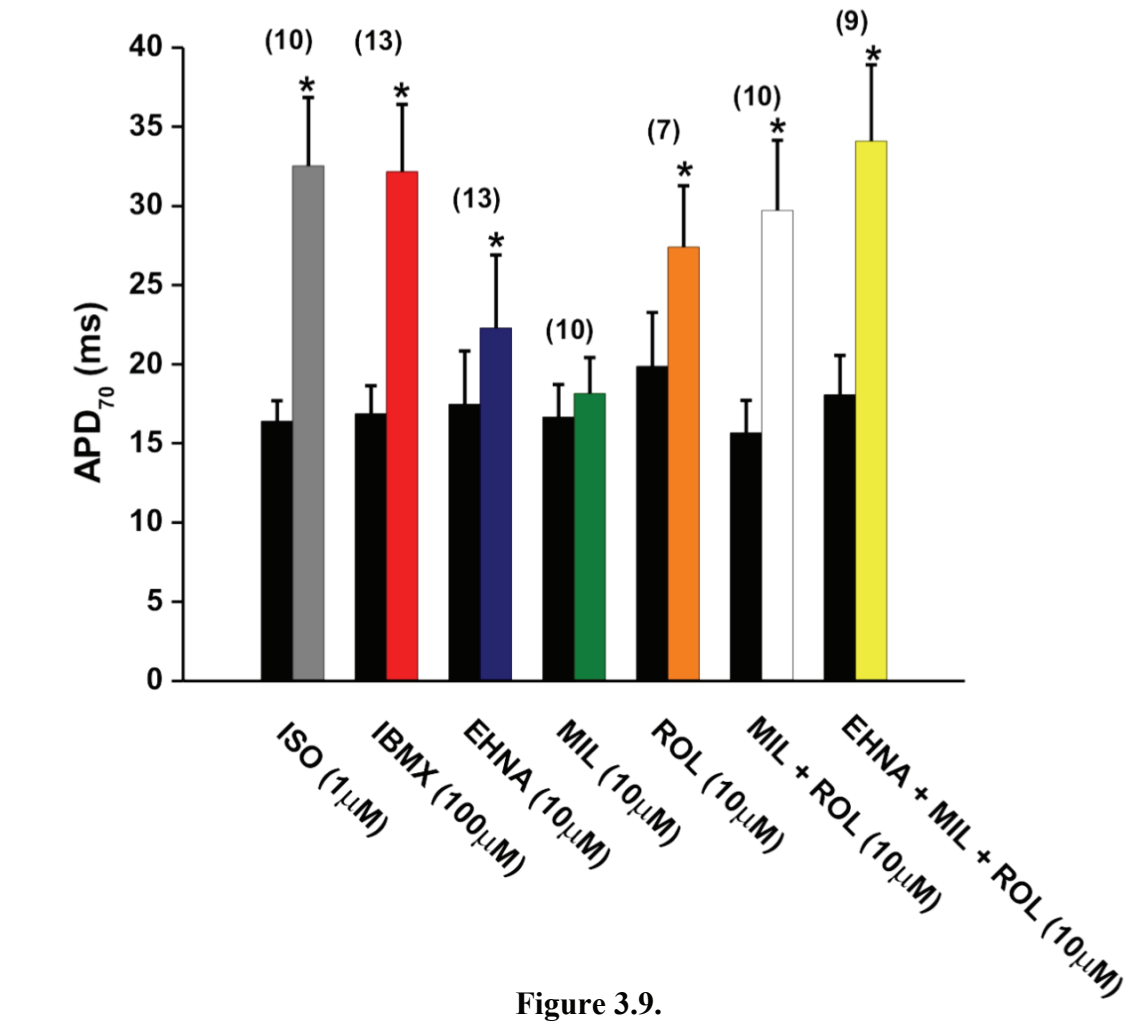
A
APD70 (ms)
40
35
30
25
20
15
10
5
0
(10)
(13)
(13)
(10)
(7)
(10)
(9)
*
ISO (1μM)
IBMX (100μM)
EHNA (10μM)
MIL (10μM)
ROL (10μM)
MIL + ROL (10μM)
EHNA + MIL + ROL (10μM)

Figure 3.9.

Figure 3.10. Summary data comparing the effects of isoproterenol, subtype specific and combined PDE inhibition on APD90 in adult mouse right atrial myocytes. A: Summary bar graph illustrating the effects of ISO (1 μM; gray bar), IBMX (100 μM; red bar), EHNA (10 μM; blue bar), milrinone (MIL 10 μM; green bar), rolipram (ROL 10 μM; orange bar) MIL+ROL (10 μM; white bar) and EHNA+MIL+ROL (10 μM; yellow bar) on 90% repolarization time (APD90) in comparison to control (black bars). Data are means ±SEM, with *n* values in parentheses, **P*<0.05 versus control.

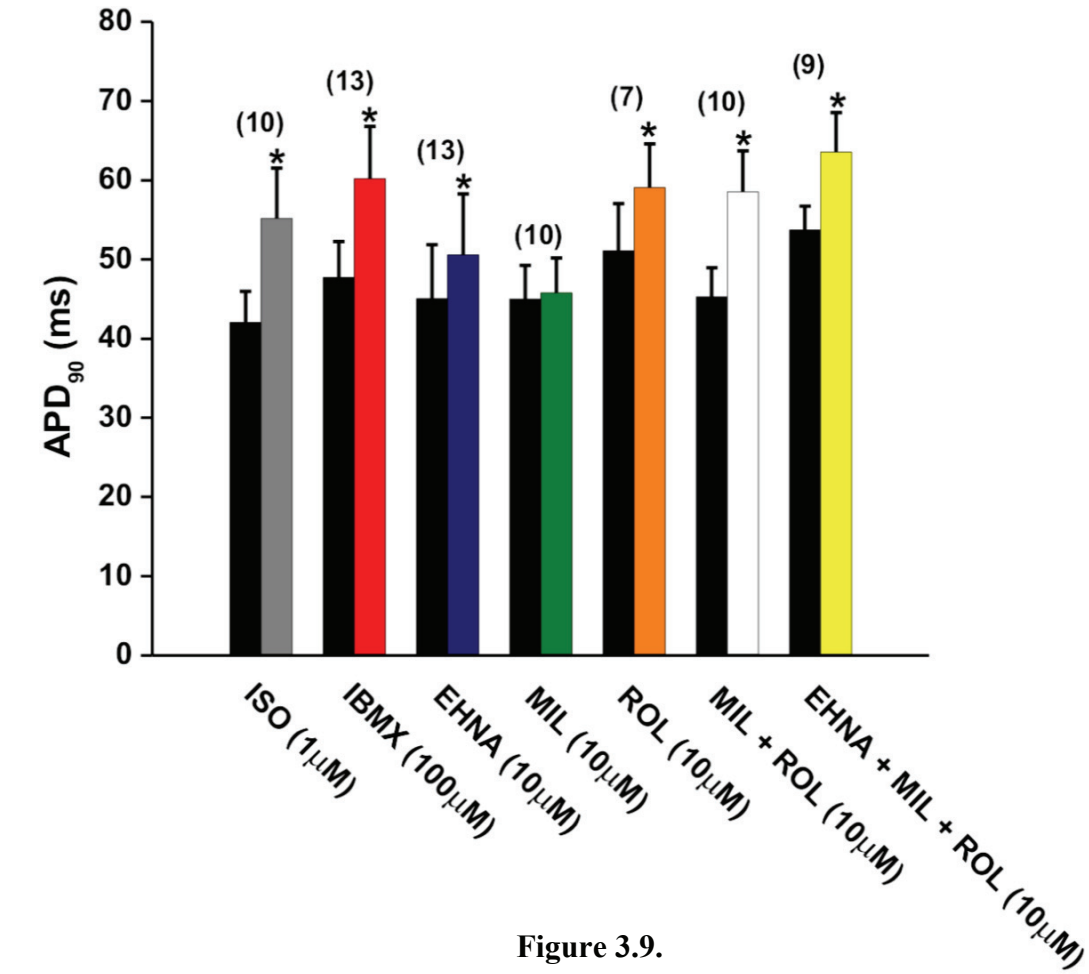
A
80
70
60
50
40
30
20
10
0
APD90 (ms)
(10)
(13)
(13)
(10)
(7)
(10)
(9)
*
ISO (1μM)
IBMX (100μM)
EHNA (10μM)
MIL (10μM)
ROL (10μM)
MIL + ROL (10μM)
EHNA + MIL + ROL (10μM)

Figure 3.9.

3.2 Effects of ISO and PDE Inhibitors on Basal $I_{Ca,L}$

ISO is well known to affect APD by increasing $I_{Ca,L}$, which is the result of increasing cAMP dependant phosphorylation of the channel by PKA leading to an increase in channel mean open probability (McDonald *et al.*, 1994;Hartzell *et al.*, 1991;Hove-Madsen *et al.*, 1996). The effects of the PDE inhibitors on APD described above, particularly on APD50 and APD70, are also suggestive of a role for $I_{Ca,L,}$ which plays a prominent role in this region of the cardiac AP. Accordingly, the next series of experiments measured the effects of ISO and PDE inhibition on right atrial $I_{Ca,L}$.

Figure 3.11A shows representative $I_{Ca,L}$ recordings in control conditions and following the application of ISO (1μM), as well as the time course of the ISO effect during a voltage clamp step to 0 mV. ISO increased $I_{Ca,L}$ rapidly (within 2 min) and this effect was completely reversible upon washout of the drug. $I_{Ca,L}$ current density was increased (P<0.05) in the presence of ISO as shown in Figure 3.11B (-3.64 ± 0.6 pA/pF in control versus -9.31 ± 1.3 pA/pF ISO, n=6). Steady state conductance was also analyzed and showed that ISO increased $I_{Ca,L}$ maximum conductance (G_{max}) (P<0.05) to 186.9 ± 19.3 pS/pF from 111.5 ± 14.3 pS/pF in control conditions in atrial myocytes (Figure 3.11C). Furthermore, the voltage required for 50% channel activation ($V_{1/2}$) was left shifted (P<0.05) compared to control (-7.71 ± 2.7 mV control versus -15.4 ± 1.6 mV ISO, Figure 3.11C).

Next, the effects of IBMX (100μM) on atrial $I_{Ca,L}$ were measured. Figure 3.12A shows representative $I_{Ca,L}$ recordings before and after application of IBMX, as well as the time course of the IBMX effect. $I_{Ca,L}$ current densities were larger (P<0.05) in the presence of IBMX as shown in Figure 3.12B by the change in the peak of the I-V curve

(-3.93 ± 0.2 pA/pF in control versus - 9.67 ± 0.4 pA/pF in IBMX, *n*=10). IBMX resulted in an increase (*P*<0.05) in G_{max} (198.4 ± 10.4 pS/pF) compared to control (112.1 ± 8.8 pS/pF) in single right atrial myocytes (Figure 3.12C). Furthermore, $V_{1/2}$ was left shifted (*P*<0.05) compared to control (-9.4 ± 1.2 mV in control versus -18.4 ± 1.1 mV in IBMX, Figure 3.12C). The effects of ISO and IBMX on $I_{Ca,L}$ were similar in magnitude (Table 2.1). All kinetic data (G_{max}, $V_{1/2}$ and slope factor (k)) are summarized in Table 2.2.

The next step was to investigate the effects of subtype specific PDE inhibitors on $I_{Ca,L}$ starting with the PDE2 inhibitor EHNA (10μM). The application of EHNA to the superfusate resulted in an increase in peak $I_{Ca,L}$ when compared to control, which was reversible upon washout as shown in Figure 3.13A. $I_{Ca,L}$ current densities were increased (*P*<0.05) upon application of EHNA as shown in Figure 3.13B by the change in the peak of I-V curve (-4.24 ± 0.45 pA/pF in control versus -5.73 ± 0.61 pA/pF in EHNA, *n*=6). Although EHNA resulted in a significant (*P*<0.05) increase in G_{max} (143.7 ± 16 pS/pF) compared to control (108.2 ± 9.2 pS/pF) in single atrial myocytes (Figure 3.13C), no change in $V_{1/2}$ (*P*=0.46) was observed compared to control (-8.3 ± 0.9 mV control versus -7.0 ± 2.2 mV EHNA, Figure 3.13C).

In agreement with the AP recordings presented in Figure 3.4, PDE3 inhibition with milrinone (MIL,10μM) had no effect on $I_{Ca,L}$ as shown in both representative recordings and time course experiments (Figure 3.14A). This was also clear by the lack of change (*P*>0.05 at all recorded potentials) in the I-V relationships (-3.54 ± 0.33 pA/pF in control versus -3.61 ± 0.14 pA/pF in MIL, *n*= 12; Figure 3.14B). Milrinone also had no effect (*P*=0.43) on G_{max} (96.7 ± 10.4 pS/pF control versus 103.5 ± 4.1 pS/pF MIL, *n*=12) or $V_{1/2}$ (-9.59 ± 1.3 mV control versus -9.01 ± 1.5 mV MIL; *P*=0.65, *n*=12) in single atrial

myocytes (Figure 3.14C).The effects of milrinone on APs and $I_{Ca,L}$ are summarized in Table 3.1.

PDE4 inhibition with rolipram (ROL, 10μM) increased right atrial myocyte $I_{Ca,L}$ and this effect was reversible upon washout (Figure 3.15A). $I_{Ca,L}$ current densities were increased (P<0.05) during the application of rolipram as shown in Figure 3.15B by the change in the peak of the I-V curve (-4.05 ± 0.3 pA/pF control versus - 6.95 ± 0.7 pA/pF ROL, n=8). Rolipram also resulted in an increase (P<0.05) in G_{max} (186 ± 20.6 pS/pF) compared to control (126 ± 8.9 pS/pF) in single atrial myocytes (Figure 3.14C). Furthermore, $V_{1/2}$ was left shifted (P<0.05) compared to control (-7.82 ± 1.5 mV in control versus -11.2 ± 2.2 mV in ROL, Figure 3.15C).

We next tested a combination of milrinone + rolipram (both at 10μM) and EHNA + milrinone + rolipram (all at 10μM) on right atrial myocyte $I_{Ca,L}$. Similar to the AP measurements and despite the lack of effect of milrinone on $I_{Ca,L}$ (Figure 3.14B), milrinone applied in conjunction with rolipram induced a large increase in $I_{Ca,L}$ that reversed upon washout (Figure 3.16A). $I_{Ca,L}$ current densities were larger (P<0.05) in the presence of milrinone + rolipram as shown in Figure 3.16B by the change in the peak of the I-V curve (-3.12 ± 0.2 pA/pF in control versus -7.69 ± 0.6 pA/pF MIL+ROL, n=9). Milrinone and rolipram together resulted in an increase (P<0.05) in G_{max} (179.7 ± 11.5 pS/pF) compared to control (87.4 ± 5.7 pS/pF) in single atrial myocytes (Figure 3.16C) and $V_{1/2}$ left shifted (P<0.05) compared to control (-7.1 ± 1.6 mV in control versus -12.5 ± 1.4 mV in MIL+ROL, Figure 3.16C).

Application of EHNA + milrinone + rolipram (all at 10 μM) also increased $I_{Ca,L}$ as is evident by the representative $I_{Ca,L}$ recordings and time course experiment (Figure 3.17A). Although there was a clear increase, the effect was not larger than MIL+ROL (Table 3.1). EHNA + milrinone + rolipram increased $I_{Ca,L}$ densities (Figure 3.17B) from -3.53 ± 0.2 pA/pF in control to - 8.7 ± 0.6 pA/pF (P<0.05; n=8). EHNA + milrinone + rolipram also resulted in an increase (P<0.05) in G_{max} (208.6 ± 21 pS/pF) compared to control (108.9 ± 11 pS/pF) in single atrial myocytes (Figure 3.17C) and $V_{1/2}$ was left shifted (P<0.05) compared to control (-6.12 ± 1.7 mV control versus -11.6 ± 1.7 mV EHNA+MIL+ROL, Figure 3.17C). A summary of the effects of each drug application on peak right atrial myocyte $I_{Ca,L}$ is provided in Figure 3.18 and their respective changes in channel kinetics are presented in Table 3.2.

Figure 3.11. Effects of ISO on $I_{Ca,L}$ in adult mouse right atrial myocytes.

A: Representative $I_{Ca,L}$ and time course recordings (250 ms voltage-clamp step to 0 mV) from single atrial myocytes before and after the application of ISO (1μM), as indicated by the labelled arrows. B: Summary I-V curves demonstrating that atrial $I_{Ca,L}$ current density increased after the application of ISO (1μM; red) in comparison to control (black). C: Activation curves for $I_{Ca,L}$ conductance in single right atrial myocytes showing that G_{max} was significantly elevated and $V_{1/2}$ was shifted to the left while under the presence of ISO . Data are means ±SEM, *n*=6 myocytes,**P*<0.05 at the given membrane potentials. Refer to Table 3.1 and Table 3.2.

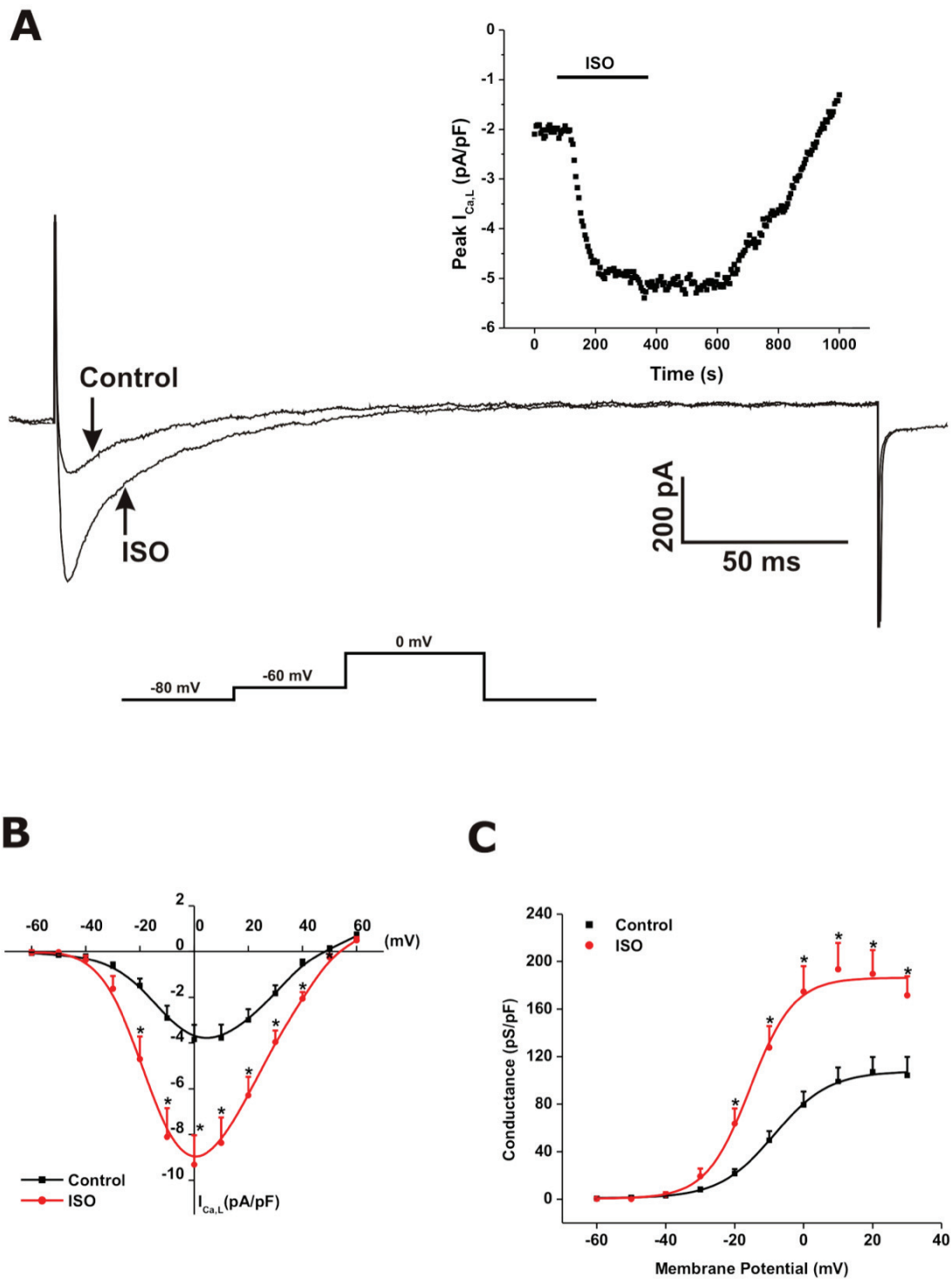
A
ISO
Peak $I_{Ca,L}$ (pA/pF)
Time (s)
Control
ISO
200 pA
50 ms
0 mV
-80 mV
-60 mV
B
(mV)
Control
ISO
$I_{Ca,L}$(pA/pF)
C
Control
ISO
Conductance (pS/pF)
Membrane Potential (mV)

Figure 3.11.

Figure 3.12. Effects of IBMX on $I_{Ca,L}$ in adult mouse right atrial myocytes.

A: Representative $I_{Ca,L}$ and time course (250 ms voltage-clamp step to 0 mV) recordings from single atrial myocytes before and after the application of IBMX (100μM), as indicated by the labelled arrows. B: Summary I-V curves demonstrating that atrial $I_{Ca,L}$ current density increased after the application of IBMX (100μM; red) in comparison to control (black). C: Activation curves for $I_{Ca,L}$ conductance in single right atrial myocytes showing that G_{max} was significantly elevated and $V_{1/2}$ was shifted to the left while under the presence of IBMX. Data are means ±SEM, n=12 myocytes,*P<0.05 at the given membrane potentials. Refer to Table 3.1 and Table 3.2.

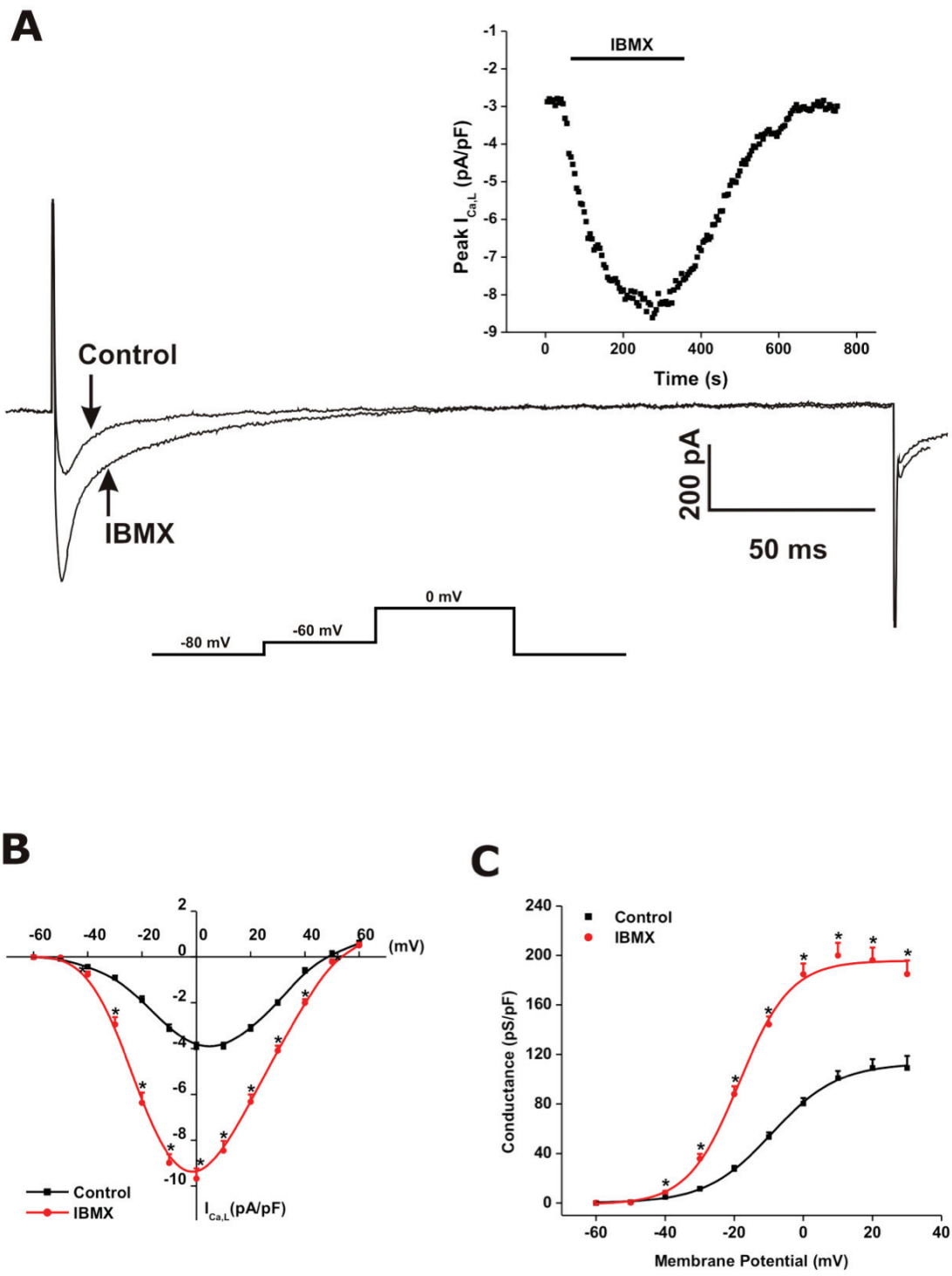
A
IBMX
Peak $I_{Ca,L}$ (pA/pF)
Time (s)
Control
IBMX
200 pA
50 ms
0 mV
-80 mV
-60 mV
B
(mV)
Control
IBMX
$I_{Ca,L}$(pA/pF)
C
Control
IBMX
Conductance (pS/pF)
Membrane Potential (mV)

Figure 3.12.

Figure 3.13. Effects of EHNA on $I_{Ca,L}$ in adult mouse right atrial myocytes.

A: Representative $I_{Ca,L}$ and time course (250 ms voltage-clamp step to 0 mV) recordings from single atrial myocytes before and after the application of EHNA (10μM), as indicated by the labelled arrows. B: Summary I-V curves demonstrating that atrial $I_{Ca,L}$ current density increased after the application of EHNA (10μM; red) in comparison to control (black). C: Activation curves for $I_{Ca,L}$ conductance in single right atrial myocytes showing that G_{max} was significantly elevated; however there was no significant difference in $V_{1/2}$ under the presence of EHNA. Data are means ±SEM, n=6 myocytes,*P<0.05 at the given membrane potentials. Refer to Table 3.1 and Table 3.2.

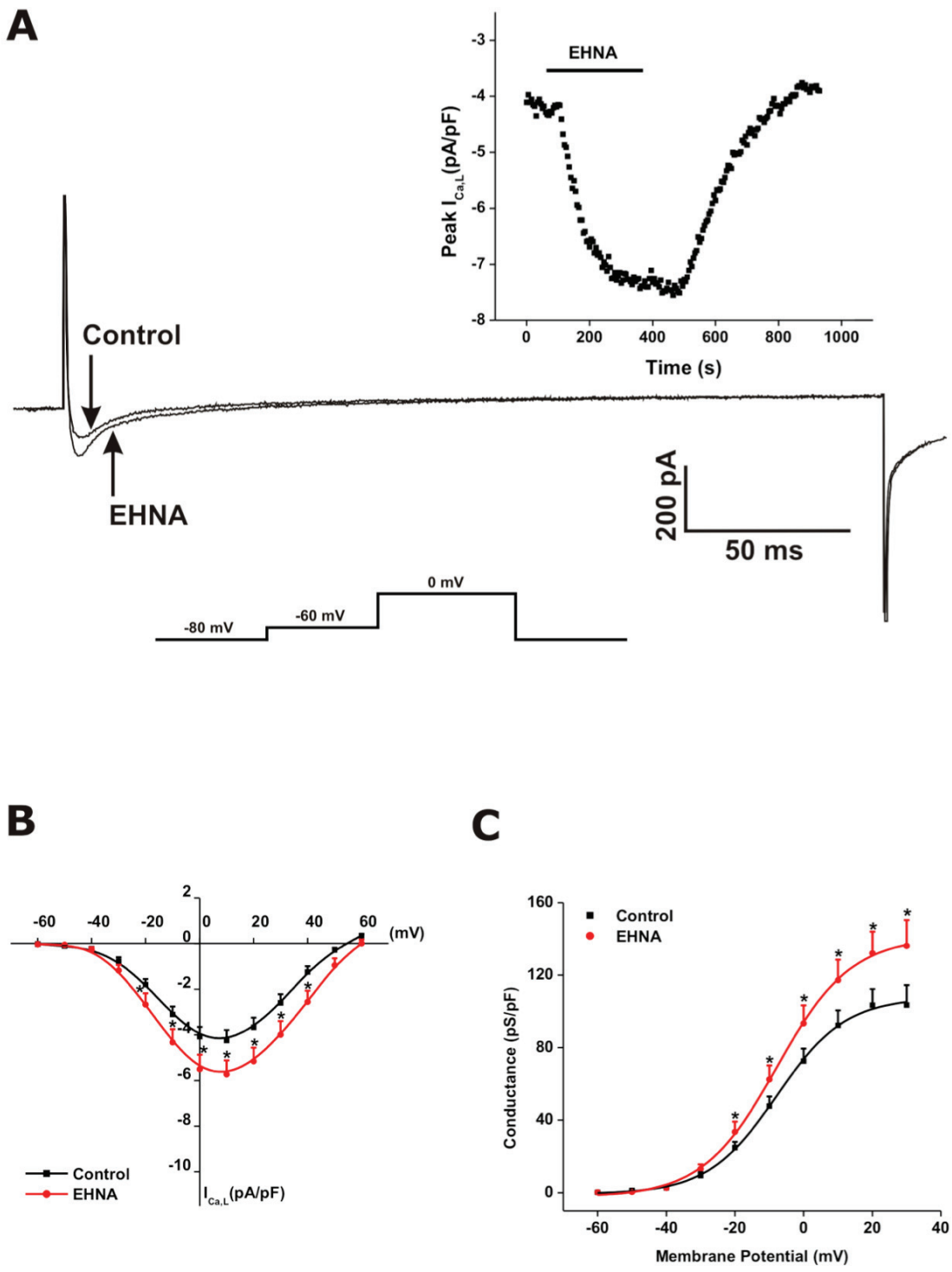
A
EHNA
Peak $I_{Ca,L}$ (pA/pF)
Time (s)
Control
EHNA
200 pA
50 ms
0 mV
-60 mV
-80 mV
B
(mV)
Control
EHNA
$I_{Ca,L}$(pA/pF)
C
Control
EHNA
Conductance (pS/pF)
Membrane Potential (mV)

Figure 3.13.

Figure 3.14. Effects of milrinone on $I_{Ca,L}$ in adult mouse right atrial myocytes.

A: Representative $I_{Ca,L}$ and time course (250 ms voltage-clamp step to 0 mV) recordings from single atrial myocytes before and after the application of milrinone (10μM), as indicated by the labelled arrows. B: Summary I-V curve demonstrating that atrial $I_{Ca,L}$ current density did not change after the application of milrinone (10μM; red) in comparison to control (black). C: Activation curves for $I_{Ca,L}$ conductance in single right atrial myocytes showing that there was no significant difference between control and milrinone application for G_{max} and $V_{1/2}$. Data are means ±SEM, n=12 myocytes, P>0.05 at all given membrane potentials. Refer to Table 3.1 and Table 3.2.

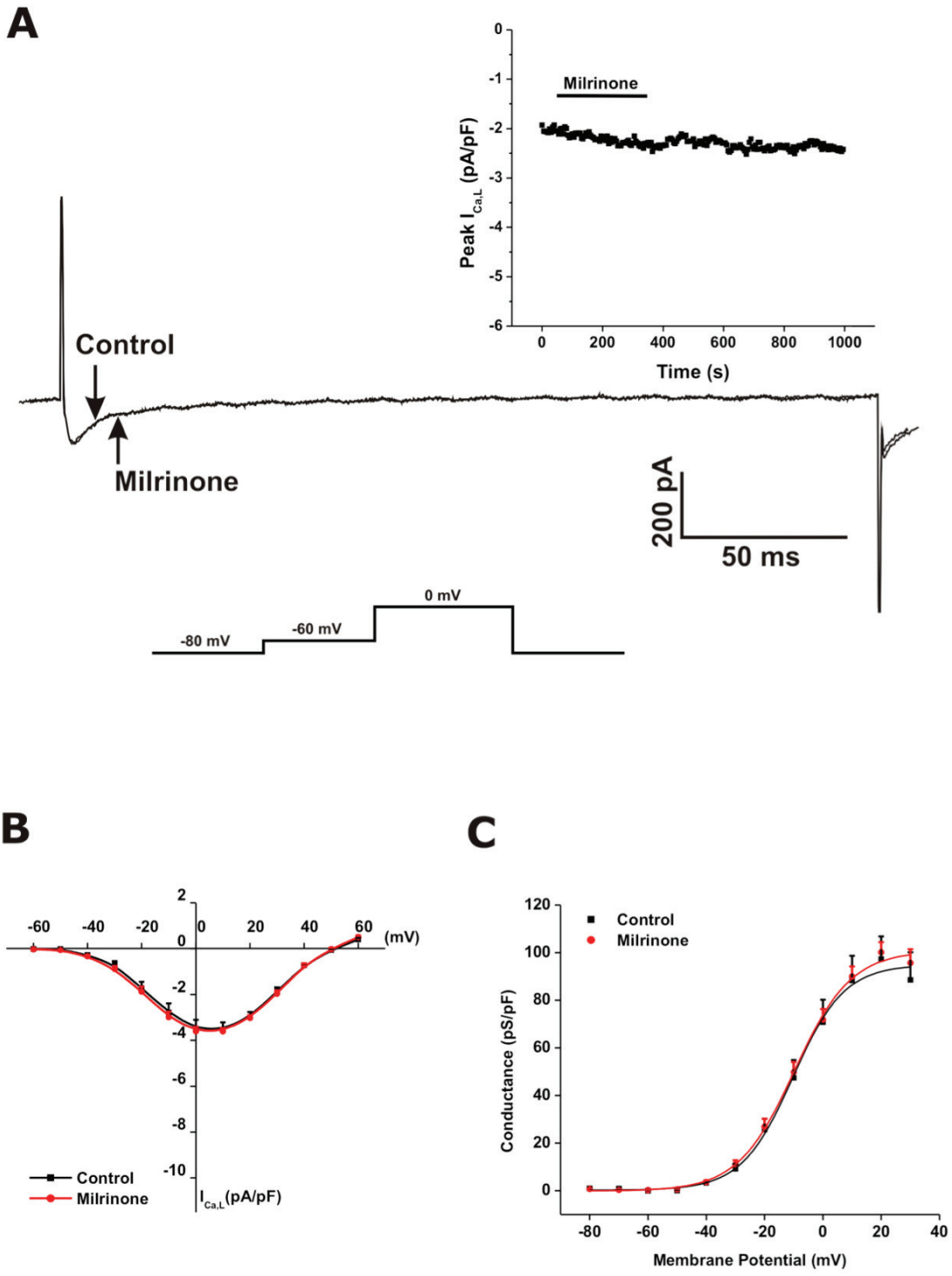
A
Milrinone
Peak $I_{Ca,L}$ (pA/pF)
Time (s)
Control
Milrinone
200 pA
50 ms
0 mV
-60 mV
-80 mV
B
(mV)
Control
Milrinone
$I_{Ca,L}$(pA/pF)
C
Control
Milrinone
Conductance (pS/pF)
Membrane Potential (mV)

Figure 3.14.

Figure 3.15. Effects of rolipram on $I_{Ca,L}$ in adult mouse right atrial myocytes.

A: Representative $I_{Ca,L}$ and time course (250 ms voltage-clamp step to 0 mV) recordings from single atrial myocytes before and after the application of rolipram (10μM), as indicated by the labelled arrows. B: Summary I-V curves demonstrating that atrial $I_{Ca,L}$ current density increased after the application of rolipram (10μM; red) in comparison to control (black). C: Activation curves for $I_{Ca,L}$ conductance in single right atrial myocytes showing that G_{max} was significantly elevated and $V_{1/2}$ was shifted to the left while under the presence of rolipram. Data are means ±SEM, n=8 myocytes, *P<0.05 at the given membrane potentials. Refer to Table 3.1 and Table 3.2.

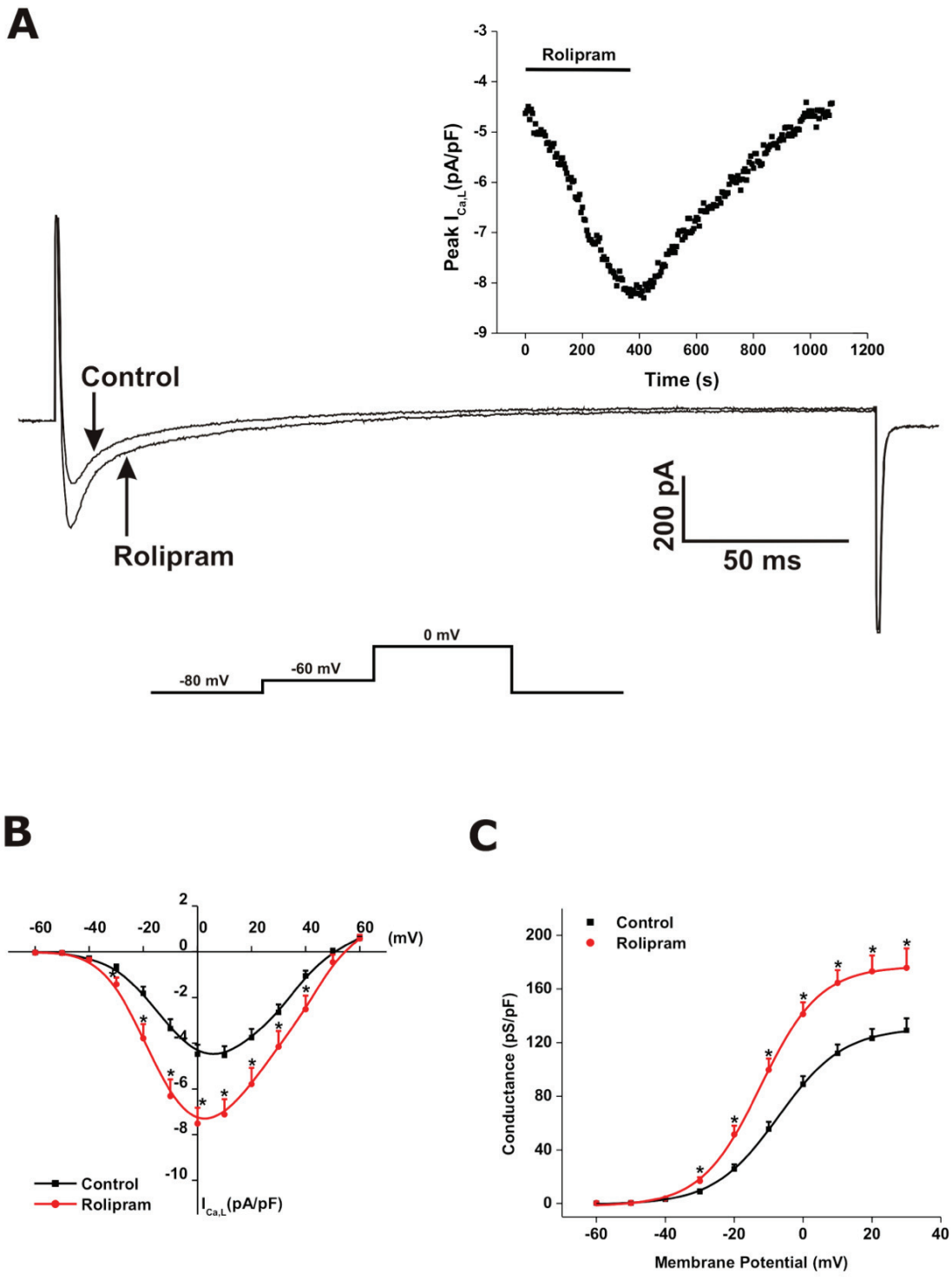
A
Rolipram
Peak $I_{Ca,L}$ (pA/pF)
Time (s)
Control
Rolipram
200 pA
50 ms
0 mV
-60 mV
-80 mV
B
(mV)
Control
Rolipram
$I_{Ca,L}$ (pA/pF)
C
Control
Rolipram
Conductance (pS/pF)
Membrane Potential (mV)

Figure 3.15.

Figure 3.16. Effects of milrinone + rolipram on $I_{Ca,L}$ in adult mouse right atrial myocytes. A: Representative $I_{Ca,L}$ and time course (250 ms voltage-clamp step to 0 mV) recordings from single atrial myocytes before and after the application of MIL+ROL (both at 10μM), as indicated by the labeled arrows. B: Summary I-V curves demonstrating that atrial $I_{Ca,L}$ current density increased after the application of MIL+ROL (boht at 10μM; red) in comparison to control (black). C: Activation curves for $I_{Ca,L}$ conductance in single right atrial myocytes showing that G_{max} was significantly elevated and $V_{1/2}$ was shifted to the left while under the presence of MIL+ROL. Data are means ±SEM, n=9 myocytes, *P<0.05 at the given membrane potentials. Refer to Table 3.1 and Table 3.2.

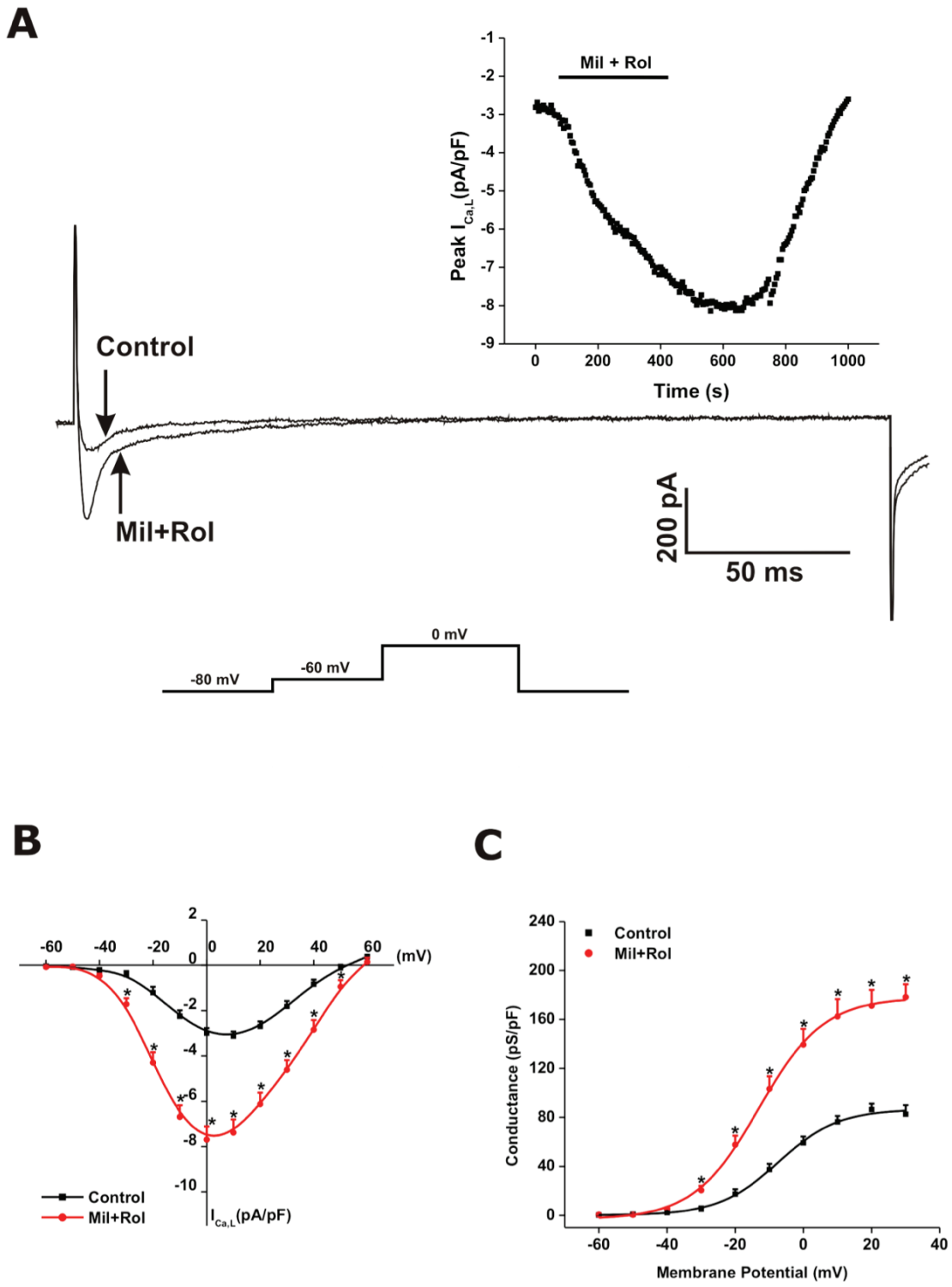
A
Mil + Rol
Peak $I_{Ca,L}$(pA/pF)
Time (s)
Control
Mil+Rol
200 pA
50 ms
0 mV
-60 mV
-80 mV
B
(mV)
Control
Mil+Rol
$I_{Ca,L}$(pA/pF)
C
Control
Mil+Rol
Conductance (pS/pF)
Membrane Potential (mV)

Figure 3.16.

Figure 3.17. Effects of EHNA+ milrinone + rolipram on $I_{Ca,L}$ in adult mouse right atrial myocytes. A: Representative $I_{Ca,L}$ and time course (250 ms voltage-clamp step to 0 mV) recordings from single atrial myocytes before and after the application of EHNA+ MIL+ROL (all at 10μM), as indicated by the labeled arrows. B: Summary I-V curves demonstrating that atrial $I_{Ca,L}$ current density increased after the application of EHNA+ MIL+ROL (all at 10μM; red) in comparison to control (black). C: Activation curves for $I_{Ca,L}$ conductance in single right atrial myocytes showing that G_{max} was significantly elevated and $V_{1/2}$ was shifted to the left while under the presence of EHNA+ MIL+ROL. Data are means ±SEM, n=8 myocytes, *P<0.05 at the given membrane potentials. Refer to Table 3.1 and Table 3.2.

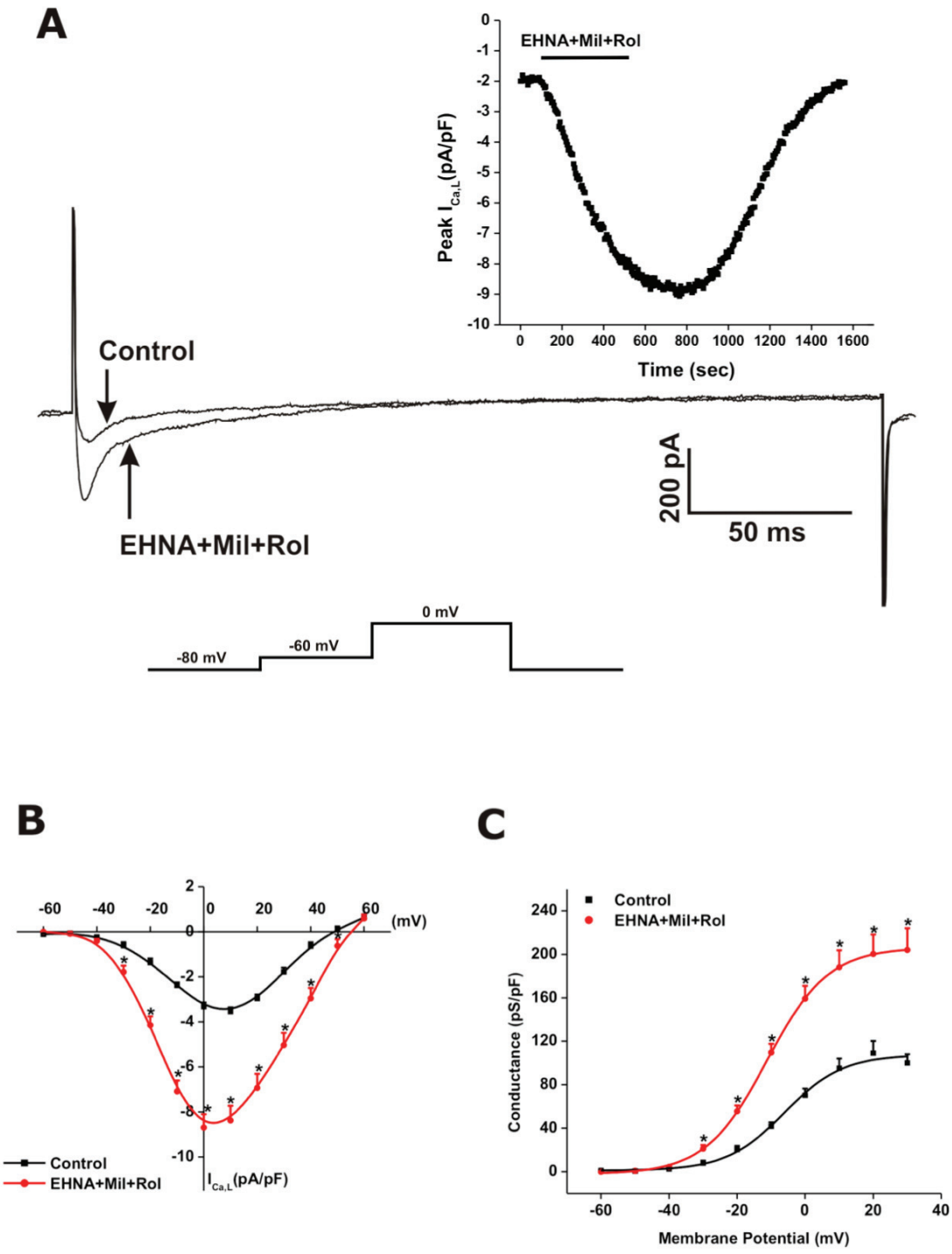
A
EHNA+Mil+Rol
Peak $I_{Ca,L}$ (pA/pF)
Time (sec)
Control
EHNA+Mil+Rol
200 pA
50 ms
0 mV
-80 mV
-60 mV
B
(mV)
Control
EHNA+Mil+Rol
$I_{Ca,L}$(pA/pF)
C
Control
EHNA+Mil+Rol
Conductance (pS/pF)
Membrane Potential (mV)

Figure 3.17.

Figure 3.18. Summary data comparing the effects of isoproterenol, isoform specific and combined PDE inhibition on peak $I_{Ca,L}$ densities in adult mouse right atrial myocytes. A: Summary bar graph illustrating the effects of ISO (1 μM; gray bar), IBMX (100 μM; red bar), EHNA (10 μM; blue bar), milrinone (MIL10 μM; green bar), rolipram (ROL 10 μM; orange bar) MIL+ROL (boht at 10 μM; white bar) and EHNA+MIL+ROL (all at 10 μM; yellow bar) on peak $I_{Ca,L}$ densities. Data are means ±SEM, with *n* values in parentheses. **P*<0.05 versus control. Refer to Table 3.1 and Table 3.2.

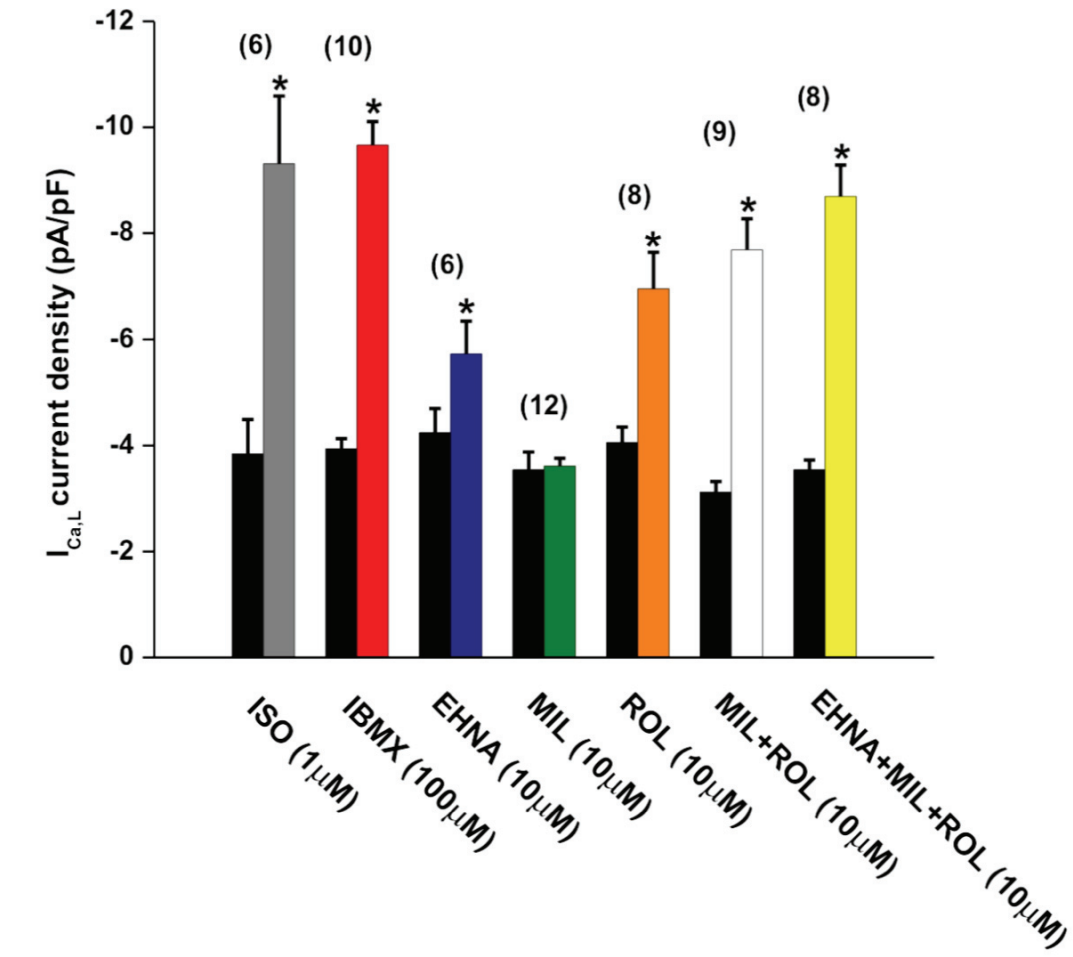
A
-12
-10
-8
-6
-4
-2
0
$I_{Ca,L}$ current density (pA/pF)
(6)
(10)
(6)
(12)
(8)
(9)
(8)
*
ISO (1μM)
IBMX (100μM)
EHNA (10μM)
MIL (10μM)
ROL (10μM)
MIL+ROL (10μM)
EHNA+MIL+ROL (10μM)

Figure 3.18.

Table 3.1. Effects of isoproterenol and PDE inhibitors on APD50 and $I_{Ca,L}$ (% change)

Drugs and concentrations	*$I_{Ca,L}$*		*APD50*	
Iso (1μM)	149 ± 17.2*	(*n*=6)	96.3 ± 7.9*	(*n*=10)
IBMX (100μM)	142 ± 8.3*	(*n*=10)	105.9 ± 15.4*	(*n*=13)
EHNA (10μM)	38.4 ± 14.5*$^{+}$	(*n*=6)	21.7 ± 9.5*$^{+}$	(*n*=13)
Milrinone (MIL; 10μM)	7.2 ± 5.6 $^{+}$	(*n*=12)	6.7 ± 4.1^{+}	(*n*=9)
Rolipram (ROL; 10μM)	71.5 ± 8.0*$^{+}$	(*n*=8)	32.2 ± 6.7*$^{+}$	(*n*=7)
MIL+ROL (10μM)	143 ± 8.9*	(*n*=9)	110.6 ± 18.8*	(*n*=10)
EHNA+MIL+ROL (10μM)	147 ± 9.7*	(*n*=8)	108 ± 15.4*	(*n*=9)

The results are presented as means ± SEM and the numbers of cells used are presented in parenthesis. Values are expressed as % variation of both basal $I_{Ca,L}$ amplitude and action potential duration at 50% repolarization times (APD50). Asterisks indicate when effects were statistically significant compared to control, *P<0.05. A plus sign indicates when the effect is statistically significant compared to IBMX, ^{+}P<0.05.

Table 3.2. Summary $I_{Ca,L}$ channel kinetics

Drugs	*Condition*	G_{max} *(pS/pF)*	$V_{1/2}$ *(mV)*	*Slope (k)*
Iso (1μM) *n*=6	Control	111.5 ± 14.3	-7.7 ± 2.7	8.1 ± 0.9
	Drug	186.9 ± 19.3*	-15.4 ± 1.6*	6.3 ± 0.2
IBMX (100μM) *n*=10	Control	112.1 ± 8.8	-9.0 ± 1.2	8.9 ± 0.5
	Drug	198.4 ± 10.4*	-18.4 ± 1.1*	7.4 ± 0.3*
EHNA (10μM) *n*=6	Control	108.2± 9.2	-8.3 ± 0.9	8.7 ± 0.4
	Drug	143.7 ± 16.0*	-7.0 ± 2.2	10.6 ± 1.5
Milrinone (MIL; 10μM) *n*=12	Control	96.7 ± 10.4	-9.6 ± 1.3	8.9 ± 0.4
	Drug	103.5 ± 9.1	-9.0 ± 1.5	9.8 ± 0.4
Rolipram (ROL; 10μM) *n*=8	Control	126 ± 8.8	-7.8 ± 1.5	8.2 ± 0.6
	Drug	186 ± 20.6*	-11.2 ± 2.2*	8.7 ± 1.2
MIL+ROL (10μM) *n*=9	Control	87.4 ± 5.7	-7.1 ± 1.6	8.1 ± 0.6
	Drug	179.7 ± 11.5*	-12.5 ± 1.4*	9.6 ± 0.6
EHNA+MIL+ROL (10μM) *n*=8	Control	108.9 ± 1.6	-6.1 ± 1.6	8.4 ± 0.5
	Drug	208.6 ± 21.3*	-11.6 ± 1.7*	8.7 ± 0.7

The results are presented as means ± SEM and the numbers of cells used are presented in parenthesis. Values are changes in G_{max}, $V_{1/2}$ and slope factor (k) from control after drug application. Asterisks indicate when effects were statistically significant compared to control, *P<0.05.

CHAPTER 4: DISCUSSION

The cyclic nucleotides, cAMP and cGMP, have proven over the years to be two very important second messengers involved in cardiac signaling (Fischmeister *et al.*, 2006). Changes in the intracellular concentration of these two second messengers is controlled by two mechanisms: 1) their synthesis via adenylyl and guanylyl cyclases and 2) their degradation by CN specific phosphosdiesterases, which hydrolize cAMP and cGMP into their biologically inactive forms (Conti & Beavo, 2007). Presently, out of the 11 known PDE families (PDE1-11), seven have been found to be expressed in the heart: PDE1, PDE2, PDE3, PDE4, PDE5, PDE8 and PDE9 (Loughney *et al.*, 1996;Meacci *et al.*, 1992;Kostic *et al.*, 1997b;Senzaki *et al.*, 2001;Soderling & Beavo, 2000;Soderling *et al.*, 1998;Onody *et al.*, 2003), of which five subtypes (PDE1-5) have demonstrated significant contributions in regards to the regulation of cardiac electrophysiology and tissue remodelling. This study however, has focused on the characterization of PDE2, PDE3 and PDE4 and their electrophysiological effects in mouse right atrial myocytes for reasons discussed in the introduction.

The ability to investigate PDE2, PDE3 and PDE4's respective functional roles within atrial myocytes has been made possible by the development of PDE selective pharmacological blockers. In the present study, we used the broad spectrum PDE inhibitor IBMX as well as the PDE selective inhibitors EHNA, which selectively inhibits PDE2, milrinone which selectively inhibits PDE3 and rolipram, which selectively inhibits PDE4, to assess the respective roles of these PDEs in their ability modulate action potentials as well as basal $I_{Ca,L}$ in mouse right atrial myocytes (Bender & Beavo, 2006).

Isoproterenol was also used as a β-adrenergic agonist for comparative purposes. The following sections will summarize our key findings and the significance of these data.

4.1 Effects of ISO on Action Potentials and $I_{Ca,L}$ in Mouse Right Atrial Myocytes

It is well known that regulation of heart function by the sympathetic nervous system is mediated by the β-adrenergic receptors that couple primarily to G_s. When these receptors are stimulated by extracellular signaling molecules, such as catecholamines, G_s stimulates AC to start synthesizing cAMP from ATP (Bers, 2002). This rise in cAMP results in an increase of cAMP-dependant PKA acticity. This occurs when cAMP binds to the regulatory domains of PKA activating the catalytic subunits, which then allow for the phosphorylation of multiple proteins found within the cell. The cardiac L-type Ca^{2+} channel is a well known example of an ion channel regulated by protein phosphorylation, resulting in an increase in the mean open probability of individual channels; hence, an increase in its macroscopic current (McDonald *et al.*, 1994;Hartzell *et al.*, 1991).

Isoproterenol (ISO), which is a well characterized β-adrenergic agonist, when bound to β_1-AR results in the stimulation of the cAMP-PKA pathway, in turn enabling it to stimulate $I_{Ca,L}$ as well as prolong APD (Verde *et al.*, 1999;Rose *et al.*, 2003). Consistent with this, my data demonstrate robust effects of ISO on both APD and peak $I_{Ca,L}$. This experiment was conducted to illustrate the maximal effects of the extracellular stimulatory pathway on intracellular cAMP levels and its ability to modulate APD and $I_{Ca,L}$. Subsequently, our goal was to investigate how the intracellular levels of cAMP could be regulated by the inhibition of phosphodiesterases.

4.2 Effects of IBMX on Action Potentials and $I_{Ca,L}$ in Mouse Right Atrial Myocytes

Application of IBMX has previously been shown to lead to large increases in basal $I_{Ca,L}$ in cardiac myoctytes of many mammals, such as guinea-pig ventricular myocytes (Mubagwa *et al.*, 1993) , rabbit ventricular myocytes (Akita *et al.*, 1994), rat ventricular myocytes (Verde *et al.*, 1999) and human atrial myocytes (Kajimoto *et al.*, 1997). Our data similarly show that IBMX results in a increase in basal $I_{Ca,L}$ in mouse atrial myocytes, which caused an increase in the duration of the action potential. This is also the first study that we know of that has tested PDE inhibition on atrial action potentials.

The fact that the application of IBMX resulted in a significant increase in $I_{Ca,L}$ in basal conditions demonstrates that, in mouse atrial myocytes, constitutively active AC generates enough cAMP and downstream PKA to be able to phosphorylate LTCCs and significantly increase $I_{Ca,L}$ peak amplitude. Although this effect may seem ubiquitous among species, this pattern is not observed in frog ventricular myocytes (Fischmeister & Hartzell, 1990;Fischmeister & Hartzell, 1991), unless pre stimulated by ISO, forskolin or cAMP, suggesting that in this species, even when all PDEs are blocked, the basal AC activity is not sufficient to increase cAMP levels past the threshold level for activation of $I_{Ca,L}$.

4.3 Effects of Subtype Specific PDE Inhibitors on Action Potentials and $I_{Ca,L}$ in Mouse Right Atrial Myocytes

We next proceeded to test three subtype specific PDE inhibitors and their ability to regulate APs and $I_{Ca,L}$ in mouse right atrial myocytes. The first compound tested was the selective PDE2 inhibitor, EHNA. Previous studies using EHNA have shown variable

results. In rat atrial and ventricular cells as well as frog ventricular cells, application of EHNA was unable to modulate $I_{Ca,L}$ in basal conditions (Fischmeister & Hartzell, 1990;Rivet-Bastide *et al.*, 1997). However, in human atrial myocytes, EHNA was able to increase $I_{Ca,L}$ to a similar extent as ISO (Rivet-Bastide *et al.*, 1997). In our experiments, EHNA significantly increased peak $I_{Ca,L}$ and prolonged the AP; but these effects were much smaller than those observed following application of ISO.

The next selective PDE inhibitor tested was milrinone, which is well known to selectively inhibit PDE3. PDE3 has received considerable attention over the years as its pharmacological block has been examined as a potential treatment for heart failure for the past two decades. In fact it is still used today in situations of acute heart failure in order to improve hemodynamic function (Zaccolo & Movsesian, 2007). Pharmacological inhibition of PDE3 activity has been associated with increases in $I_{Ca,L}$ in various species, an effect contributing to the positive inotropic effects of these inhibitors.

PDE3 inhibition has been associated with increases in basal $I_{Ca,L}$ in rabbit atrial cardiomyocytes (Kajimoto *et al.*, 1997), and increased atrial contractility in guinea pigs (Muller *et al.*, 1990). In human atrial myocytes, inhibition of PDE3 significantly increased $I_{Ca,L}$ in basal conditions to a similar extent as saturating concentrations of ISO (Kirstein *et al.*, 1995;Rivet-Bastide *et al.*, 1997). Significant increases in $I_{Ca,L}$ have been observed in human ventricular myocytes as well (Li *et al.*, 1994). This makes sense as PDE3 provides a major component of the cAMP hydrolyzing activity in the microsomal fraction of human myocardial tissue and more than 50% of the total PDE activity in the cytosolic fraction in the absence of Ca^{+}/calmodulin (Wechsler *et al.*, 2002;Hambleton *et al.*, 2005). In fact, PDE3 is the most abundant PDE subtype in the myocardial tissue of

most mammalian species. For example, in both rabbit and dog ventricular tissue, PDE3 accounts for 70-85% of the total cAMP hydrolyzing activity in microsomal fraction and about 30-40% in cytosol (Smith *et al.*, 1997;Lugnier *et al.*, 1993;Shakur *et al.*, 2002).

In the present study; however, when PDE3 was selectively blocked by milrinone there was no significant change observed on AP parameters or peak $I_{Ca,L}$ in isolated atrial myocytes. It is important to note that although PDE3 is very important in regulating intracellular cAMP, as well as contractile properties and $I_{Ca,L}$ in various mammalian species, such as human, dog and rabbit, its ability to do so in all species is not the case. In rat ventricular myocytes for example, although PDE3 and PDE4 account for about 90% of cAMP hydrolyzing activity, PDE3 inhibition under basal conditions was unable to increase $I_{Ca,L}$, but was able to do so in cells pre stimulated with ISO or when inhibited in conjunction with PDE4 (Verde *et al.*, 1999). In the presence of ISO, PDE4 inhibition was actually the one to result in the greatest increase in $I_{Ca,L,}$ not PDE3 inhibition. The inability of selective PDE3 blockade to elicit changes in $I_{Ca,L}$ in basal conditions was also observed in mouse ventricular myocytes (Kerfant *et al.*, 2007). This could be linked to the fact that in mice, contrary to most other mammalian species, PDE4 seems to be the major contributor in the regulation of intracellular cAMP hydrolyzing activity, representing 63% of total cAMP hydrolyzing activity and PDE3 contributing 28% (Osadchii, 2007;Xiang *et al.*, 2005;Georget *et al.*, 2003). Taking this into consideration, it is possible that the hydrolyzing activity of PDE3 in mouse atrial myocytes on its own is not significant enough to raise cAMP levels past threshold levels to activate $I_{Ca,L}$ or modulate other potential ionic currents based on AP data.

The next step was to then test rolipram, a PDE4 selective inhibitor, in order to investigate if in fact this PDE subtype played a more prominent role in the atrial region of the mouse heart. Upon application of the drug in both sets of experiments, APD and peak $I_{Ca,L}$ were significantly increased in comparison to control under basal conditions. This was a novel discovery, as it is the first time to our knowledge that inhibition of PDE4 alone has been shown to increase in peak $I_{Ca,L}$ or modulate the AP under basal conditions in any animal model. When increases were observed in the past under the presence of a PDE4 inhibitor, the cells had either been pre stimulated with ISO or were applied in conjunction with PDE3 inhibitors (Verde *et al.*, 1999;Kajimoto *et al.*, 1997).

To summarize, the application of EHNA a selective PDE2 inhibitor and rolipram a PDE4 selective inhibitor, both resulted in an increase in APD and peak $I_{Ca,L}$ in mouse right atrial myocytes. Although the increases observed in both sets of experiments were not as robust as those observed under the presence of the broad spectrum PDE inhibitor IBMX, they were significant in comparison to control. The PDE3 selective inhibitor milrinone; however, was unable to produce any change in APs or $I_{Ca,L}$.

The fact that PDE2 inhibition alone was able to significantly modulate both APs and $I_{Ca,L}$ and PDE3 inhibition was unable to do so may seem a bit counterintuitive based on the respective contributions of each to cAMP hydrolysis in mouse cardiac myocytes, PDE2 contributing less than 10% based on the numbers mentioned earlier (Osadchii, 2007). However, it is well known that PDE2 is a dual specific PDE able to hydrolyze both cAMP and cGMP, which is allosterically regulated by both with positive and cooperative kinetics; however, favours cGMP as a substrate and effector (Erneux *et al.*, 1981). Whereas PDE3; on the other hand, is inhibited at submicromolar concentrations of

cGMP (Vandecasteele *et al.*, 2001;Kirstein *et al.*, 1995). Therefore, it is quite possible that by inhibiting PDE2, and increasing intracellular cAMP and cGMP levels, the increase in cGMP could have blocked PDE3 as well, resulting in higher cAMP/PKA levels and enough to surpass the threshold of activation for $I_{Ca,L}$. More experiments would be needed to test this hypothesis, such as applying EHNA and milrinone in conjunction with each other to see if a similar pattern would result.

4.4 Effects of Combined PDE Inhibition on Action Potentials and $I_{Ca,L}$ in Mouse Right Atrial Myocytes

As mentioned in the above section, in mouse and rat ventricular myocytes, no changes occurred in $I_{Ca,L}$ after single inhibition of PDE2, PDE3 or PDE4 under basal conditions, but increases in $I_{Ca,L}$ did occur when PDE3 and PDE4 were inhibited in combination (Verde *et al.*, 1999;Kerfant *et al.*, 2007). Therefore, the next step in this study was to test combined PDE inhibition. The first combination examined was PDE3 and PDE4. The studies mentioned above that tested this combination in rat and mouse ventricular myocytes demonstrated that combined PDE3 and PDE4 blockade results in a significant increase in $I_{Ca,L}$ even though each inhibitor had no effect when applied alone (Verde *et al.*, 1999;Kerfant *et al.*, 2007); however, the increase observed was submaximal when compared to ISO or IBMX. When this combination was tested in human atrial myocyte, the increase in $I_{Ca,L}$ was comparable to that seen under the presence of IBMX (Kajimoto *et al.*, 1997). In our experiments, blocking both PDE3 and PDE4 together using the combination of milrinone and rolipram, resulted in a significant increase in both APD and $I_{Ca,L}$ in which the percent increases for both were highly comparable to that observed in the presence of IBMX. These data suggest that the inhibition of PDE3 can

have a considerable influence on the regulation of cAMP concentrations in mouse atrial cells, but only when inhibited in combination with PDE4. This observation could potentially explain the lack of effect observed when PDE3 is inhibited alone, as it is possible that PDE4 is compensating for the lack of PDE3 activity and was preventing cAMP levels from reaching threshold levels able to activate $I_{Ca,L}$.

We also tested the effects of combined PDE2, PDE3 and PDE4 inhibition to determine if the effects observed under single inhibition of PDE2 by EHNA would be additive. As mentioned earlier, in rat ventricular myocytes, combined PDE3 and PDE4 inhibition resulted in a submaximal increase of $I_{Ca,L}$; however, in this same study the inhibition of PDE2, PDE3 and PDE4 combined resulted in increases similar to those observed in the presence of saturating concentrations of ISO and inhibition of all PDEs by IBMX (Verde *et al.*, 1999). Our experiments; on the other hand, had already demonstrated near maximal effects in the presence of milrinone and rolipram; therefore, it was no surprise that when PDE2, PDE3 and PDE4 were inhibited in combination, no further increase in APD or $I_{Ca,L}$ was observed. This leads us to believe that PDE3 and PDE4 are still the major contributors of cAMP hydrolysis in mouse atrial myocytes, and that when they are blocked in combination they potentially saturate the levels of cAMP that can be generated by PDE inhibition within the cell from constitutively active AC. It does remain possible that cAMP levels could be further increased if stimulated by extracellular stimuli, such as ISO in addition to PDE blockade (Leroy *et al.*, 2008;Jurevicius *et al.*, 2003;Afzal *et al.*, 2011)

4.5 How Does the Atrial Region of the Myocardium Differ From the Other Regions of the Heart with Respect to the Roles of Specific PDE Subtypes?

First, to summarize the effects observed for APs and $I_{Ca,L}$ in mouse right atrial myocytes, ISO and IBMX both resulted in similar robust effects in both sets of experiments. The average percent increase observed in AP and $I_{Ca,L}$ for both were almost identical with respect to control, demonstrating that cAMP levels can be similarly increased from either extracellular stimulation of β-ARs or intracellular inhibition of PDEs (Table 3.1). However, there is also the possibility that maximal stimulation of the LTCC was reached for both but that one is in fact able to result in higher levels of intracellular cAMP than the other. cAMP levels were not measured in these experiments; therefore, this is only speculation. In the presence of specific PDE subtype inhibition, significant increases in APD and $I_{Ca,L}$ were observed following selective inhibition of PDE2 and PDE4; however, no changes in APD and $I_{Ca,L}$ were observed following single inhibition of PDE3. Combined inhibition of PDE3 and 4 elicited similar effects to ISO and IBMX. Further addition of the PDE2 inhibitor EHNA did not result in any further increase in APD or $I_{Ca,L}$.

These results differ from those observed in the ventricular region of the mouse heart when comparing the effects of single PDE2 and PDE4 inhibition on $I_{Ca,L}$ (Figure 4.1). In mouse ventricular myocytes, selective inhibition of PDE2, PDE3 and PDE4 on their own resulted in no change in peak $I_{Ca,L}$. Combined PDE3 and PDE4 inhibition results in a significant submaximal increase in $I_{Ca,L}$ and when PDE2 inhibition is added to this combination, the average percent increase observed in $I_{Ca,L}$ is similar to that observed under the presence of saturating concentrations of ISO and the broad spectrum PDE

inhibitor IBMX. These effects reflect those observed in rat ventricular myocytes (Verde *et al.*, 1999).

The pacemaker of the heart, the SAN, exhibits its own characteristic effects as well. Single inhibition of PDE2, PDE3 and PDE4, contrary to ventricular myocytes, are all able to cause a significant increase in spontaneous AP firing frequency in the SAN (Figure 4.2). Therefore, contrary to atrial myocytes, selective inhibition of PDE3 in the SAN is able to modulate the AP. This could be potentially associated with the higher levels of basal cAMP found in the SAN region of the heart (Vinogradova *et al.*, 2008); therefore, enabling PDE3 inhibition to result in a more significant contribution to the increase in intracellular cAMP potentiating the channels involved in diastolic depolarization slope which is responsible for the spontaneous firing of APs in the SAN.

Based on this comparison, it is clear that there are regional differences when it comes to the role of selective PDE subtypes and their ability to regulate mouse atrial myocyte electrophysiology. Where each PDE specific inhibitor was able to increase spontaneous AP firing frequency in the SAN, no PDE specific inhibitors were able to result in changes in $I_{Ca,L}$ in ventricular myocytes. The atria; on the other hand, which was analyzed in this study demonstrated an intermediate pattern, whereby inhibition of PDE2 and PDE4 elicited effects on APs and $I_{Ca,L}$ but the inhibition of PDE3 did not. These data therefore provide insight into the regional differences in the ability of PDEs to regulate CN sensitive ion channels.

Figure 4.1. Summary data comparing the effects of isoproterenol, isoform specific and combined PDE inhibition on peak $I_{Ca,L}$ densities in adult mouse ventricular myocytes. A: Summary bar graph illustrating the effects of ISO (1 μM; gray bar), IBMX (100 μM; red bar), EHNA (10 μM; blue bar), milrinone (MIL 10 μM; green bar), rolipram (ROL 10 μM; orange bar) MIL+ROL (both at 10 μM; white bar) and EHNA+MIL+ROL (all at 10 μM; yellow bar) on peak $I_{Ca,L}$ densities. Data are means ±SEM, with *n* values in parentheses. **P*<0.05 versus control. Data provided by R.Hua

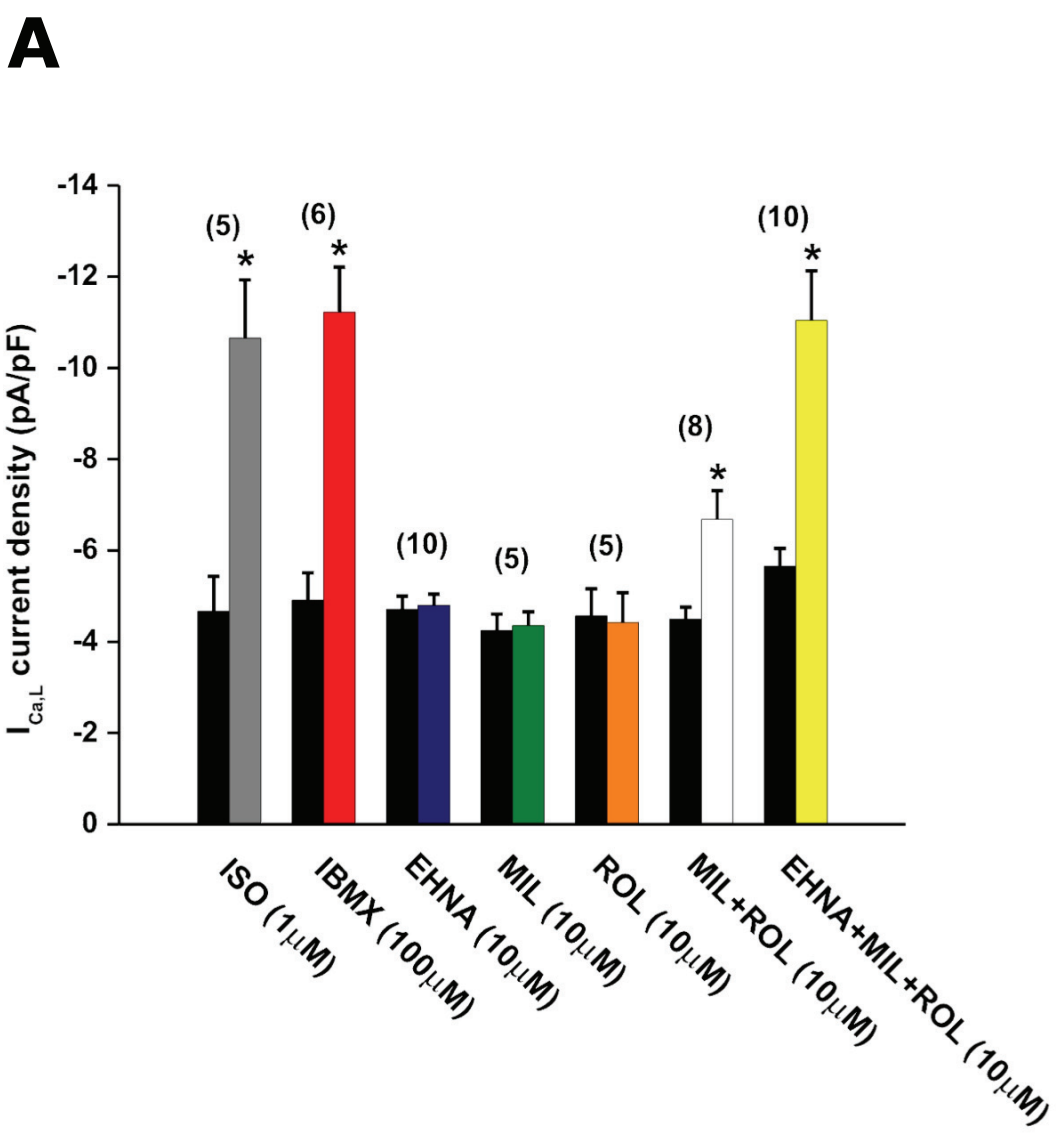
A
-14
-12
-10
-8
-6
-4
-2
0
$I_{Ca,L}$ current density (pA/pF)
(5)
(6)
(10)
(5)
(5)
(8)
(10)
*
ISO (1μM)
IBMX (100μM)
EHNA (10μM)
MIL (10μM)
ROL (10μM)
MIL+ROL (10μM)
EHNA+MIL+ROL (10μM)

Figure 4.1.

Figure 4.2. Summary data comparing the effects of isoproterenol and subtype specific PDE inhibition on spontaneous AP firing frequency in adult mouse SAN myocytes. A: Summary bar graph illustrating the effects of ISO (1 μM; gray bar), IBMX (100 μM; red bar), EHNA (10 μM; blue bar), milrinone (MIL10 μM; green bar) and rolipram (ROL 10 μM) on spontaneous AP firing frequency. Data are means ±SEM, with *n* values in parentheses. **P*<0.05 versus control. Data provided by R.Rose

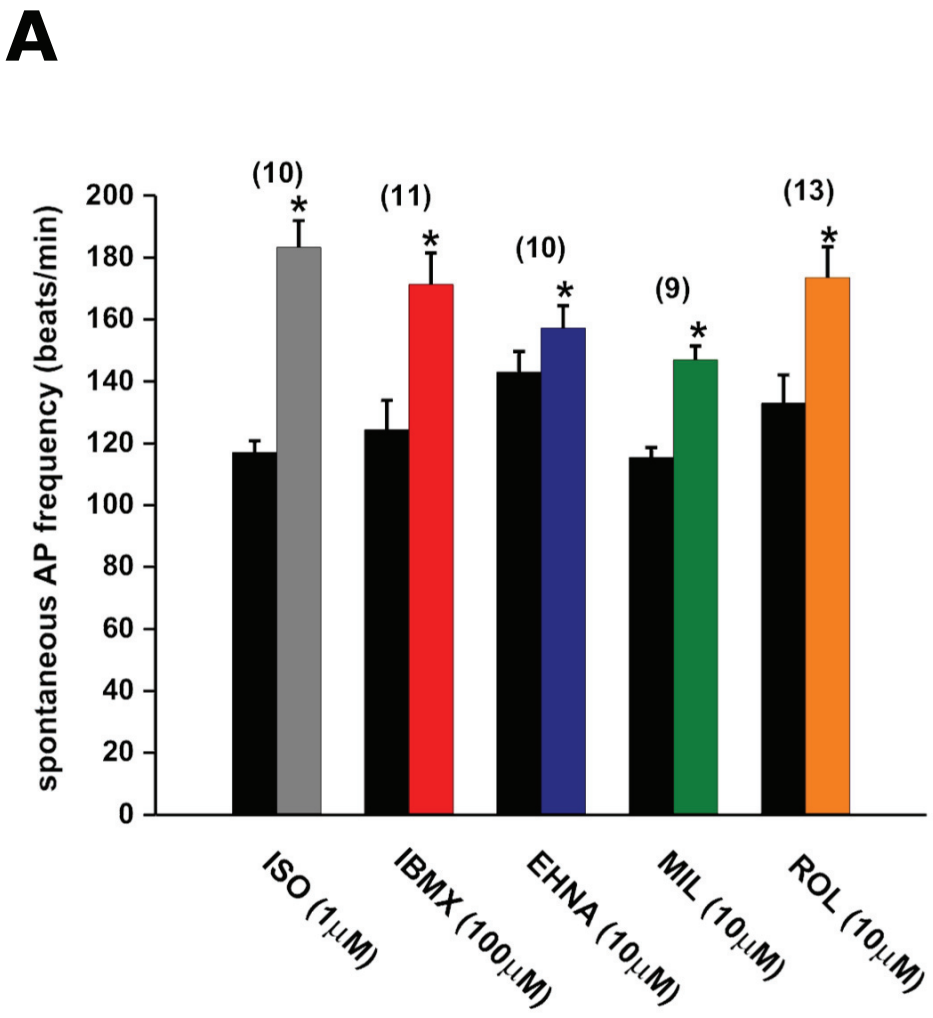
A
spontaneous AP frequency (beats/min)
200
180
160
140
120
100
80
60
40
20
0
(10)
(11)
(10)
(9)
(13)
*
ISO (1μM)
IBMX (100μM)
EHNA (10μM)
MIL (10μM)
ROL (10μM)

Figure 4.2.

4.6 Significance

Based on the findings of this study we hope to further understand the electrophysiological effects mediated by natriuretic peptides, especially with regards to their relationship to atrial arrhythmias such as atrial fibrillation. Genetic factors relating natriuretic peptides to atrial fibrillation have been studied in a family containing a frameshift mutation in the ANP gene (Hodgson-Zingman *et al.*, 2008). This mutation resulted in higher levels of circulating ANP (mutant form), causing significant shortening of the AP. ANPs ability to shorten the effective refractory period (ERP), the period of time that a new action potential cannot be initiated, has also been shown to be reduced in other human studies as well as in dogs (Crozier *et al.*, 1993;Stambler & Guo, 2005). The shortening of the AP is most likely due to a decrease in $I_{Ca,L}$ which has been observed in previous studies looking at the effects of ANP on human atrial and rabbit ventricular myocytes (Le *et al.*, 1992;Tohse *et al.*, 1995). Short ERP favours multiple-circuit reentry which is a catalyst for atrial fibrillation (Nattel, 2003). Based on the findings of this study, certain selective PDE inhibitors (EHNA and rolipram) have shown increases in APD and $I_{Ca,L}$ in mouse atrial myocytes following their application. Therefore, PDE inhibitors could potentially be used as potential a therapeutic for the prevention of atrial arrhythmias.

4.7 Limitations of the Study

The first limitation of this study would be that not all cardiac PDEs were investigated in terms of their role in regulating cardiac electrophysiology. Only PDE2, PDE3 and PDE4 were analysed alone, and in terms of combined inhibition, only combinations of PDE3 and PDE4 inhibition and PDE2, PDE3 and PDE4 were performed.

As mentioned early in the discussion, the heart expresses PDEs 1-5 along with PDE8 and PDE9 as well; therefore, it is possible that some of these other subtypes also contribute to the regulation of cardiac electrophysiology. In future experiments it would be important to investigate the respective roles of the PDE subtypes that were not looked at in this study and their ability to mediate atrial myocyte electrophysiology. It would also be important to examine the individual contributions of PDE's 1-5, as well as PDE8 and PDE9 to atrial myocyte electrophysiology under conditions pre stimulated with ISO. Another limitation of this study is that we have yet to perform any mRNA or protein expression work in these tissues. Although we can say that PDE2, PDE3 and PDE4 all have a functional role in regulating cardiac electrophysiology in mouse atrial myocytes, and their contributions to this regulation is regionally dependant, performing expression work may help clarify these findings.

4.8 Conclusion

In conclusion, although the intracellular localization and/or respective activities of specific PDE subtypes may vary depending on the animal species and/or cardiac tissue (Osadchii, 2007), the findings of this study demonstrate that the atrial region of the heart plays an intermediate role in terms of the ability for its electrophysiology to be regulated by PDEs in basal conditions when compared to the ventricular and SAN regions of the heart as discussed in section 4.5. This is also the first time that PDEs and their selective roles have been characterized in mouse atrial myocytes. These data; therefore, have implications for understanding regional differences in signaling processes in the myocardium that involve PDEs, especially those of interest to our lab which have focused on natriuretic peptides. Based on these findings and the association of natriuretic peptides

with atrial fibrillation, PDEs could potentially serve as a target for the prevention of this common cardiac arrhythmia.

REFERENCE LIST

Afzal F, Aronsen JM, Moltzau LR, Sjaastad I, Levy FO, Skomedal T, Osnes JB, & Qvigstad E (2011). Differential regulation of beta2 -adrenoceptor-mediated inotropic and lusitropic response by PDE3 and PDE4 in failing and non-failing rat cardiac ventricle. *Br J Pharmacol* **162**, 54-71.

Akita T, Joyner RW, Lu C, Kumar R, & Hartzell HC (1994). Developmental changes in modulation of calcium currents of rabbit ventricular cells by phosphodiesterase inhibitors. *Circulation* **90**, 469-478.

Ashman DF, Lipton R, Melicow MM, & Price TD (1963). Isolation of adenosine 3', 5'-monophosphate and guanosine 3', 5'-monophosphate from rat urine. *Biochem Biophys Res Commun* **11**, 330-334.

Baillie GS (2009). Compartmentalized signalling: spatial regulation of cAMP by the action of compartmentalized phosphodiesterases. *FEBS J* **276**, 1790-1799.

Baillie GS & Houslay MD (2005). Arrestin times for compartmentalised cAMP signalling and phosphodiesterase-4 enzymes. *Curr Opin Cell Biol* **17**, 129-134.

Baillie GS, Huston E, Scotland G, Hodgkin M, Gall I, Peden AH, MacKenzie C, Houslay ES, Currie R, Pettitt TR, Walmsley AR, Wakelam MJ, Warwicker J, & Houslay MD (2002). TAPAS-1, a novel microdomain within the unique N-terminal region of the PDE4A1 cAMP-specific phosphodiesterase that allows rapid, Ca2+-triggered membrane association with selectivity for interaction with phosphatidic acid. *J Biol Chem* **277**, 28298-28309.

Barnett CF & Machado RF (2006). Sildenafil in the treatment of pulmonary hypertension. *Vasc Health Risk Manag* **2**, 411-422.

Baruscotti M, Bucchi A, & Difrancesco D (2005). Physiology and pharmacology of the cardiac pacemaker ("funny") current. *Pharmacol Ther* **107**, 59-79.

Beavo JA (1995). Cyclic nucleotide phosphodiesterases: functional implications of multiple isoforms. *Physiol Rev* **75**, 725-748.

Beavo JA & Brunton LL (2002). Cyclic nucleotide research -- still expanding after half a century. *Nat Rev Mol Cell Biol* **3**, 710-718.

Beavo JA, Hansen RS, Harrison SA, Hurwitz RL, Martins TJ, & Mumby MC (1982). Identification and properties of cyclic nucleotide phosphodiesterases. *Mol Cell Endocrinol* **28**, 387-410.

Beavo JA, Hardman JG, & SUTHERLAND EW (1971). Stimulation of adenosine 3',5'-monophosphate hydrolysis by guanosine 3',5'-monophosphate. *J Biol Chem* **246**, 3841-3846.

Bender AT & Beavo JA (2006). Cyclic nucleotide phosphodiesterases: molecular regulation to clinical use. *Pharmacol Rev* **58**, 488-520.

Bers DM (2002). Cardiac excitation-contraction coupling. *Nature* **415**, 198-205.

Bers DM (2008). Calcium cycling and signaling in cardiac myocytes. *Annu Rev Physiol* **70**, 23-49.

bi-Gerges A, Richter W, Lefebvre F, Mateo P, Varin A, Heymes C, Samuel JL, Lugnier C, Conti M, Fischmeister R, & Vandecasteele G (2009). Decreased expression and activity of cAMP phosphodiesterases in cardiac hypertrophy and its impact on beta-adrenergic cAMP signals. *Circ Res* **105**, 784-792.

Bjorgo E, Solheim SA, Abrahamsen H, Baillie GS, Brown KM, Berge T, Okkenhaug K, Houslay MD, & Tasken K (2010). Cross talk between phosphatidylinositol 3-kinase and cyclic AMP (cAMP)-protein kinase a signaling pathways at the level of a protein kinase B/beta-arrestin/cAMP phosphodiesterase 4 complex. *Mol Cell Biol* **30**, 1660-1672.

Bode DC, Kanter JR, & Brunton LL (1991). Cellular distribution of phosphodiesterase isoforms in rat cardiac tissue. *Circ Res* **68**, 1070-1079.

Bolger G, Michaeli T, Martins T, St JT, Steiner B, Rodgers L, Riggs M, Wigler M, & Ferguson K (1993). A family of human phosphodiesterases homologous to the dunce learning and memory gene product of Drosophila melanogaster are potential targets for antidepressant drugs. *Mol Cell Biol* **13**, 6558-6571.

Bolger GB, McCahill A, Huston E, Cheung YF, McSorley T, Baillie GS, & Houslay MD (2003). The unique amino-terminal region of the PDE4D5 cAMP phosphodiesterase isoform confers preferential interaction with beta-arrestins. *J Biol Chem* **278**, 49230-49238.

Borlaug BA, Melenovsky V, Marhin T, Fitzgerald P, & Kass DA (2005). Sildenafil inhibits beta-adrenergic-stimulated cardiac contractility in humans. *Circulation* **112**, 2642-2649.

Bos JL (2003). Epac: a new cAMP target and new avenues in cAMP research. *Nat Rev Mol Cell Biol* **4**, 733-738.

Bou-Abboud E, Li H, & Nerbonne JM (2000). Molecular diversity of the repolarizing voltage-gated K+ currents in mouse atrial cells. *J Physiol* **529 Pt 2**, 345-358.

Brette F, Leroy J, Le Guennec JY, & Salle L (2006). Ca2+ currents in cardiac myocytes: Old story, new insights. *Prog Biophys Mol Biol* **91**, 1-82.

Brodde OE & Michel MC (1999). Adrenergic and muscarinic receptors in the human heart. *Pharmacol Rev* **51**, 651-690.

Burke JP, Sander S, Shah H, Zarotsky V, & Henk H (2010). Impact of persistence with antiplatelet therapy on recurrent ischemic stroke and predictors of nonpersistence among ischemic stroke survivors. *Curr Med Res Opin* **26**, 1023-1030.

Butcher RW & Sutherland EW (1962). Adenosine 3',5'-phosphate in biological materials. I. Purification and properties of cyclic 3',5'-nucleotide phosphodiesterase and use of this enzyme to characterize adenosine 3',5'-phosphate in human urine. *J Biol Chem* **237**, 1244-1250.

Castro LR, Schittl J, & Fischmeister R (2010). Feedback control through cGMP-dependent protein kinase contributes to differential regulation and compartmentation of cGMP in rat cardiac myocytes. *Circ Res* **107**, 1232-1240.

Castro LR, Verde I, Cooper DM, & Fischmeister R (2006). Cyclic guanosine monophosphate compartmentation in rat cardiac myocytes. *Circulation* **113**, 2221-2228.

Clapham JC & Wilderspin AF (2001). Cloning of dog heart PD. *Gene* **268**, 165-171.

Conti M & Beavo J (2007). Biochemistry and physiology of cyclic nucleotide phosphodiesterases: essential components in cyclic nucleotide signaling. *Annu Rev Biochem* **76**, 481-511.

Corbin JD, Turko IV, Beasley A, & Francis SH (2000). Phosphorylation of phosphodiesterase-5 by cyclic nucleotide-dependent protein kinase alters its catalytic and allosteric cGMP-binding activities. *Eur J Biochem* **267**, 2760-2767.

Coward RM & Carson CC (2008). Tadalafil in the treatment of erectile dysfunction. *Ther Clin Risk Manag* **4**, 1315-1330.

Crozier I, Richards AM, Foy SG, & Ikram H (1993). Electrophysiological effects of atrial natriuretic peptide on the cardiac conduction system in man. *Pacing Clin Electrophysiol* **16**, 738-742.

D'Souza SP, Davis M, & Baxter GF (2004). Autocrine and paracrine actions of natriuretic peptides in the heart. *Pharmacol Ther* **101**, 113-129.

Das A, Xi L, & Kukreja RC (2005). Phosphodiesterase-5 inhibitor sildenafil preconditions adult cardiac myocytes against necrosis and apoptosis. Essential role of nitric oxide signaling. *J Biol Chem* **280**, 12944-12955.

Defer N, Best-Belpomme M, & Hanoune J (2000). Tissue specificity and physiological relevance of various isoforms of adenylyl cyclase. *Am J Physiol Renal Physiol* **279**, F400-F416.

Dengler R, Diener HC, Schwartz A, Grond M, Schumacher H, Machnig T, Eschenfelder CC, Leonard J, Weissenborn K, Kastrup A, & Haberl R (2010). Early treatment with aspirin plus extended-release dipyridamole for transient ischaemic attack or ischaemic stroke within 24 h of symptom onset (EARLY trial): a randomised, open-label, blinded-endpoint trial. *Lancet Neurol* **9**, 159-166.

DiBianco R, Shabetai R, Kostuk W, Moran J, Schlant RC, & Wright R (1989). A comparison of oral milrinone, digoxin, and their combination in the treatment of patients with chronic heart failure. *N Engl J Med* **320**, 677-683.

Ding B, Abe J, Wei H, Huang Q, Walsh RA, Molina CA, Zhao A, Sadoshima J, Blaxall BC, Berk BC, & Yan C (2005a). Functional role of phosphodiesterase 3 in cardiomyocyte apoptosis: implication in heart failure. *Circulation* **111**, 2469-2476.

Ding B, Abe J, Wei H, Xu H, Che W, Aizawa T, Liu W, Molina CA, Sadoshima J, Blaxall BC, Berk BC, & Yan C (2005b). A positive feedback loop of phosphodiesterase 3 (PDE3) and inducible cAMP early repressor (ICER) leads to cardiomyocyte apoptosis. *Proc Natl Acad Sci U S A* **102**, 14771-14776.

Dodge KL, Khouangsathiene S, Kapiloff MS, Mouton R, Hill EV, Houslay MD, Langeberg LK, & Scott JD (2001). mAKAP assembles a protein kinase A/PDE4 phosphodiesterase cAMP signaling module. *EMBO J* **20**, 1921-1930.

Dorsey P, Keel C, Klavens M, & Hellstrom WJ (2010). Phosphodiesterase type 5 (PDE5) inhibitors for the treatment of erectile dysfunction. *Expert Opin Pharmacother* **11**, 1109-1122.

Erneux C, Couchie D, Dumont JE, Baraniak J, Stec WJ, Abbad EG, Petridis G, & Jastorff B (1981). Specificity of cyclic GMP activation of a multi-substrate cyclic nucleotide phosphodiesterase from rat liver. *Eur J Biochem* **115**, 503-510.

Eu JP, Sun J, Xu L, Stamler JS, & Meissner G (2000). The skeletal muscle calcium release channel: coupled O2 sensor and NO signaling functions. *Cell* **102**, 499-509.

Fabiato A & Fabiato F (1978). Calcium-induced release of calcium from the sarcoplasmic reticulum of skinned cells from adult human, dog, cat, rabbit, rat, and frog hearts and from fetal and new-born rat ventricles. *Ann N Y Acad Sci* **307**, 491-522.

Feron O, Saldana F, Michel JB, & Michel T (1998). The endothelial nitric-oxide synthase-caveolin regulatory cycle. *J Biol Chem* **273**, 3125-3128.

Fimia GM & Sassone-Corsi P (2001). Cyclic AMP signalling. *J Cell Sci* **114**, 1971-1972.

Fischmeister R, Castro L, bi-Gerges A, Rochais F, & Vandecasteele G (2005). Species- and tissue-dependent effects of NO and cyclic GMP on cardiac ion channels. *Comp Biochem Physiol A Mol Integr Physiol* **142**, 136-143.

Fischmeister R, Castro LR, bi-Gerges A, Rochais F, Jurevicius J, Leroy J, & Vandecasteele G (2006). Compartmentation of cyclic nucleotide signaling in the heart: the role of cyclic nucleotide phosphodiesterases. *Circ Res* **99**, 816-828.

Fischmeister R & Hartzell HC (1987). Cyclic guanosine 3',5'-monophosphate regulates the calcium current in single cells from frog ventricle. *J Physiol* **387**, 453-472.

Fischmeister R & Hartzell HC (1990). Regulation of calcium current by low-Km cyclic AMP phosphodiesterases in cardiac cells. *Mol Pharmacol* **38**, 426-433.

Fischmeister R & Hartzell HC (1991). Cyclic AMP phosphodiesterases and Ca2+ current regulation in cardiac cells. *Life Sci* **48**, 2365-2376.

Fowkes RC & McArdle CA (2000). C-type natriuretic peptide: an important neuroendocrine regulator? *Trends Endocrinol Metab* **11**, 333-338.

Francis SH, Bessay EP, Kotera J, Grimes KA, Liu L, Thompson WJ, & Corbin JD (2002). Phosphorylation of isolated human phosphodiesterase-5 regulatory domain induces an apparent conformational change and increases cGMP binding affinity. *J Biol Chem* **277**, 47581-47587.

Francis SH, Blount MA, & Corbin JD (2011). Mammalian cyclic nucleotide phosphodiesterases: molecular mechanisms and physiological functions. *Physiol Rev* **91**, 651-690.

Francis SH, Turko IV, & Corbin JD (2001). Cyclic nucleotide phosphodiesterases: relating structure and function. *Prog Nucleic Acid Res Mol Biol* **65**, 1-52.

Galie N, Brundage BH, Ghofrani HA, Oudiz RJ, Simonneau G, Safdar Z, Shapiro S, White RJ, Chan M, Beardsworth A, Frumkin L, & Barst RJ (2009). Tadalafil therapy for pulmonary arterial hypertension. *Circulation* **119**, 2894-2903.

Gao T, Puri TS, Gerhardstein BL, Chien AJ, Green RD, & Hosey MM (1997). Identification and subcellular localization of the subunits of L-type calcium channels and adenylyl cyclase in cardiac myocytes. *J Biol Chem* **272**, 19401-19407.

Garcia-Cardena G, Martasek P, Masters BS, Skidd PM, Couet J, Li S, Lisanti MP, & Sessa WC (1997). Dissecting the interaction between nitric oxide synthase (NOS) and caveolin. Functional significance of the nos caveolin binding domain in vivo. *J Biol Chem* **272**, 25437-25440.

Georget M, Mateo P, Vandecasteele G, Lipskaia L, Defer N, Hanoune J, Hoerter J, Lugnier C, & Fischmeister R (2003). Cyclic AMP compartmentation due to increased cAMP-phosphodiesterase activity in transgenic mice with a cardiac-directed expression of the human adenylyl cyclase type 8 (AC8). *FASEB J* **17**, 1380-1391.

Hambleton R, Krall J, Tikishvili E, Honeggar M, Ahmad F, Manganiello VC, & Movsesian MA (2005). Isoforms of cyclic nucleotide phosphodiesterase PDE3 and their contribution to cAMP hydrolytic activity in subcellular fractions of human myocardium. *J Biol Chem* **280**, 39168-39174.

Hamill OP, Marty A, Neher E, Sakmann B, & Sigworth FJ (1981). Improved patch-clamp techniques for high-resolution current recording from cells and cell-free membrane patches. *Pflugers Arch* **391**, 85-100.

Han SJ, Vaccari S, Nedachi T, Andersen CB, Kovacina KS, Roth RA, & Conti M (2006). Protein kinase B/Akt phosphorylation of PDE3A and its role in mammalian oocyte maturation. *EMBO J* **25**, 5716-5725.

Han X, Kobzik L, Severson D, & Shimoni Y (1998). Characteristics of nitric oxide-mediated cholinergic modulation of calcium current in rabbit sino-atrial node. *J Physiol* **509 (Pt 3)**, 741-754.

Hare JM, Givertz MM, Creager MA, & Colucci WS (1998). Increased sensitivity to nitric oxide synthase inhibition in patients with heart failure: potentiation of beta-adrenergic inotropic responsiveness. *Circulation* **97**, 161-166.

Hartzell HC & Fischmeister R (1986). Opposite effects of cyclic GMP and cyclic AMP on Ca2+ current in single heart cells. *Nature* **323**, 273-275.

Hartzell HC, Mery PF, Fischmeister R, & Szabo G (1991). Sympathetic regulation of cardiac calcium current is due exclusively to cAMP-dependent phosphorylation. *Nature* **351**, 573-576.

Hatzelmann A, Morcillo EJ, Lungarella G, Adnot S, Sanjar S, Beume R, Schudt C, & Tenor H (2010). The preclinical pharmacology of roflumilast--a selective, oral phosphodiesterase 4 inhibitor in development for chronic obstructive pulmonary disease. *Pulm Pharmacol Ther* **23**, 235-256.

Hodgson-Zingman DM, Karst ML, Zingman LV, Heublein DM, Darbar D, Herron KJ, Ballew JD, de AM, Burnett JC, Jr., & Olson TM (2008). Atrial natriuretic peptide frameshift mutation in familial atrial fibrillation. *N Engl J Med* **359**, 158-165.

Hofmann F (2005). The biology of cyclic GMP-dependent protein kinases. *J Biol Chem* **280**, 1-4.

Houslay MD (2010). Underpinning compartmentalised cAMP signalling through targeted cAMP breakdown. *Trends Biochem Sci* **35**, 91-100.

Houslay MD & Adams DR (2003). PDE4 cAMP phosphodiesterases: modular enzymes that orchestrate signalling cross-talk, desensitization and compartmentalization. *Biochem J* **370**, 1-18.

Houslay MD & Baillie GS (2003). The role of ERK2 docking and phosphorylation of PDE4 cAMP phosphodiesterase isoforms in mediating cross-talk between the cAMP and ERK signalling pathways. *Biochem Soc Trans* **31**, 1186-1190.

Houslay MD, Baillie GS, & Maurice DH (2007). cAMP-Specific phosphodiesterase-4 enzymes in the cardiovascular system: a molecular toolbox for generating compartmentalized cAMP signaling. *Circ Res* **100**, 950-966.

Houslay MD, Sullivan M, & Bolger GB (1998). The multienzyme PDE4 cyclic adenosine monophosphate-specific phosphodiesterase family: intracellular targeting, regulation, and selective inhibition by compounds exerting anti-inflammatory and antidepressant actions. *Adv Pharmacol* **44**, 225-342.

Hove-Madsen L, Mery PF, Jurevicius J, Skeberdis AV, & Fischmeister R (1996). Regulation of myocardial calcium channels by cyclic AMP metabolism. *Basic Res Cardiol* **91 Suppl 2**, 1-8.

Huai Q, Wang H, Zhang W, Colman RW, Robinson H, & Ke H (2004). Crystal structure of phosphodiesterase 9 shows orientation variation of inhibitor 3-isobutyl-1-methylxanthine binding. *Proc Natl Acad Sci U S A* **101**, 9624-9629.

Jarnaess E & Tasken K (2007). Spatiotemporal control of cAMP signalling processes by anchored signalling complexes. *Biochem Soc Trans* **35**, 931-937.

Jurevicius J, Skeberdis VA, & Fischmeister R (2003). Role of cyclic nucleotide phosphodiesterase isoforms in cAMP compartmentation following beta2-adrenergic stimulation of ICa,L in frog ventricular myocytes. *J Physiol* **551**, 239-252.

Kajimoto K, Hagiwara N, Kasanuki H, & Hosoda S (1997). Contribution of phosphodiesterase isozymes to the regulation of the L-type calcium current in human cardiac myocytes. *Br J Pharmacol* **121**, 1549-1556.

Kakkar R, Raju RV, & Sharma RK (1999). Calmodulin-dependent cyclic nucleotide phosphodiesterase (PDE1). *Cell Mol Life Sci* **55**, 1164-1186.

Kambayashi J, Liu Y, Sun B, Shakur Y, Yoshitake M, & Czerwiec F (2003). Cilostazol as a unique antithrombotic agent. *Curr Pharm Des* **9**, 2289-2302.

Keef KD, Hume JR, & Zhong J (2001). Regulation of cardiac and smooth muscle Ca(2+) channels (Ca(V)1.2a,b) by protein kinases. *Am J Physiol Cell Physiol* **281**, C1743-C1756.

Kenan Y, Murata T, Shakur Y, Degerman E, & Manganiello VC (2000). Functions of the N-terminal region of cyclic nucleotide phosphodiesterase 3 (PDE 3) isoforms. *J Biol Chem* **275**, 12331-12338.

Kerfant BG, Zhao D, Lorenzen-Schmidt I, Wilson LS, Cai S, Chen SR, Maurice DH, & Backx PH (2007). PI3Kgamma is required for PDE4, not PDE3, activity in subcellular microdomains containing the sarcoplasmic reticular calcium ATPase in cardiomyocytes. *Circ Res* **101**, 400-408.

Kirstein M, Rivet-Bastide M, Hatem S, Benardeau A, Mercadier JJ, & Fischmeister R (1995). Nitric oxide regulates the calcium current in isolated human atrial myocytes. *J Clin Invest* **95**, 794-802.

Kostic MM, Erdogan S, Rena G, Borchert G, Hoch B, Bartel S, Scotland G, Huston E, Houslay MD, & Krause EG (1997a). Altered expression of PDE1 and PDE4 cyclic nucleotide phosphodiesterase isoforms in 7-oxo-prostacyclin-preconditioned rat heart. *J Mol Cell Cardiol* **29**, 3135-3146.

Kotera J, Fujishige K, Akatsuka H, Imai Y, Yanaka N, & Omori K (1998). Novel alternative splice variants of cGMP-binding cGMP-specific phosphodiesterase. *J Biol Chem* **273**, 26982-26990.

Kuhn M (2003). Structure, regulation, and function of mammalian membrane guanylyl cyclase receptors, with a focus on guanylyl cyclase-A. *Circ Res* **93**, 700-709.

Laflamme MA & Becker PL (1999). G(s) and adenylyl cyclase in transverse tubules of heart: implications for cAMP-dependent signaling. *Am J Physiol* **277**, H1841-H1848.

Layland J, Li JM, & Shah AM (2002). Role of cyclic GMP-dependent protein kinase in the contractile response to exogenous nitric oxide in rat cardiac myocytes. *J Physiol* **540**, 457-467.

Layland J, Solaro RJ, & Shah AM (2005). Regulation of cardiac contractile function by troponin I phosphorylation. *Cardiovasc Res* **66**, 12-21.

Le GB, Deroubaix E, Couetil JP, & Coraboeuf E (1992). Effects of atrionatriuretic factor on Ca2+ current and Cai-independent transient outward K+ current in human atrial cells. *Pflugers Arch* **421**, 486-491.

Lehnart SE, Wehrens XH, Reiken S, Warrier S, Belevych AE, Harvey RD, Richter W, Jin SL, Conti M, & Marks AR (2005). Phosphodiesterase 4D deficiency in the ryanodine-receptor complex promotes heart failure and arrhythmias. *Cell* **123**, 25-35.

Leroy J, bi-Gerges A, Nikolaev VO, Richter W, Lechene P, Mazet JL, Conti M, Fischmeister R, & Vandecasteele G (2008). Spatiotemporal dynamics of beta-adrenergic cAMP signals and L-type Ca2+ channel regulation in adult rat ventricular myocytes: role of phosphodiesterases. *Circ Res* **102**, 1091-1100.

Li Q, Himmel HM, & Ravens U (1994). Effects of the new phosphodiesterase-III inhibitor R80122 on contractility and calcium current in human cardiac tissue. *J Cardiovasc Pharmacol* **24**, 133-143.

Liu L, Underwood T, Li H, Pamukcu R, & Thompson WJ (2002). Specific cGMP binding by the cGMP binding domains of cGMP-binding cGMP specific phosphodiesterase. *Cell Signal* **14**, 45-51.

Lohmann SM, Fischmeister R, & Walter U (1991). Signal transduction by cGMP in heart. *Basic Res Cardiol* **86**, 503-514.

Lomax AE, Kondo CS, & Giles WR (2003). Comparison of time- and voltage-dependent K+ currents in myocytes from left and right atria of adult mice. *Am J Physiol Heart Circ Physiol* **285**, H1837-H1848.

Loughney K, Martins TJ, Harris EA, Sadhu K, Hicks JB, Sonnenburg WK, Beavo JA, & Ferguson K (1996). Isolation and characterization of cDNAs corresponding to two human calcium, calmodulin-regulated, 3',5'-cyclic nucleotide phosphodiesterases. *J Biol Chem* **271**, 796-806.

Lugnier C (2006). Cyclic nucleotide phosphodiesterase (PDE) superfamily: a new target for the development of specific therapeutic agents. *Pharmacol Ther* **109**, 366-398.

Lugnier C, Gauthier C, Le BA, & Soustre H (1992). Cyclic nucleotide phosphodiesterases from frog atrial fibers: isolation and drug sensitivities. *Am J Physiol* **262**, H654-H660.

Lugnier C, Muller B, Le BA, Beaudry C, & Rousseau E (1993). Characterization of indolidan- and rolipram-sensitive cyclic nucleotide phosphodiesterases in canine and human cardiac microsomal fractions. *J Pharmacol Exp Ther* **265**, 1142-1151.

Lukowski R, Rybalkin SD, Loga F, Leiss V, Beavo JA, & Hofmann F (2010). Cardiac hypertrophy is not amplified by deletion of cGMP-dependent protein kinase I in cardiomyocytes. *Proc Natl Acad Sci U S A* **107**, 5646-5651.

MacKenzie SJ, Baillie GS, McPhee I, Bolger GB, & Houslay MD (2000). ERK2 mitogen-activated protein kinase binding, phosphorylation, and regulation of the PDE4D cAMP-specific phosphodiesterases. The involvement of COOH-terminal docking sites and NH2-terminal UCR regions. *J Biol Chem* **275**, 16609-16617.

MacKenzie SJ, Baillie GS, McPhee I, MacKenzie C, Seamons R, McSorley T, Millen J, Beard MB, van HG, & Houslay MD (2002). Long PDE4 cAMP specific phosphodiesterases are activated by protein kinase A-mediated phosphorylation of a single serine residue in Upstream Conserved Region 1 (UCR1). *Br J Pharmacol* **136**, 421-433.

MacLennan DH & Kranias EG (2003). Phospholamban: a crucial regulator of cardiac contractility. *Nat Rev Mol Cell Biol* **4**, 566-577.

Mangoni ME & Nargeot J (2008). Genesis and regulation of the heart automaticity. *Physiol Rev* **88**, 919-982.

Martinez SE, Beavo JA, & Hol WG (2002). GAF domains: two-billion-year-old molecular switches that bind cyclic nucleotides. *Mol Interv* **2**, 317-323.

Martins TJ, Mumby MC, & Beavo JA (1982). Purification and characterization of a cyclic GMP-stimulated cyclic nucleotide phosphodiesterase from bovine tissues. *J Biol Chem* **257**, 1973-1979.

Marx SO, Reiken S, Hisamatsu Y, Jayaraman T, Burkhoff D, Rosemblit N, & Marks AR (2000). PKA phosphorylation dissociates FKBP12.6 from the calcium release channel (ryanodine receptor): defective regulation in failing hearts. *Cell* **101**, 365-376.

Massion PB & Balligand JL (2003). Modulation of cardiac contraction, relaxation and rate by the endothelial nitric oxide synthase (eNOS): lessons from genetically modified mice. *J Physiol* **546**, 63-75.

Maurice DH, Palmer D, Tilley DG, Dunkerley HA, Netherton SJ, Raymond DR, Elbatarny HS, & Jimmo SL (2003). Cyclic nucleotide phosphodiesterase activity, expression, and targeting in cells of the cardiovascular system. *Mol Pharmacol* **64**, 533-546.

McCahill AC, Huston E, Li X, & Houslay MD (2008). PDE4 associates with different scaffolding proteins: modulating interactions as treatment for certain diseases. *Handb Exp Pharmacol* 125-166.

McDonald TF, Pelzer S, Trautwein W, & Pelzer DJ (1994). Regulation and modulation of calcium channels in cardiac, skeletal, and smooth muscle cells. *Physiol Rev* **74**, 365-507.

Meacci E, Taira M, Moos M, Jr., Smith CJ, Movsesian MA, Degerman E, Belfrage P, & Manganiello V (1992). Molecular cloning and expression of human myocardial cGMP-inhibited cAMP phosphodiesterase. *Proc Natl Acad Sci U S A* **89**, 3721-3725.

Mebazaa A, Pitsis AA, Rudiger A, Toller W, Longrois D, Ricksten SE, Bobek I, De HS, Wieselthaler G, Schirmer U, von Segesser LK, Sander M, Poldermans D, Ranucci M, Karpati PC, Wouters P, Seeberger M, Schmid ER, Weder W, & Follath F (2010). Clinical review: practical recommendations on the management of perioperative heart failure in cardiac surgery. *Crit Care* **14**, 201.

Mery PF, Lohmann SM, Walter U, & Fischmeister R (1991). Ca2+ current is regulated by cyclic GMP-dependent protein kinase in mammalian cardiac myocytes. *Proc Natl Acad Sci U S A* **88**, 1197-1201.

Mery PF, Pavoine C, Pecker F, & Fischmeister R (1995). Erythro-9-(2-hydroxy-3-nonyl)adenine inhibits cyclic GMP-stimulated phosphodiesterase in isolated cardiac myocytes. *Mol Pharmacol* **48**, 121-130.

Miller CL, Oikawa M, Cai Y, Wojtovich AP, Nagel DJ, Xu X, Xu H, Florio V, Rybalkin SD, Beavo JA, Chen YF, Li JD, Blaxall BC, Abe J, & Yan C (2009). Role of Ca2+/calmodulin-stimulated cyclic nucleotide phosphodiesterase 1 in mediating cardiomyocyte hypertrophy. *Circ Res* **105**, 956-964.

Mohan P, Brutsaert DL, Paulus WJ, & Sys SU (1996). Myocardial contractile response to nitric oxide and cGMP. *Circulation* **93**, 1223-1229.

Moncada GA, Kishi Y, Numano F, Hiraoka M, & Sawanobori T (2000). Effects of acidosis and NO on nicorandil-activated K(ATP) channels in guinea-pig ventricular myocytes. *Br J Pharmacol* **131**, 1097-1104.

Mongillo M, Tocchetti CG, Terrin A, Lissandron V, Cheung YF, Dostmann WR, Pozzan T, Kass DA, Paolocci N, Houslay MD, & Zaccolo M (2006). Compartmentalized phosphodiesterase-2 activity blunts beta-adrenergic cardiac inotropy via an NO/cGMP-dependent pathway. *Circ Res* **98**, 226-234.

Morel E, Marcantoni A, Gastineau M, Birkedal R, Rochais F, Garnier A, Lompre AM, Vandecasteele G, & Lezoualc'h F (2005). cAMP-binding protein Epac induces cardiomyocyte hypertrophy. *Circ Res* **97**, 1296-1304.

Movsesian MA (2000). Therapeutic potential of cyclic nucleotide phosphodiesterase inhibitors in heart failure. *Expert Opin Investig Drugs* **9**, 963-973.

Movsesian MA (2002). PDE3 cyclic nucleotide phosphodiesterases and the compartmentation of cyclic nucleotide-mediated signalling in cardiac myocytes. *Basic Res Cardiol* **97 Suppl 1**, I83-I90.

Movsesian MA & Alharethi R (2002). Inhibitors of cyclic nucleotide phosphodiesterase PDE3 as adjunct therapy for dilated cardiomyopathy. *Expert Opin Investig Drugs* **11**, 1529-1536.

Mubagwa K, Shirayama T, Moreau M, & Pappano AJ (1993). Effects of PDE inhibitors and carbachol on the L-type Ca current in guinea pig ventricular myocytes. *Am J Physiol* **265**, H1353-H1363.

Muller B, Lugnier C, & Stoclet JC (1990). Involvement of rolipram-sensitive cyclic AMP phosphodiesterase in the regulation of cardiac contraction. *J Cardiovasc Pharmacol* **16**, 796-803.

Muller B, Stoclet JC, & Lugnier C (1992). Cytosolic and membrane-bound cyclic nucleotide phosphodiesterases from guinea pig cardiac ventricles. *Eur J Pharmacol* **225**, 263-272.

Muller FU, Boknik P, Knapp J, Linck B, Luss H, Neumann J, & Schmitz W (2001). Activation and inactivation of cAMP-response element-mediated gene transcription in cardiac myocytes. *Cardiovasc Res* **52**, 95-102.

Murthy KS & Makhlouf GM (2000). Heterologous desensitization mediated by G protein-specific binding to caveolin. *J Biol Chem* **275**, 30211-30219.

Nattel S (2003). Atrial electrophysiology and mechanisms of atrial fibrillation. *J Cardiovasc Pharmacol Ther* **8 Suppl 1**, S5-11.

Nerbonne JM & Kass RS (2005). Molecular physiology of cardiac repolarization. *Physiol Rev* **85**, 1205-1253.

Nikolaev VO, Bunemann M, Schmitteckert E, Lohse MJ, & Engelhardt S (2006). Cyclic AMP imaging in adult cardiac myocytes reveals far-reaching beta1-adrenergic but locally confined beta2-adrenergic receptor-mediated signaling. *Circ Res* **99**, 1084-1091.

Omori K & Kotera J (2007). Overview of PDEs and their regulation. *Circ Res* **100**, 309-327.

Onody A, Zvara A, Hackler L, Jr., Vigh L, Ferdinandy P, & Puskas LG (2003). Effect of classic preconditioning on the gene expression pattern of rat hearts: a DNA microarray study. *FEBS Lett* **536**, 35-40.

Osadchii OE (2007). Myocardial phosphodiesterases and regulation of cardiac contractility in health and cardiac disease. *Cardiovasc Drugs Ther* **21**, 171-194.

Padayatti PS, Pattanaik P, Ma X, & van den AF (2004). Structural insights into the regulation and the activation mechanism of mammalian guanylyl cyclases. *Pharmacol Ther* **104**, 83-99.

Patrucco E, Notte A, Barberis L, Selvetella G, Maffei A, Brancaccio M, Marengo S, Russo G, Azzolino O, Rybalkin SD, Silengo L, Altruda F, Wetzker R, Wymann MP, Lembo G, & Hirsch E (2004). PI3Kgamma modulates the cardiac response to chronic pressure overload by distinct kinase-dependent and -independent effects. *Cell* **118**, 375-387.

Pawson T & Scott JD (2005). Protein phosphorylation in signaling--50 years and counting. *Trends Biochem Sci* **30**, 286-290.

Perry SJ, Baillie GS, Kohout TA, McPhee I, Magiera MM, Ang KL, Miller WE, McLean AJ, Conti M, Houslay MD, & Lefkowitz RJ (2002). Targeting of cyclic AMP degradation to beta 2-adrenergic receptors by beta-arrestins. *Science* **298**, 834-836.

Podzuweit T, Nennstiel P, & Muller A (1995). Isozyme selective inhibition of cGMP-stimulated cyclic nucleotide phosphodiesterases by erythro-9-(2-hydroxy-3-nonyl) adenine. *Cell Signal* **7**, 733-738.

Potter LR, bbey-Hosch S, & Dickey DM (2006). Natriuretic peptides, their receptors, and cyclic guanosine monophosphate-dependent signaling functions. *Endocr Rev* **27**, 47-72.

Preckel B, Kojda G, Schlack W, Ebel D, Kottenberg K, Noack E, & Thamer V (1997). Inotropic effects of glyceryl trinitrate and spontaneous NO donors in the dog heart. *Circulation* **96**, 2675-2682.

Pyriochou A & Papapetropoulos A (2005). Soluble guanylyl cyclase: more secrets revealed. *Cell Signal* **17**, 407-413.

Rae J, Cooper K, Gates P, & Watsky M (1991). Low access resistance perforated patch recordings using amphotericin B. *J Neurosci Methods* **37**, 15-26.

Richter W & Conti M (2002). Dimerization of the type 4 cAMP-specific phosphodiesterases is mediated by the upstream conserved regions (UCRs). *J Biol Chem* **277**, 40212-40221.

Richter W, Day P, Agrawal R, Bruss MD, Granier S, Wang YL, Rasmussen SG, Horner K, Wang P, Lei T, Patterson AJ, Kobilka B, & Conti M (2008). Signaling from beta1- and beta2-adrenergic receptors is defined by differential interactions with PDE4. *EMBO J* **27**, 384-393.

Richter W, Xie M, Scheitrum C, Krall J, Movsesian MA, & Conti M (2010). Conserved expression and functions of PDE4 in rodent and human heart. *Basic Res Cardiol*.

Rivet-Bastide M, Vandecasteele G, Hatem S, Verde I, Benardeau A, Mercadier JJ, & Fischmeister R (1997). cGMP-stimulated cyclic nucleotide phosphodiesterase regulates the basal calcium current in human atrial myocytes. *J Clin Invest* **99**, 2710-2718.

Rochais F, bi-Gerges A, Horner K, Lefebvre F, Cooper DM, Conti M, Fischmeister R, & Vandecasteele G (2006). A specific pattern of phosphodiesterases controls the cAMP signals generated by different Gs-coupled receptors in adult rat ventricular myocytes. *Circ Res* **98**, 1081-1088.

Rose RA & Giles WR (2008). Natriuretic peptide C receptor signalling in the heart and vasculature. *J Physiol* **586**, 353-366.

Rose RA, Kabir MG, & Backx PH (2007). Altered heart rate and sinoatrial node function in mice lacking the cAMP regulator phosphoinositide 3-kinase-gamma. *Circ Res* **101**, 1274-1282.

Rose RA, Lomax AE, & Giles WR (2003). Inhibition of L-type Ca2+ current by C-type natriuretic peptide in bullfrog atrial myocytes: an NPR-C-mediated effect. *Am J Physiol Heart Circ Physiol* **285**, H2454-H2462.

Rosman GJ, Martins TJ, Sonnenburg WK, Beavo JA, Ferguson K, & Loughney K (1997). Isolation and characterization of human cDNAs encoding a cGMP-stimulated 3',5'-cyclic nucleotide phosphodiesterase. *Gene* **191**, 89-95.

Rybalkin SD, Bornfeldt KE, Sonnenburg WK, Rybalkina IG, Kwak KS, Hanson K, Krebs EG, & Beavo JA (1997). Calmodulin-stimulated cyclic nucleotide phosphodiesterase (PDE1C) is induced in human arterial smooth muscle cells of the synthetic, proliferative phenotype. *J Clin Invest* **100**, 2611-2621.

Rybalkin SD, Rybalkina I, Beavo JA, & Bornfeldt KE (2002). Cyclic nucleotide phosphodiesterase 1C promotes human arterial smooth muscle cell proliferation. *Circ Res* **90**, 151-157.

Schroder F, Klein G, Fiedler B, Bastein M, Schnasse N, Hillmer A, Ames S, Gambaryan S, Drexler H, Walter U, Lohmann SM, & Wollert KC (2003). Single L-type Ca(2+) channel regulation by cGMP-dependent protein kinase type I in adult cardiomyocytes from PKG I transgenic mice. *Cardiovasc Res* **60**, 268-277.

Schwencke C, Yamamoto M, Okumura S, Toya Y, Kim SJ, & Ishikawa Y (1999). Compartmentation of cyclic adenosine 3',5'-monophosphate signaling in caveolae. *Mol Endocrinol* **13**, 1061-1070.

Sears CE, Bryant SM, Ashley EA, Lygate CA, Rakovic S, Wallis HL, Neubauer S, Terrar DA, & Casadei B (2003). Cardiac neuronal nitric oxide synthase isoform regulates myocardial contraction and calcium handling. *Circ Res* **92**, e52-e59.

Semigran MJ (2005). Type 5 phosphodiesterase inhibition: the focus shifts to the heart. *Circulation* **112**, 2589-2591.

Senzaki H, Smith CJ, Juang GJ, Isoda T, Mayer SP, Ohler A, Paolocci N, Tomaselli GF, Hare JM, & Kass DA (2001). Cardiac phosphodiesterase 5 (cGMP-specific) modulates beta-adrenergic signaling in vivo and is down-regulated in heart failure. *FASEB J* **15**, 1718-1726.

Shah AM & MacCarthy PA (2000). Paracrine and autocrine effects of nitric oxide on myocardial function. *Pharmacol Ther* **86**, 49-86.

Shakur Y, Fong M, Hensley J, Cone J, Movsesian MA, Kambayashi J, Yoshitake M, & Liu Y (2002). Comparison of the effects of cilostazol and milrinone on cAMP-PDE activity, intracellular cAMP and calcium in the heart. *Cardiovasc Drugs Ther* **16**, 417-427.

Shakur Y, Takeda K, Kenan Y, Yu ZX, Rena G, Brandt D, Houslay MD, Degerman E, Ferrans VJ, & Manganiello VC (2000). Membrane localization of cyclic nucleotide phosphodiesterase 3 (PDE3). Two N-terminal domains are required for the efficient targeting to, and association of, PDE3 with endoplasmic reticulum. *J Biol Chem* **275**, 38749-38761.

Smith CJ, Huang R, Sun D, Ricketts S, Hoegler C, Ding JZ, Moggio RA, & Hintze TH (1997). Development of decompensated dilated cardiomyopathy is associated with decreased gene expression and activity of the milrinone-sensitive cAMP phosphodiesterase PDE3A. *Circulation* **96**, 3116-3123.

Soderling SH, Bayuga SJ, & Beavo JA (1998). Cloning and characterization of a cAMP-specific cyclic nucleotide phosphodiesterase. *Proc Natl Acad Sci U S A* **95**, 8991-8996.

Soderling SH & Beavo JA (2000). Regulation of cAMP and cGMP signaling: new phosphodiesterases and new functions. *Curr Opin Cell Biol* **12**, 174-179.

Sonnenburg WK, Mullaney PJ, & Beavo JA (1991). Molecular cloning of a cyclic GMP-stimulated cyclic nucleotide phosphodiesterase cDNA. Identification and distribution of isozyme variants. *J Biol Chem* **266**, 17655-17661.

Sonnenburg WK, Seger D, & Beavo JA (1993). Molecular cloning of a cDNA encoding the "61-kDa" calmodulin-stimulated cyclic nucleotide phosphodiesterase. Tissue-specific expression of structurally related isoforms. *J Biol Chem* **268**, 645-652.

Stambler BS & Guo GB (2005). Atrial natriuretic peptide has dose-dependent, autonomically mediated effects on atrial refractoriness and repolarization in anesthetized dogs. *J Cardiovasc Electrophysiol* **16**, 1341-1347.

Sutherland EW & Rall TW (1958). Fractionation and characterization of a cyclic adenine ribonucleotide formed by tissue particles. *J Biol Chem* **232**, 1077-1091.

Takasago T, Imagawa T, & Shigekawa M (1989). Phosphorylation of the cardiac ryanodine receptor by cAMP-dependent protein kinase. *J Biochem* **106**, 872-877.

Takimoto E, Champion HC, Belardi D, Moslehi J, Mongillo M, Mergia E, Montrose DC, Isoda T, Aufiero K, Zaccolo M, Dostmann WR, Smith CJ, & Kass DA (2005a). cGMP catabolism by phosphodiesterase 5A regulates cardiac adrenergic stimulation by NOS3-dependent mechanism. *Circ Res* **96**, 100-109.

Takimoto E, Champion HC, Li M, Belardi D, Ren S, Rodriguez ER, Bedja D, Gabrielson KL, Wang Y, & Kass DA (2005b). Chronic inhibition of cyclic GMP phosphodiesterase 5A prevents and reverses cardiac hypertrophy. *Nat Med* **11**, 214-222.

Thompson WJ, Terasaki WL, Epstein PM, & Strada SJ (1979). Assay of cyclic nucleotide phosphodiesterase and resolution of multiple molecular forms of the enzyme. *Adv Cyclic Nucleotide Res* **10**, 69-92.

Tohse N, Nakaya H, Takeda Y, & Kanno M (1995). Cyclic GMP-mediated inhibition of L-type Ca2+ channel activity by human natriuretic peptide in rabbit heart cells. *Br J Pharmacol* **114**, 1076-1082.

Tsang TS, Miyasaka Y, Barnes ME, & Gersh BJ (2005). Epidemiological profile of atrial fibrillation: a contemporary perspective. *Prog Cardiovasc Dis* **48**, 1-8.

Vandecasteele G, Rochais F, bi-Gerges A, & Fischmeister R (2006). Functional localization of cAMP signalling in cardiac myocytes. *Biochem Soc Trans* **34**, 484-488.

Vandecasteele G, Verde I, Rucker-Martin C, Donzeau-Gouge P, & Fischmeister R (2001). Cyclic GMP regulation of the L-type Ca(2+) channel current in human atrial myocytes. *J Physiol* **533**, 329-340.

Vandeput F, Wolda SL, Krall J, Hambleton R, Uher L, McCaw KN, Radwanski PB, Florio V, & Movsesian MA (2007). Cyclic nucleotide phosphodiesterase PDE1C1 in human cardiac myocytes. *J Biol Chem* **282**, 32749-32757.

Verde I, Pahlke G, Salanova M, Zhang G, Wang S, Coletti D, Onuffer J, Jin SL, & Conti M (2001). Myomegalin is a novel protein of the golgi/centrosome that interacts with a cyclic nucleotide phosphodiesterase. *J Biol Chem* **276**, 11189-11198.

Verde I, Vandecasteele G, Lezoualc'h F, & Fischmeister R (1999). Characterization of the cyclic nucleotide phosphodiesterase subtypes involved in the regulation of the L-type Ca2+ current in rat ventricular myocytes. *Br J Pharmacol* **127**, 65-74.

Vila-Petroff MG, Younes A, Egan J, Lakatta EG, & Sollott SJ (1999). Activation of distinct cAMP-dependent and cGMP-dependent pathways by nitric oxide in cardiac myocytes. *Circ Res* **84**, 1020-1031.

Vinogradova TM, Sirenko S, Lyashkov AE, Younes A, Li Y, Zhu W, Yang D, Ruknudin AM, Spurgeon H, & Lakatta EG (2008). Constitutive phosphodiesterase activity restricts spontaneous beating rate of cardiac pacemaker cells by suppressing local Ca2+ releases. *Circ Res* **102**, 761-769.

Wang H, Kohr MJ, Traynham CJ, & Ziolo MT (2009). Phosphodiesterase 5 restricts NOS3/Soluble guanylate cyclase signaling to L-type Ca2+ current in cardiac myocytes. *J Mol Cell Cardiol* **47**, 304-314.

Wang H, Liu Y, Chen Y, Robinson H, & Ke H (2005). Multiple elements jointly determine inhibitor selectivity of cyclic nucleotide phosphodiesterases 4 and 7. *J Biol Chem* **280**, 30949-30955.

Wang TJ, Larson MG, Levy D, Vasan RS, Leip EP, Wolf PA, D'Agostino RB, Murabito JM, Kannel WB, & Benjamin EJ (2003). Temporal relations of atrial fibrillation and congestive heart failure and their joint influence on mortality: the Framingham Heart Study. *Circulation* **107**, 2920-2925.

Wechsler J, Choi YH, Krall J, Ahmad F, Manganiello VC, & Movsesian MA (2002). Isoforms of cyclic nucleotide phosphodiesterase PDE3A in cardiac myocytes. *J Biol Chem* **277**, 38072-38078.

Wedel BJ & Garbers DL (1998). Guanylyl cyclases: approaching year thirty. *Trends Endocrinol Metab* **9**, 213-219.

Wehrens XH, Lehnart SE, & Marks AR (2005). Intracellular calcium release and cardiac disease. *Annu Rev Physiol* **67**, 69-98.

Wolf PA, Abbott RD, & Kannel WB (1991). Atrial fibrillation as an independent risk factor for stroke: the Framingham Study. *Stroke* **22**, 983-988.

Wu AY, Tang XB, Martinez SE, Ikeda K, & Beavo JA (2004). Molecular determinants for cyclic nucleotide binding to the regulatory domains of phosphodiesterase 2A. *J Biol Chem* **279**, 37928-37938.

Xiang Y, Naro F, Zoudilova M, Jin SL, Conti M, & Kobilka B (2005). Phosphodiesterase 4D is required for beta2 adrenoceptor subtype-specific signaling in cardiac myocytes. *Proc Natl Acad Sci U S A* **102**, 909-914.

Xiao RP, Zhu W, Zheng M, Chakir K, Bond R, Lakatta EG, & Cheng H (2004). Subtype-specific beta-adrenoceptor signaling pathways in the heart and their potential clinical implications. *Trends Pharmacol Sci* **25**, 358-365.

Xu KY, Huso DL, Dawson TM, Bredt DS, & Becker LC (1999). Nitric oxide synthase in cardiac sarcoplasmic reticulum. *Proc Natl Acad Sci U S A* **96**, 657-662.

Xu L, Eu JP, Meissner G, & Stamler JS (1998). Activation of the cardiac calcium release channel (ryanodine receptor) by poly-S-nitrosylation. *Science* **279**, 234-237.

Xu RX, Hassell AM, Vanderwall D, Lambert MH, Holmes WD, Luther MA, Rocque WJ, Milburn MV, Zhao Y, Ke H, & Nolte RT (2000). Atomic structure of PDE4: insights into phosphodiesterase mechanism and specificity. *Science* **288**, 1822-1825.

Yan C, Miller CL, & Abe J (2007). Regulation of phosphodiesterase 3 and inducible cAMP early repressor in the heart. *Circ Res* **100**, 489-501.

Yanaka N, Kurosawa Y, Minami K, Kawai E, & Omori K (2003). cGMP-phosphodiesterase activity is up-regulated in response to pressure overload of rat ventricles. *Biosci Biotechnol Biochem* **67**, 973-979.

Yang Q, Paskind M, Bolger G, Thompson WJ, Repaske DR, Cutler LS, & Epstein PM (1994). A novel cyclic GMP stimulated phosphodiesterase from rat brain. *Biochem Biophys Res Commun* **205**, 1850-1858.

Zaccolo M (2009). cAMP signal transduction in the heart: understanding spatial control for the development of novel therapeutic strategies. *Br J Pharmacol* **158**, 50-60.

Zaccolo M & Movsesian MA (2007). cAMP and cGMP signaling cross-talk: role of phosphodiesterases and implications for cardiac pathophysiology. *Circ Res* **100**, 1569-1578.

Zhang KY, Card GL, Suzuki Y, Artis DR, Fong D, Gillette S, Hsieh D, Neiman J, West BL, Zhang C, Milburn MV, Kim SH, Schlessinger J, & Bollag G (2004). A glutamine switch mechanism for nucleotide selectivity by phosphodiesterases. *Mol Cell* **15**, 279-286.

Ziolo MT, Lewandowski SJ, Smith JM, Romano FD, & Wahler GM (2003). Inhibition of cyclic GMP hydrolysis with zaprinast reduces basal and cyclic AMP-elevated L-type calcium current in guinea-pig ventricular myocytes. *Br J Pharmacol* **138**, 986-994.

Zoraghi R, Bessay EP, Corbin JD, & Francis SH (2005). Structural and functional features in human PDE5A1 regulatory domain that provide for allosteric cGMP binding, dimerization, and regulation. *J Biol Chem* **280**, 12051-12063.

Zoraghi R, Corbin JD, & Francis SH (2004). Properties and functions of GAF domains in cyclic nucleotide phosphodiesterases and other proteins. *Mol Pharmacol* **65**, 267-278.